University of Alberta

Tumor Control Probability Models

by

Jiafen Gong

A thesis submitted to the Faculty of Graduate Studies and Research
in partial fulfillment of the requirements for the degree of

Doctor of Philosophy

in

Applied Mathematics

Department of Mathematical and Statistical Sciences

©Jiafen Gong
Fall 2011
Edmonton, Alberta

Abstract

Cancer is one of the major causes of death in the world. In the field of Oncology, clinical trials form the crux of medical effort to find better treatment schedules. These trials are expensive, time consuming, and carry great risks for the patients involved. Mathematical models provide a complimentary, non-invasive tool in the development of improved treatments. Examples of such modeling efforts are the tumor control probability (TCP), used to measure the probability of tumor cell eradication; the cumulative radiation effect (CRE) and the normal tissue complication probability (NTCP), used for quantifying normal tissue complication.

In this thesis, I begin with a simple Poisson TCP based on mean cell population dynamics. Optimal treatment schedules are obtained by maximizing this TCP while constraining the CRE under a given threshold. Some of the optimal results suggest the usage of hyperfractionated treatments, which are applied in the treatment of prostate cancer.

A TCP derived from a birth-death process is obtained to include stochastic effects. The Poisson TCP is suitable for larger tumors whereas the new TCP is preferable for smaller ones. Furthermore, by using the birth-death process, I also derive an NTCP model. The calculation of this NTCP model provides an alternative proof to a formula derived by Hanin [36] to compute the probability distribution of the tumor size from its generating function. My formula is

computationally more efficient, compared to Hanin's.

Inspired by Ecology, I also study a third TCP model derived from the first passage time problem. This problem has been used in animal movement to find the mean time for a predator to target a motionless prey. I apply this idea to the radiation treatment of tumors to find the mean time to reduce the tumor size to zero.

Overall, my main contributions in this thesis are,

- A generalization of the hazard function for radiation induced damage, which includes various hazard functions from the literature (Chapter 2);

- An optimization of TCP under CRE constraints for realistic treatments (Chapter 3 and 4);

- A generalization of the birth-death approaches from Zaider-Minerbo and Dawson-Hillen into one framework (Chapter 5);

- A derivation of a TCP which includes tumor stem cells (Chapter 5);

- A new model for the NTCP which includes logistic growth (Chapter 6);

- A new model for the TCP, based on the first passage time problem (Chapter 7).

Acknowledgements

Contents

List of Tables

List of Figures

List of Symbols

Symbols	Meaning
BED	Biological effective dose
CRE	Cumulative radiation effect
DSB(SSB)	Double (single) strand break
LQ	Linear Quadratic model
LPL	Lethal potential-lethal model
MTSH	Multitarget single-hit model
NTCP	Normal tissue complication probability
ODE	Ordinary differential equation
RBD	Relative biological effect
RMR	Repair and misrepair model
PDE	partial differential equation
STSH	Single-target single-hit model
TCP	Tumor Control Probability
TSF	Total survival fraction

Chapter 1

Introduction

Cancer, mostly malignant tumor, is a class of diseases characterized by uncontrolled growth and the ability to invade into neighboring tissue or metastasize into distant tissues. It is not until the 18th century that people gained more knowledge about causes of cancer. Epidemiologic studies show that most human cancer is developed as the result of exposure to unhealthy environment or factors, such as chemicals in diet, tobacco, radiation (nature or medical), etc [22]. There are many types of cancer which affect different parts of human bodies. Usually, a particular type of cancer is named in conjunction with the location where it occurs. For example, skin cancer, breast cancer, brain cancer and prostate cancer. Even after the cancer metastasizes and affects another part of the body, it is still referred to the organ of origin. For instance, if a breast cancer spread to the liver, it is called (metastatic) breast cancer rather than liver cancer. To differentiate from the metastatic cancer, the original position of cancer is also called a primary cancer [7].

Cancer has brought great burden to the world. Based on a recent report from World Health Organization (WHO), the diagnosed incidence of cancer in 2004 is 11.4 million [68]. Compared the death rate caused by malignant tumor (per 100,000 persons) in 2000 and 2004 in Canada, it increased from 188.6 to 196.9 for women and from 218.8 to 222.9 for men, respectively. The current cancer treatment methods include surgery, chemotherapy, radiotherapy, immunotherapy. Although improvements have been obtained in early cancer diagnosis and

in cancer treatment, it is still the second largest cause of death in the world based on the report of the WHO in 2011 [68].

Therefore, even today, clinical trials still form the crux of medical efforts to find new or better treatment. Unfortunately, these trials are expensive, time consuming, and carry risks for the patients involved. Thus mathematical models provide an alternative, non-invasive tool in the search and development of new and improved treatment protocols. Example of the clinical trial oriented by the mathematical models is: in 2003, Citron *et al* [13] tested the dose densification that is proposed by Norton and Simon in 1986 [66] as a hypothesis based on mathematical models.

In this thesis, I mainly focus on the mathematical models that can be used to measure and compare cancer radiation treatment schedules. I will use prostate cancer as a test example for my models.

Radiotherapy or radiation treatment is a method to use ionizing particles or waves (such as fast neutrons, X-rays) to transfer energy and kill cancer cells in the treated area. Over half of all cancer patients receive radiotherapy at some stage of their diseases, either alone or in combination with other types of treatment (such as surgery or chemotherapy) [41, 59]. Radiation is energy. Its original unit is *radiation absorbed dose* (rad), which is the dose of radiation needed for deposition of 100 ergs per gram. Now it is replaced by the SI unit Gray (Gy), or 1 J/kg [1], where 1 Gy = 100 rad.

Two types of radiotherapy methods are available: brachytherapy, where a radiation probe is inserted into the tumor; and external beam radiotherapy, in which the tumor is irradiated from outside of the patient. Many tumors are treated by external beam radiotherapy. Before the treatment is given, the treatment volume must be determined. There are three levels of volume: (1) gross tumor volume (GTV) includes visible extent and location of the malignant tumor; (2) clinical target volume (CTV) contains GTV plus its surrounded area which might have subclinical disease; (3) planning target volume (PTV) is CTV with another layer of edge surrounded. In most treatments,

---

[1]1J/kg means the amount of radiation required to deposit 1 Joule of energy in any 1 kilogram matter.

the total dose is split into several smaller fractions to allow normal tissues to recover between fractions in external beam radiotherapy. For simplicity, we will use a tuple (d, T, n) to denote the treatment schedules: n fractions of treatment with dose d; T is a constant or vector to record the time intervals between each two fractions.

1.1 Cell Survival Models

To understand how the radiation kills the cancer cells, experiments have been carried out and different cell survival models have been proposed to explain these data. I review some of these cell survival models in Chapter 2, which describes the cell surviving as a function of radiation dose. One main such model is the linear quadratic model (LQ),

$$\sigma(D) = e^{-\alpha D - \beta D^2},\tag{1.1}$$

where α, β are radiosensitivity parameters which depend on the treated tissue and D is the total dose delivered to the tissue.

A highly related concept to the LQ model is the *Biological Effective Dose* (BED). The BED is defined based on the exponent of the fractionated - LQ model (see (2.44) in Subsection 2.2.3) as follows:

$$E = \frac{-\ln(\sigma(d))}{\alpha} = nd\left(1 + \frac{d}{\alpha/\beta}\right) = D\left(1 + \frac{d}{\alpha/\beta}\right),\tag{1.2}$$

where d is the dose used per fraction, n is the number of fractions, $D = nd$ is the total dose of the treatment, and α/β is called α/β-ratio of the corresponding tissue.

Another function which comes from the LQ model is the hazard function. It describes the death rate caused by radiation. I will review some choices of the hazard functions and summarize them into one general form in Section 2.3.

1.2 Poissonian Tumor Control Probability (TCP)

Cell survival models can be used to derive the Tumor Control Probability (TCP) model. It is the probability that no tumor cell exists and can be used

to quantify the effect of the treatments. The simplest TCP models are based on the linear quadratic survival fraction model (1.1) and the Poisson or the Binomial distribution. They both assume that the initial number of tumor cells N_0 is large. After one fraction of delivering dose D, the surviving fraction of tumor cells is $\sigma(D)$, as described in (1.1). Let X denote a random variable for the amount of surviving cells. If the deaths of tumor cells are stochastically independent of each other, and cell survival is a rare event, the probability of k tumor cells surviving is then,

$$P_P(X = k) = \frac{\lambda^k e^{-\lambda}}{k!}, \quad P_B(X = k) = \begin{pmatrix} k \\ N_0 \end{pmatrix} p^k (1 - p)^{N_0 - k}. \tag{1.3}$$

where P_P is the Poisson distribution and P_B is the Binomial distribution. The parameter λ is the expectation of Poisson distribution and p is the probability of one cell survival. We could use $N_0 \sigma(D)$ and $\sigma(D)$ to approximate them, respectively. Therefore we have the two TCPs as

$$TCP_P = p(X = 0) = e^{-\lambda} = e^{-N_0 \sigma(D)}. \tag{1.4}$$

or

$$TCP_B = (1 - \sigma(D))^{N_0}, \tag{1.5}$$

The Poisson approximation tells us that the Binomial distribution approaches the Poisson distribution when $N_0 \to \infty, \sigma(D) \to 0$ and the product of $N_0 \sigma(D)$ approaches the constant λ (i.e. $N_0 \sigma(D) \to \lambda$). Therefore, both TCP models are categorized into the Poissonian TCP.

These two Poissonian TCPs do not include tumor regrowth. Usher [89] extended these models to include regrowth between treatments. He found an explicit Poissonian TCP formula for the most commonly used growth laws: exponential growth, logistic growth and Gompertzian growth. It turns out that these TCP formulae are algebraic function of the treatment protocol (n, T, d) for uniform treatment (T=constant). I will adapt this approach in Chapter 3 to include realistic treatments with radiation during the week and treatment breaks over the weekend.

Usher tried to find optimal treatment schedules by maximizing the Poisson TCP under the constraint of normal tissue complication. The formula he used

to quantify the normal tissue complication is the cumulative radiation effect (CRE). It is defined as

$$CRE = \frac{n^c d}{T^b}, \tag{1.6}$$

where (n, T, d) denote the treatment schedule. The exponents b and c depend on the type of radiation used. They have been found through data fitting to be $c = 0.65, b = 0.11$ for X- and γ-rays radiation [45] and $c = 0.85, b = 0.11$ for fast-neutron radiotherapy [27]. The unit for CRE is *radiation effective unit* (reu) with the unit of days for T and rad[1] for dose d. The largest CRE value for normal tissue recommended by clinicians is 1800 *reu* [89].

However, Usher's results are not global optimal as he did optimization coordinate by coordinate. In Chapter 4, we verified Usher's results are not global optima, although his results are close to the real maxima. We further calculate Poissonian TCP values and CRE values for ten existent prostate cancer treatment schedules. We find that higher dose treatments result in quicker tumor killing at risk of more normal tissue complication; and that hyperfractionated treatments have effective reduction on normal tissue damage compared to their standard treatments. The success of the simplest TCP model encouraged us to develop more sophisticated TCP models and models for quantifying normal tissue complication.

1.3 TCP Derived From a Birth-Death Process

The Poisson TCP model, as described above, is entirely based on the expected number of surviving cells $\lambda = N_0 \sigma(D)$. This approach is suitable for large number of tumor cells. However, when tumor cell number is small, the stochastic effect will dominate. The stochastic process is a description of random phenomena changing with time [70]. It has been widely applied in physics, biology, chemistry, economics etc.

In a stochastic process, the variable we are interested in is a random variable $X(t)$, depending on a parameter $t \in T$. The parameter set T could be an abstract set. In my thesis, I will choose X to represent the tumor size and

---

[1]1rad=1cGy, 1Gy=100rad.

$t \in [0, \infty)$ or $t \in [0, T]$ and interpret t as 'time'. For each time t, the random variable $X(t)$ has values on a sample space Ω. We could define a Borel set[1] $\mathcal{R}$ of Ω and a probability measure on $\mathcal{R}$. Therefore, $x \in \Omega$ is called 'space' or 'state' and $X(t) = x$ means X is at position x at time t. The 'space' could have different meaning based on the field of study. For example, in population genetics [87], $X(t)$ is the number of certain genes present at time t; in gamble ruin problem or stock market, $X(t)$ can be the balance in the account; and $X(t)$ can be the density of molecules in chemical compounds.

In this thesis, we assume that the stochastic process $X(t)$ has the Markov property: the probability of the state of $X(t)$ at a future time $t + \Delta t$ only depends on the current time t, there is no memory of states in previous time. Mathematically, it can be written as: given any finite set of time moments, $t_1 < t_2 < \cdots < t_r < t$, we will have

$$Prob\{X(t + \Delta t)|\, X(t), X(t_r), \cdots, X(t_2), X(t_1)\} = Prob\{X(t + \Delta t)|\, X(t)\}.$$
(1.7)

The stochastic process with Markov property is either called a Markov process or a Markov chain, depending on whether the state are continuous or discrete. This transition probability also satisfies the Chapman-Kolmogorov equation

$$
\begin{aligned}
&Prob\{X(s) = y|X(t) = x\} \\
= &\int_z Prob\{X(s) = y|X(t') = z\}Prob\{X(t') = z|X(t) = x\}dz.
\end{aligned}
$$
(1.8)

or the discrete Chapman-Kolmogorov equation

$$Prob\{X(s) = y|X(t) = x\}$$
(1.9)
$$= \sum_z Prob\{X(s) = y|X(t') = z\}Prob\{X(t') = z|X(t) = x\}.$$
(1.10)

for any $t < t' < s$, where the states $X(t) = x$ represents that the size of the population at time t is x.

A special case of continuous time Markov chain is a birth-death process [30]. The birth-death process is based on the assumption that only a finite number

---

[1] In Measure Theory, Borel sets are elements of a sigma algebra, which is closed with respect to countable union, countable intersections and relative complement [8].
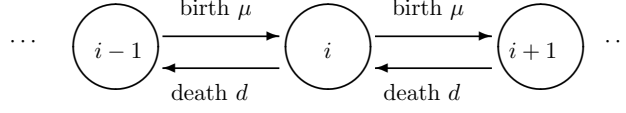
Figure 1.1: **The diagram of birth-death process.**

of $X(t)$ are born or die in a given small time interval [30]. Suppose (x, t) are on the grid

$$\cdots, i - 1, i, i + 1, \cdots$$

and

$$0, \Delta t, \cdots, t - \Delta t, t, t + \Delta t, \cdots$$

Δt is small enough such that only one event (either birth or death) will happen in Δt. The transition probability of birth-death process is

$$Prob\{X(t + \Delta t) = i + 1 | X(t) = i\} = i\mu\Delta t + o(\Delta t) \qquad (1.11)$$

$$Prob\{X(t + \Delta t) = i - 1 | X(t) = i\} = id\Delta t + o(\Delta t) \qquad (1.12)$$

$$Prob\{X(t + \Delta t) = i | X(t) = i\} = 1 - (d + \mu)i\Delta t + o(\Delta t) \qquad (1.13)$$

$$Prob\{X(t + \Delta t) = i + k | X(t) = i\} = o(\Delta t), \quad |k| \geq 2 \qquad (1.14)$$

where μ is the growth rate per capita and d is the death rate per capita. This could also be displayed as a diagram shown in Figure 1.1.

For a given initial tumor size x_0, we abbreviate $Prob\{X(t) = i | X(t_0) = x_0\} := P_i(t)$, and substituting (1.11)-(1.14) into (1.9), we have

$$P_i(t+\Delta t) = (i-1)\mu\Delta t P_{i-1}(t) + (i+1)d\Delta t P_{i+1}(t) + (1 - (d + \mu)i\Delta t) P_i(t) + o(\Delta t).$$
$$(1.15)$$

Letting $\Delta t \to 0$, we formally obtain an ordinary differential equation system to describe the evolution of probability of each state. This system is called a master equation:

$$\frac{dP_0}{dt} = dP_1(t), \qquad (1.16)$$

$$\frac{dP_i}{dt} = \mu(i - 1)P_{i-1}(t) + d(i + 1)P_{i+1} - (\mu + d)iP_i(t), \quad i \geq 1. \quad (1.17)$$

One way to solve the above systems is to use the generating function. The generating function for this system is

$$A(s,t) = \sum_{i=0}^{\infty} P_i(t)s^i. \tag{1.18}$$

We show later that the generating function will satisfy a hyperbolic equation

$$\frac{\partial A(s,t)}{\partial t} = (s-1)(ds - \mu)\frac{\partial A(s,t)}{\partial s}. \tag{1.19}$$

Zaider and Minerbo [101] derived a TCP model from the above birth-death process with the assumption that all the tumor cells are identical. Once they solve the hyperbolic equation (1.19) by the method of characteristics, they obtain a TCP formula defined as

$$TCP = A(0,t). \tag{1.20}$$

Cell regeneration and tumor regrowth is not only a matter of birth and death. For cells to multiply, they transit through the cell cycle. The cell cycle, or cell division cycle, is the process that a cell divides and duplicates into two new cells, often called 'daughter cells' [55]. For cells with a nucleus, the cell cycle includes four phases: G_1, S, G_2, or M phase. The first three phases are also called Interphase, during which the cell prepares for the division. Cell size will increase in the G_1 phase, DNA replication occurs during the S phase, cell continues to increase necessary protein and RNA synthesis in the G_2 phase. When everything is ready, the cell division happens in the M phase and two daughter cells are generated. Cells could leave the cycle and stop dividing; in this case, they enter a resting phase which is called G_0 phase. Cells in the G_0 phase could also return back to the cell cycle and undergo mitosis. Cells in different stages of the cell cycle show different radiosensitivities. For example, quiescent cells (G_0) are much less radiosensitive than cells in S or M phases. Dawson and Hillen [20] extended the Zaider and Minerbo model to include the cell cycle effect and they divide the tumor cells into two compartments: active (G_1, S, G_2, M) and quiescent compartment (G_0). In Chapter 5, I will first review these two TCP models, then I will present my contribution to a TCP model in this category, which is a generalization of the above two
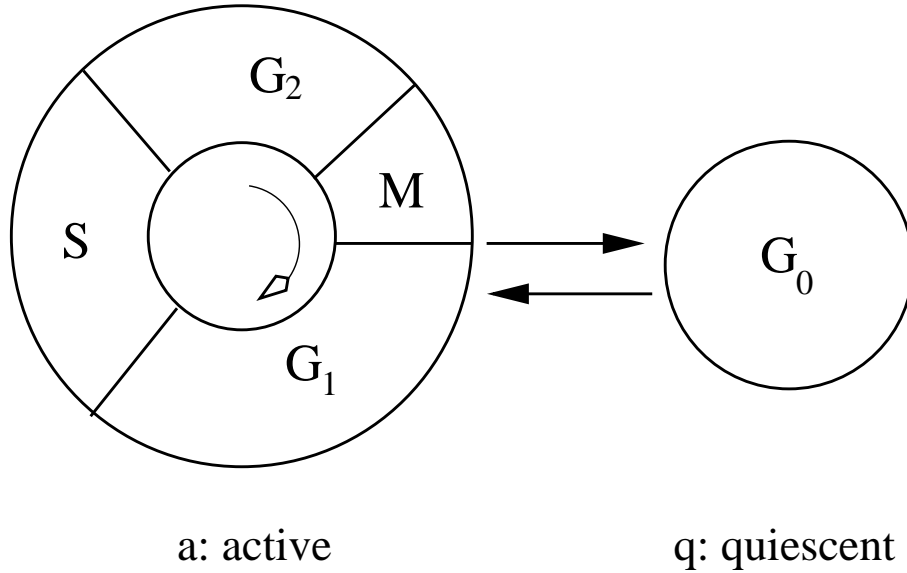
Figure 1.2: **A schematic of cell cycle dynamics.** Cells in the G_1, S, G_2, and M phases are grouped in one compartment, and labeled as active. Cells in the G_0 phase are grouped in a second compartment, and labeled as quiescent. Figure redraw from [37].

models, where the Zaider-Minerbo and Dawson-Hillen TCP arise as special cases. Furthermore, we adapted this approach to derive a TCP model under the assumption of tumor stem cells.

1.4 Stochastic Normal Tissue Complication Probability

As mentioned above, not only tumor cells can be killed in the radiation treatment, normal tissue will also be affected by the treatment. In Chapter 6, I derive a new formula for measuring the normal tissue damage - normal tissue complication probability (NTCP). First I introduce two existent NTCP models: the Lyman NTCP [53] and the structural NTCP Model. Both above NTCP models do not consider normal tissue regrowth. I use a birth-death process to derive a NTCP model characterized by logistic growth. The calculation of NTCP will also provide an alternative proof to the formula pro-

posed by Hanin [36] to compute the probability distribution $P_i(t)$ of tumor cell amount from the generating function $A(s,t)$. However, our formula leads to faster computer simulations.

1.5 TCP from First Passage Time Problem

Stochastic Processes can not only be studied by discrete space birth death processes as shown above, they could also be studied by a diffusion equation like backward Kolmogorov equation and forward Kolmogorov equation, or Fokker Planck equations. Inspired by models from Ecology, I finally study a TCP model based on the backward Kolmogorov equation and the first passage time problem. The first passage time problem is used to study the probability that a random variable X arrives at a preset target for the first time. Applying this idea to the tumor radiation treatment, we want to study the time needed for the numbers of tumor cells X to arrive the target $X = 0$ and the probability that the amount of tumor cells reduces to 0.

Between these three TCP models (Poisson TCP, birth-death TCP, first passage time TCP), it turns out that the Poisson TCP is the most useful model in daily practice. The first passage time TCP can only be used for constant treatment, since the corresponding equations cannot be solved for arbitrary treatments. The Poisson TCP and birth-death TCP both can be used for any treatments. However, Poisson TCP is simple, easy to calculate, and the most important thing is that it can make the same prediction as the complicated birth-death TCP and Monte Carlo TCP when proper parameters are chosen (see [31]).

Chapter 2

Cell Survival Models and Hazard Functions

As pointed out by Alpen [4], most modern radiobiology theories are based on the *cell survival model*. It describes the fraction of surviving radiated cells as a function of radiation dose. Therefore, in this chapter, I mainly review the *cell survival models* that have nice fitting to experimental data done *in vitro*. Furthermore, I also review the *hazard function* related to the cell survival models, which will be used in differential equations in later chapters.

2.1 Data for Cell Survival Models

In radiobiology, cell death, the converse of cell survival, is defined as cells losing the reproductive integrity, which is also called reproductive death [34]. By definition, a survivor retains its reproductive capability and is able to grow indefinitely to form a large colony, which can be seen with the naked eye. This is also the way that experimentalists determine whether or not a cell is still alive. Before the late 1950s, experimentalists mainly worked on classic microbiological organisms that would grow in a petri dish to measure cell survival after treatment. Examples are Escherichia Coli, Bacteroides subtilis, Sacbharomycep Sp., Tetrahymena Sp., and many more. In 1955, Puck and Marcus [72] discovered a method to grow mammalian cells *in vitro*, which made

these experimental methods available to mammalian cells. Quite often, cells taken from mammals or other animals which are placed in the petri dish only grow for a few weeks before they peter out and die. Some cell lines, which pass through a 'crisis' become 'immortal': they could grow for many years. These 'immortal' cell lines will be preserved and fed regularly, and they are called established cell lines. Commonly used cell lines are Hela cells from human cervical cancer; V97 and CHO cells from hamster lung or ovary, respectively; 9L cells from rat glioscarcoma and T1 cells from human kidney [4]. Single cells can be obtained from the cell lines by the use of an enzyme called *Trypsin*. These single cells are then seeded into several cultured dishes. Besides one unirradiated control dish, each other dish will be radiated by different doses. Then all the dishes are incubated for several weeks at temperature 37 ^{o}C under the same environment. Figure 2.1 shows how this experiment proceeds.
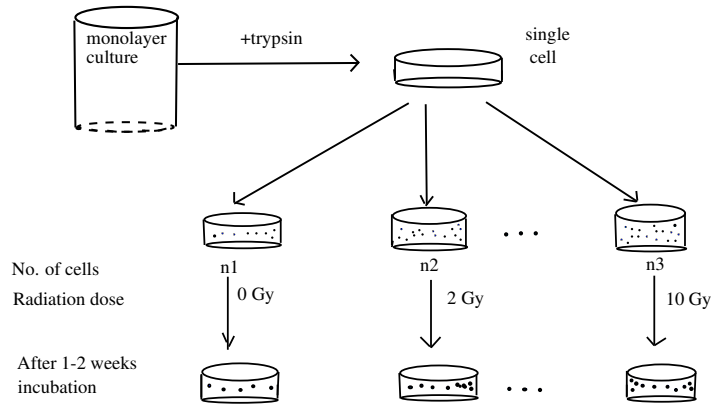
Figure 2.1: **Experiments to generate the cell survival curve.** Single cells are obtained from an 'immortal' cell line by trypsinization. Then known numbers of cells are placed into different petri dishes and irradiated with different doses, with one unirradiated petri dish as control. All the petri dishes will be incubated in the same environment until a single cell grows into a colony. Figure has been redrawn from the original graph in Hall's book [34].

To calculate the cell survival, we first calculate the *plating efficiency (PE)* by counting the visible colonies in the control dish as follows,

$$PE = \frac{\text{counted colonies in the control dish}}{\text{cell seeds}}.$$

Then each dish will receive a *survival fraction* (σ) at dose D

$$\sigma(D) = \frac{\text{counted colonies (after dose D)}}{\text{cell seeds} * PE}.$$

2.2 Theoretical Model for Cell Survival

There were several theories developed in order to explain these data. One type of earliest models is the target theory model proposed by Lea in 1955 [48]. The basic assumption of his model is that there are some critical volumes in a cell, once all the targets in the critical volumes are inactivated, the cell dies. People find that the target models have fatal shortcoming when it comes to the data of mammalian cell lines. Another alternative model, the linear quadratic (LQ) model, has been developed to solve the problem and is still widely used today [4]. Many scholars have contributed to the explanation of this model since its original proposal. The most famous ones include the molecular theory of radiation action by Chadwick and Leenhouts in 1981 [12], the dual radiation action proposed by Kellerer and Rossi in 1972 [44], the repair-misrepair model of cell survival developed by Tobias *et al* in 1980 [85] and the lethal-potential lethal model by Curtis in 1986 [16]. We will discuss all these models in the following subsections.

2.2.1 Target Model

The target theory was developed by Lea [48] using data on microorganism cells. All the target theories base on the essential assumption that cells will die as a result of a multi-step process,

(1). Absorbing energy in the cell,

(2). Deposited energy causes ionization and excitation which lead to molecular lesions,

(3). Cells lose reproductive capability.

At the time that Lea published the target theory, the energy absorption was well understood, but there was only limited understanding in the other two

steps. Although nobody knew the importance of DNA at that time, Lea did predict the need of inactivating of critical volumes (CV) to kill a cell. Lea assumes that the critical volume is a discrete target in a cell which is a space-occupying entity. There might be multiple targets in a single cell, say n targets, inactivating all the n targets will lead to cell death.

In the model derivation, Lea assumes that the cell population is exposed to low LET[1] radiation (high LET radiation will have similar derivation with rescaled units), so the interactions of ionizing events are rare. The energy deposition can produce biological damage which is called *active event*. Mathematically, he denotes

- V: the total cell volume =(the average cell volume)*(number of cells);

- ν: the sensitive volume(s) in a cell, an *active event* happens in this area is called a *hit*;

- D: the density of *active events*, that is, events occuring per unit volume. It is assumed to be proportional to the dose.

Therefore, the number of *active events* in all cells exposed to radiation is $\mathfrak{D} = VD$, the hit probability ρ, or the probability of an *active event* happening in sensitive volume, is given by $\rho = \frac{\nu D}{VD} = \frac{\nu}{V}$.

The probability that a cell has k hits is given by the binomial distribution

$$p_k = \left(\begin{array}{c} \mathfrak{D} \\ k \end{array} \right) \rho^k (1-\rho)^{\mathfrak{D}-k}. \tag{2.1}$$

The probability of a cell surviving k hits is called *hit-survival function*. If we denoted it as $H(k)$, the survival probability with k hits is given by

$$p(k, \mathfrak{D}, \rho) = p_k H(k) = \left(\begin{array}{c} \mathfrak{D} \\ k \end{array} \right) \rho^k (1-\rho)^{\mathfrak{D}-k} H(k). \tag{2.2}$$

The total survival probability of a cell, denoted as σ, is given by

$$\sigma(\mathfrak{D}, \rho) = \sum_{k=0}^{\mathfrak{D}} p_k H(k) = \sum_{k=0}^{\mathfrak{D}} \left(\begin{array}{c} \mathfrak{D} \\ k \end{array} \right) \rho^k (1-\rho)^{\mathfrak{D}-k} H(k). \tag{2.3}$$

---

[1]Linear energy transfer (LET), is a measure of the loss of energy per unit distance along the path of a charged particle [32].

- **Single-target Single-hit Model**

  The Single-target Single-hit (STSH) model assumes that a cell only contains one target and the target will be inactivated if it is hit once or more times, that means the *hit-survival function* has the following form

  $$H(k) = \begin{cases} 0, & k \geq 1 \\ 1, & k = 0 \end{cases} \tag{2.4}$$

  Therefore the survival model (2.3) is specified as

  $$\sigma(\mathfrak{D}, \rho) = p(0, \mathfrak{D}, \rho) = (1 - \rho)^{\mathfrak{D}} = e^{\mathfrak{D} \ln(1-\rho)} = e^{-p_0 \mathfrak{D}}. \tag{2.5}$$

  where $p_0 = -\ln(1 - \rho)$. For small ρ, we approximate p_0 by ρ because of the Taylor expansion $\ln(1 - \rho) = -\rho - \frac{1}{2}\rho^2 - \frac{1}{3}\rho^3 - \cdots$.

  Notice that $\mathfrak{D} = VD$ and denote $p = p_0 V$, we have

  $$\sigma(\mathfrak{D}, \rho) = e^{-pD}. \tag{2.6}$$

  Recall D is the density of active events, which is proportional to the dose. We could let the proportional coefficient be combined into the parameter p and denote D the dose. Therefore p has the unit of $\frac{1}{\text{dose}}$. More generally, p is written as $\frac{1}{D_0}$, where D_0 is called *mean lethal dose* [23] or the average dose absorbed by each cell before it dies because

  $$D_0 = \int_0^\infty e^{-pD} dD = \frac{1}{p}.$$

  The STSH model is also referred as exponential survival function.

- **Multi-target Single-hit Model**

  The Multi-target Single-hit (MTSH) model assumes that there are n targets, each target is independent of each other and is inactivated once it receives at least one hit. All the other assumptions are the same as the STSH model.

  From the STSH model, we know each target has a probability e^{-pD} to survive, so the probability that k targets are hit is

  $$p_k = \binom{n}{k} (1 - e^{-pD})^k (e^{-pD})^{n-k}. \tag{2.7}$$

15

Similarly, denote $H(k)$ as the *hit-survival function*, we have the cell survival as

$$\sigma(n, p, D) = \sum_{k=0}^{n} p_k H(k) = \sum_{k=0}^{n} \binom{n}{k} (1 - e^{-pD})^k (e^{-pD})^{n-k} H(k). \quad (2.8)$$

With the assumption that the cell die if and only if all the targets are hit, that is,

$$H(k) = \begin{cases} 0, & k = n \\ 1, & 0 \le k \le n - 1 \end{cases} \quad (2.9)$$

The MTSH model is written as

$$\sigma(n, p, D) = \sum_{k=0}^{n} p_k H(k) = \sum_{k=0}^{n-1} \binom{n}{k} (1 - e^{-pD})^k (e^{-pD})^{n-k} = 1 - (1 - e^{-pD})^n. \quad (2.10)$$

Similar to the STSH model, sometimes the MTSH model is written as

$$\sigma(n, D_0, D) = 1 - \left(1 - \exp\left(\frac{-D}{D_0}\right)\right)^n. \quad (2.11)$$

For any n, we have $\sigma = 1$ at dose $D = 0$. There is a shoulder when dose D is small for $n \ne 1$. The bigger n is, the bigger the shoulder. When D is large, the MTSH curves can be approximated by a straight line as showed by the solid lines in Figure (2.2). These linear approximations have y-intercept at n because (2.11) is dominated by $\sigma(n, D_0, D) = ne^{-\frac{D}{D_0}}$.

- **Other Developments of Target Models**
  There are other developments of the target models. MTSH model can be thought of the extension of the STSH model by increasing the target numbers. If we increase the number of hits that are needed to destroy a single target, we have the Single-target Multi-hit model. This model assumes each cell has one target and a cell can be killed only when it received more than m hits. It is much more complicated than the above two and not as popular as the two. Hence, for details, I refer the reader to the book written by Elkind and Whitmore [23].

  The MTSH model has a vital shortcoming which is the initial zero slope (see Figure 2.2), while this is not observed in the experimental data. To
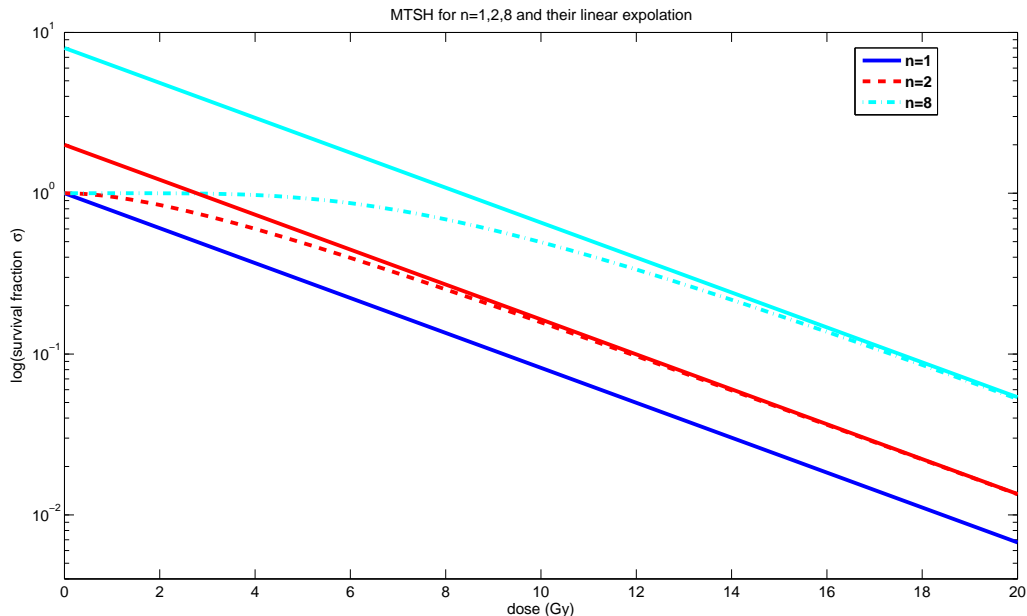
Figure 2.2: **Plot of log(MTSH) as a function of dose for** $n = 1, 2, 8$. The MTSH curve is a straight line for $n = 1$ as denoted as solid blue line, the curved dashed line and dash-dot line are MTSH curves for $n = 2$ and $n = 8$, respectively. The other two solid lines are linear approximation of the corresponding curved lines at high dose for $n > 1$. Here, we choose $D_0 = 4$ Gy. When $n \neq 1$, the survival fraction has a shoulder at low dose. The target number n are the y-intercept of each linear approximation curve.

solve this problem, a single-hit term is introduced in front of the MTSH model, which becomes

$$\sigma = e^{-p_1 D}\big[1 - (1 - e^{-p_2 D})^n\big] \tag{2.12}$$

where p_1 is the parameter in the STSH model and p_2 is the parameter from the MTSH model. The first term does not change the properties of the MTSH model except that now it has a non-zero initial slope, since at high doses, there is an exponential approximation to (2.10) i.e. $\sigma \approx ce^{-pD}$, where c is a constant.

Another aspect of the target model development comes from the *hit-survival function $H(k)$*. The above models all choose a step function for

17

$H(k)$. Hall [34] has proved that in a homogeneous population, a more general *hit-survival function* can also result in the exponential survival fraction model. *i.e.*

$$H(k) = e^{k \ln(h)}, 0 \leq h \leq 1. \tag{2.13}$$

where h is a parameter between $[0, 1]$. For the special case $h = 0$, we have the same $H(k)$ as that in the STSH model (2.4) because $e^{\ln h^k} = 1$.

There are more developments on the target models, like population heterogeneous situation, we refer readers to the Elkind and Whitmore's book [23] for detail. More recently, Dawson and Hillen [20] derived a target survival model to include cell cycle by first principles. They divided the whole cell population into active and quiescent cells based on the cell cycle. In their model assumption, each cell includes multiple targets. The differences between the active and quiescent cells lie in the way to inactivate the targets. For a cell in the active compartment, part of its targets will die followed by single hit and the others will die by two hits. All the targets in the quiescent compartment only need one single hit to inactivate. I will refer readers to [20] for the detailed model derivation.

2.2.2 Linear Quadratic (LQ) Model

The linear quadratic (LQ) model is a group of models with both linear and quadratic dose terms in the exponent of an exponential function. The classic linear quadratic model (LQ) is written as follows,

$$\sigma(D) = \exp(-\alpha D - \beta D^2). \tag{2.14}$$

where D is the dose used in the radiation, α (Gy^{-1}), β (Gy^{-2}) are radiosensitivity parameters depending on the tissue type. The ratio α/β characterizes the sensitivity of tissues to radiation and it can be used to differentiate between different kind of tissues [94]. The bigger the ratio is, the more sensitive the tissue is. For fast dividing cells (also called early responding tissue), $\alpha/\beta \approx 10$, for most normal tissue (or late responding tissue), the ratio is about 3. Example values of α/β ratios for human or animal tissues are listed in Table 2.1.

Tissue/Organ	α/β value (Gy)	Reference
Spinal Cord		
Cervical and thoracic cord	2	Human data by Nieder *et al* [63]
Lumloar cord	4	Human data by Nieder *et al* [63]
Lung	1.1-4.3	Human data by Koontz *et al*[46]
Colon	3.95*	Human data by Leith *et al* [49]
Kidney	2-3	Mouse data by Stewart *et al* [80]

* $\alpha = 0.281 Gy^{-1}, \beta = 0.0711 Gy^{-2}$ in original paper.

Table 2.1: **Example values of α/β ratios for different tissues.**

In what follows I am going to briefly review four popular models where two of them derive the LQ model, and another two have the LQ model as one of their special cases.

(1). **Molecular Theory of Radiation Action**

This model was first introduced by Chadwick and Leenhouts in 1981 [12]. It explicitly states that the radiation energy deposition will result in damage in the cell through the interaction of DNA breaks, DNA repair and lack of repair. In contrast to the critical volume considered in the target models, Chadwick and Leenhouts assume that critical molecules - double-stranded DNA - are essential for the survival of a cell. The DNA strand lesions are the ruptures of molecular bonds on a DNA strand. The damage to the molecular bonds on one DNA strand may cause scission of the backbone and therefore in a breakage of a single strand, which is called single-strand breaks (SSB); the damage resulting in the breakage of both DNA strands is called a double-strand break (DSB).

Chadwick and Leenhouts thought of DSB as the critical damage. They considered the DSB as a result of two mechanisms: (I) both strands are broken in one event, or (II) two SSBs happen close to each other in time and space. The assumptions about the DSB from mechanism one are:

– K is the fraction of DSBs in one event per unit dose.

– These DNA lesions can be repaired under certain condition, the

19

proportion of repair is r. Therefore $f_0 = 1 - r$ is the proportion of DSB unrepaired.

Let n_0 be the initial number of critical bonds that are susceptible to DSB, $N(D)$ be the number of critical bonds remaining intact after any dose, so N will changes against dose D as follows

$$\frac{dN}{dD} = -K\Delta N, \quad N(0) = n_0. \tag{2.15}$$

where Δ is the fraction of dose creating DSB in one event. Therefore, the number of remaining intact critical bonds are $N(D) = n_0 e^{-K\Delta D}$. With the consideration of repair of DNA break with rate f_0, the number of DSB created in one event by mechanism I is given by

$$N_{dbI} = f_0(n_0 - N(D)) = n_0 f_0(1 - e^{-K\Delta D}). \tag{2.16}$$

In a similar way, the generation of SSB on each DNA strand can be considered. Denote n_1 be the initial number of critical bonds susceptible to SSB on one strand and n_2 be the corresponding numbers on the other strand ($n_1 = n_2$), f_1, f_2 be the proportions of repair of the SSB on each strand, respectively. We still use K to denote the fraction of generation of SSB in one event per unit dose. By following the above process for the DSB from the mechanism I, the number of the SSB on each strand is

$$n_{sb1} = n_1 f_1(1 - e^{-KD(1-\Delta)}), \quad n_{sb2} = n_2 f_2(1 - e^{-KD(1-\Delta)}) \tag{2.17}$$

Here, we replace Δ in (2.16) by $1 - \Delta$, which is the fraction of the dose to create SSB. Therefore, the number of DSB generated by mechanism II is given by

$$n_{dbII} = E n_{sb1} n_{sb2} f_0 = E f_0 f_1 f_2 n_1 n_2 (1 - e^{-KD(1-\Delta)})^2. \tag{2.18}$$

where E is the effectiveness factor for the likelihood of two SSB close to each other in time and space and f_0 is the repair rate of DSB.

Combining both DSB mechanisms, the total number of lethal DSB is given by

$$n_{db} = p\left(n_{dbI} + n_{dbII}\right) = pn_0 f_0 (1 - e^{-K\Delta D}) + pE f_0 f_1 f_2 n_1 n_2 (1 - e^{-KD(1-\Delta)})^2,$$
(2.19)

where p is the fraction of lethal DSB. Typically the fraction of generating DSB or SSB per unit dose (K) is very small, so $K\Delta D, K(1 - \Delta)D$ are small. The number of DSB could be approximate by

$$n_{db} \approx pn_0 f_0 K \Delta D + pE f_0 f_1 f_2 n_1 n_2 K^2 (1 - \Delta)^2 D^2.$$
(2.20)

If we assume the number of lethal DSB (X) satisfying the Poisson distribution (see Equation 1.3) with parameter λ, we could use n_{db} as estimator of the expectation λ and have the probability of cell survival $P(X = 0)$ given by

$$\sigma(D) = P(X = 0) = e^{-n_{db}} = e^{-(\alpha D + \beta D^2)}.$$
(2.21)

The radiosensitivity parameters α, β are determined by the parameters for generation of DSB and DSB repair; i.e. $\alpha = pn_0 f_0 k_0 \Delta$ is from linear generation of DSB and $\beta = pE n_1 n_2 f_0 f_1 f_2 K^2 (1 - \Delta)^2$ depends on nonlinear generation of DSB.

(2). **Theory of Dual Radiation Action**

Kellerer and Rossi [44] derived the dual radiation action theory from their observation that a linear relation exists between the Relative Biological effectiveness (RBE) and the dose on the logarithmic scale. A RBE is defined as

$$RBE = \frac{D_x}{D_n}.$$
(2.22)

where D_x is the dose for X-ray radiation and D_n is the corresponding dose used in other type of radiations when both radiations have the same effect. After analyzing several clinical data, they found that on the logarithmic scale, the RBE of the high LET radiation against its dose is a straight line with slope $-\frac{1}{2}$, that is,

$$\log(RBE) = \log\left(\frac{D_x}{D_n}\right) = -\frac{1}{2}\log(D_n) + c.$$
(2.23)

where c is a constant depending on the type of radiation used. Equivalently, this formula can be written as

$$\frac{D_x}{D_n} = RBE = \sqrt{\frac{\lambda}{D_n}}, \quad \lambda = e^{2c}. \tag{2.24}$$

Therefore

$$D_n = \frac{1}{\lambda}D_x^2. \tag{2.25}$$

This tells us: to obtain the same effect, the dose needed for high LET radiation is proportional to the square of the dose of X-ray radiation. They further find that the generation of elementary lesions, denoted as L, is proportional to the absorbed high LET dose in certain range of dose,

$$L = k_n D_n. \tag{2.26}$$

So the yield of elementary lesions by X-ray will be proportional to the square of the dose,

$$L = \frac{k_n}{\lambda}D_x^2. \tag{2.27}$$

A more general expression of the yield of lesions is given by

$$L(D) = k(\lambda D + D^2). \tag{2.28}$$

where $k = \frac{k_n}{\lambda}$, and λ depends on radiation quality. For X-ray, λ is very small such that the linear term can be negligible when D is not too small; for neutron, λ is so large that the linear term dominates once D is not too big.

The main part of the dual radiation action model is to derive the parameter λ from the aspect of Microdosimetry. The microdosimetry is a field of physical study without biology. It measures and analyzes the energy deposition by the radiation within a small volume in an equipment called Rossi counter.

The Rossi counter is filled with gas at a low pressure so that the mass of the gas is the same as that of a small sphere of tissue [32]. When a Rossi counter is exposed to radiation, each interaction of radiation with the counter gas is called *energy deposition event*, or *event* for simplicity. Each

event generates a measurable pulse. By collecting the pulse intensities, we could find the probability density distribution of the absorbed energy z after the usage of dose D, denoted as $f(z; D)$. Let $l(z)$ be the generation of lesions by absorbed energy z, the experimental data [32] suggested the form of $l(z) = mz^2$, then the average yield of lesions after dose D is given by

$$L(D) = m\overline{z^2}(D) = m \int_0^\infty z^2 f(z; D)dz. \tag{2.29}$$

Assume the number of events at dose D is a Poission distribution, i.e., $p_i(D)$ is the probability of i events happening after dose D. Let $f_1(z)$ be the probability density of absorbed energy z deposited in a single event, $f(z, D)$ has the form of

$$f(z; D) = \sum_{i=1}^\infty f_i(z)p_i(D).$$

where $f_i(z)$ are the probability density of deposited energy z happening in i events and they can be computed as the i-fold convolution of $f_1(z)$ [44]. Kellerer and Rossi wrote the mean number of lesions as

$$L(D) = m\overline{z^2}(D) = m \left(\frac{\int_0^\infty z^2 f_1(z)dz}{\int_0^\infty z f_1(z)} D + D^2 \right), \tag{2.30}$$

For detailed derivation of this formula, we refer the reader to the original paper [44]. If, once again, we assume that the number of lesions satisfy the Poisson distribution, the survival of the cells can be given by

$$\sigma(D) = e^{-L(D)} = e^{-(\alpha D + \beta D^2)}. \tag{2.31}$$

where $\alpha = m\frac{\int_0^\infty z^2 f_1(z)dz}{\int_0^\infty z f_1(z)}, \beta = m$.

(3). **Repair and Misrepair Model (RMR)**

This model is derived by Tobias *et al* in 1980 [85]. It mainly tracks the number of DNA breaks. In the Molecular theory, Chadwick and Leenhouts considered the linear and nonlinear generation of DNA breaks to derive the LQ model. Here in the RMR model, Tobias and his coworker consider the number of DNA breaks, regardless of their mechanisms of

generation. It is the different mechanisms of the repair of DNA breaks that make the model include linear and quadratic terms. Tobias *et al* denote $U(t)$ as the DNA breaks, divide the repair of the DNA break into linear and quadratic process. The repair rates of each process are λ and k, respectively. Therefore the number of DNA break is governed by

$$\frac{dU}{dt} = -\lambda U - kU^2, \quad U(0) = U_0. \tag{2.32}$$

Where U_0 is the initially generated DNA break after radiation. This Bernoulli equation has a solution of the form

$$U(t) = \frac{U_0 e^{-\lambda t}}{1 + \frac{U_0}{\epsilon}(1 - e^{-\lambda t})}.$$

where $\epsilon = \lambda/k$ is the repair ratio. We find that the number of unrepaired DNA break approaches 0 as time goes to ∞.

The total number of linear and quadratic repair, can also be calculated by

$$
\begin{aligned}
R_L(t) &= \int_0^t \lambda U(s)ds = \epsilon \left(1 + \frac{U_0(1 - e^{-\lambda t})}{\epsilon}\right); \\
R_Q(t) &= \int_0^t kU^2(s)ds = -\epsilon \ln\left(1 + \frac{U_0}{\epsilon}(1 - e^{-\lambda t})\right) + \frac{(U_0 + \frac{U_0^2}{\epsilon})(1 - e^{-\lambda t})}{1 + \frac{U_0}{\epsilon}(1 - e^{-\lambda t})}.
\end{aligned}
$$

In the assumption of the RMR model, not all the repairs are correct, those accurate repairs are called 'eurepair', the unrepaired or misrepaired DNA break will lead to the death of the cell. If the fraction of linear eurepair and quadratic eurepair are denoted as ϕ and δ, respectively, the cell survival model is given by

$$\sigma(t) = e^{-\left(U(t)+(1-\phi)R_L(t)+(1-\delta)R_Q(t)\right)}. \tag{2.33}$$

A speical case of this model can be obtained under the assumption that all the linear repair are eurepair and none of the quadratic repair is eurepair, i.e. $\phi = 1, \delta = 0$. The (2.33) becomes

$$\sigma(t) = e^{-\left(U(t)+R_Q(t)\right)} = e^{-U_0}\left[1 + \frac{U_0}{\epsilon}(1 - e^{-\lambda t})\right]^\epsilon. \tag{2.34}$$

The initial yield of lesions U_0 is in general a power series of the dose D,

$$U_0 = \sum_{i=0}^{i_{\max}} \alpha_i D^i.$$

where $\alpha_i, i = 1, \cdots, i_{\max}$ are constants. In their paper, Tobias et al chose $U_0 = kD$.

When $\frac{U_0}{\epsilon}(1 - e^{-\lambda t}) = \frac{kD}{\epsilon}(1 - e^{-\lambda t})$ is small, we have the logarithm of (2.34) approximated by

$$-\ln \sigma(t) = U_0 - \epsilon \ln\left(1 + \frac{U_0}{\epsilon}(1 - e^{-\lambda t})\right) \approx ke^{-\lambda t}D + \frac{k^2}{2\epsilon}(1 - e^{-\lambda t})^2 D^2.$$

Therefore $\sigma(t)$ in (2.34) is the LQ model with $\alpha = ke^{-\lambda t}$ and $\beta = \frac{k^2}{2\epsilon}(1 - e^{-\lambda t})^2$. Note here both α and β are not constants as those in the first two models, they vary as time changes.

Another interesting special case of RMR model is that, without the assumption that all linear repairs are eurepair, we have the same form of the cell survival model as (2.34), except an extra power ϕ in the second term.

$$\sigma(t) = e^{-\left(U(t) + R_Q(t) + (1-\phi)R_L(t)\right)} = e^{-U_0}\left[1 + \frac{U_0}{\epsilon}(1 - e^{-\lambda t})\right]^{\epsilon\phi}. \quad (2.35)$$

(4). **Lethal and Potentially Lethal Model (LPL)**

The former RMR model assumes that all the newly generated DNA breaks are uniform, it is the repair process of the DNA break that generates different categories of DNA lesions. Curtis [16] explained the LQ model by dividing the yield of the DNA lesions into two categories: lethal lesions and potentially lethal lesions. Yields of both kinds of lesions are proportional to the applied dose. By tracking the number of both lesions, Curtis derived the Lethal and Potentially Lethal Model (LPL) model, one of whose special cases is the LQ model.

This model is based on the diagram shown in Figure 2.3. Here, A denotes the number of undamaged critical bonds in the DNA, B and C represent the potentially lethal and lethal lesions, respectively. Based
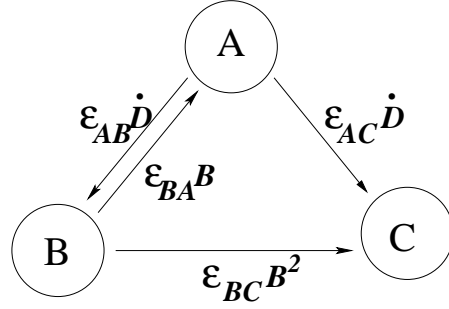
Figure 2.3: **The diagram for lethal and potential-lethal (LPL) model.**
A denotes the undamaged critical bonds in the DNA, B, C are potential-lethal
and lethal lesions, respectively.

on the assumption of the model, only potentially lethal lesions are re-
pairable by a linear progress, they could transfer to the lethal lesions if
they interact with each other as well. A lethal lesion is permanent and
can not be repaired.

Curtis further assumes that the number of undamaged DNA critical
bonds are way more than the DNA lesions, so the generation of both
categories of lesions are only dependent on the dose rate, denoted as $\dot{D}$.
Therefore the evolution of the number of both lesions can be modeled
by the following equations,

$$\frac{dB}{dt} = \epsilon_{AB}\dot{D} - \epsilon_{BA}B - \epsilon_{BC}B^2, \tag{2.36}$$

$$\frac{dC}{dt} = \epsilon_{AC}\dot{D} + \epsilon_{BC}B^2. \tag{2.37}$$

with initial condition $B(0) = C(0) = 0$, and the assumption that dose is
given constantly within the radiation time $[0, R_T]$, i.e.

$$\dot{D}(t) = \begin{cases} \frac{D}{R_T}, & t \text{ within treatment time } [0, R_T], \\ 0, & t \text{ after treatment} \end{cases} \tag{2.38}$$

we could solve the above system as follows [16]

$$
B(t) = \begin{cases} \frac{2\epsilon_{AB}\dot{D}(1-e^{-\epsilon_0 t})}{\epsilon_0+\epsilon_{BA}+(\epsilon_0-\epsilon_{BA})e^{-\epsilon_0 t}}, & 0 < t \le R_T \\\\ \frac{N_{PL}e^{-\epsilon_{BA}(t-T)}}{1+\frac{N_{PL}}{\epsilon}(1-e^{-\epsilon_{BA}(t-T)})}, & t > R_T \end{cases} \tag{2.39}
$$

$$
C(t) = \begin{cases} \epsilon_{AC}D + \epsilon \ln\left[\frac{2\epsilon_0}{\epsilon_0+\epsilon_{BA}+(\epsilon_0-\epsilon_{BA})e^{-\epsilon_0 t}}\right] \\\\ \quad + \frac{(\epsilon_0-\epsilon_{BA})^2 t}{4\epsilon_{BC}} - B(t), & 0 < t \le R_T \\\\ N_L + \frac{N_{PL}\left[1+\frac{N_{PL}}{\epsilon}\right](1-e^{-\epsilon_{BA}(t-T)})}{1+\frac{N_{PL}}{\epsilon}(1-e^{-\epsilon_{BA}(t-T)})} \\\\ \quad -\epsilon \ln\left[1+\frac{N_{PL}}{\epsilon}(1-e^{-\epsilon_{BA}(t-T)})\right], & t > R_T \end{cases} \tag{2.40}
$$

where $\epsilon_0 = \sqrt{\epsilon_{BA}^2 + 4\epsilon_{BC}\epsilon_{AB}\dot{D}}, \epsilon = \frac{\epsilon_{BA}}{\epsilon_{BC}}, N_{PL} = B(R_T)$ and $N_L = C(R_T)$. If we assume the number of lesions has Poisson distribution, the survival model has the form of

$$
\sigma(t) = e^{-(B(t)+C(t))}. \tag{2.41}
$$

At some time moment t after the treatment, that is, $t = R_T + t_r > R_T$, we have

$$
\begin{aligned} \sigma(t) &= e^{-\left(N_L+N_{PL}+\epsilon \ln\left[1+\frac{N_{PL}}{\epsilon}(1-e^{-\epsilon_{BA}t_r})\right]\right)} \\\\ &= e^{-(N_L+N_{PL})}\left[1+\frac{N_{PL}}{\epsilon}(1-e^{-\epsilon_{BA}t_r})\right]^{\epsilon}. \end{aligned} \tag{2.42}
$$

At the special case of high-dose rate $\dot{D} >> \frac{\epsilon_{BA}^2}{4\epsilon_{AB}\epsilon_{BC}}$, we have $\epsilon_0 \approx \sqrt{4\epsilon_{BC}\epsilon_{AB}\dot{D}}$ and $\epsilon_{BA} << \epsilon_0$. Therefore

$$
N_{PL} = B(R_T) = \frac{2\epsilon_{AB}\dot{D}(1-e^{-\epsilon_0 R_T})}{\epsilon_0+\epsilon_{BA}+(\epsilon_0-\epsilon_{BA})e^{-\epsilon_0 R_T}} \approx \epsilon_{AB}D.
$$

when $R_T << \frac{2}{\epsilon_0}$. Similarly, $N_L = C(R_T) \approx \epsilon_{AC}D$. Then the survival model is approximated by

$$
\sigma(t) = e^{-\left(\epsilon_{AB}+\epsilon_{AC}\right)D}\left[1+\frac{\epsilon_{AB}D}{\epsilon}(1-e^{-\epsilon_{BA}t_r})\right]^{\epsilon}. \tag{2.43}
$$

When it comes to the low dose at high-dose rate (for example, fractionated treatment), the second term in the power function is relatively

small, by ignoring the higher order terms, we have

$$
\begin{aligned}
-\ln \sigma(t) &= \left(\epsilon_{AC} + \epsilon_{AB}\right)D - \epsilon \ln \left[1 + \frac{\epsilon_{AB}D}{\epsilon}(1 - e^{-\epsilon_{BA}t_r})\right] \\
&\approx \left(\epsilon_{AC} + \epsilon_{AB}\right)D - \epsilon \frac{\epsilon_{AB}D}{\epsilon}(1 - e^{-\epsilon_{BA}t_r}) + \epsilon \frac{1}{2}\left(\frac{\epsilon_{AB}D}{\epsilon}(1 - e^{-\epsilon_{BA}t_r})\right)^2 \\
&= \left(\epsilon_{AC} + e^{-\epsilon_{BA}t_r}\epsilon_{AB}\right)D + \frac{1}{2\epsilon}\epsilon_{AB}^2(1 - e^{-\epsilon_{BA}t_r})^2 D^2.
\end{aligned}
$$

Therefore this special case of the LPL model $\sigma(t)$ is the LQ model with $\alpha = \epsilon_{AC} + \epsilon_{AB}e^{-\epsilon_{BA}t_r}, \beta = \frac{\epsilon_{AB}^2}{2\epsilon}(1 - e^{-\epsilon_{BA}t_r})^2$. These two parameters are also time-dependent.

It is worth mentioning that this model can also be used to derive the LQ model with Lea-Catcheside factor (see (2.47)), where the Lea-Catcheside factor is given by as (2.48) [19],[75]. In Dawson's derivation [19], she assumed the nonlinear term $\epsilon_{BC}B^2$ in (2.36) is negligible, Sachs *et al* [75] states that this is a reasonable assumption when the dose D is not too big, say $D < 5$ Gy.

Besides the four derivations of the LQ model we reviewed here, there are many more explanations of the LQ model in the literature. The latter two models, the RMR and LPL models can be thought of extensions of the LQ model which include a time factor explicitly. However, because of its simplicity and nice fitting of data, the LQ model has been widely accepted in this area. As Alpen [4] pointed out, the LQ model is adequate for the survival fraction larger than 10^{-3}, most of the clinical results are in this range. Therefore, in this thesis, we are mainly using the LQ model and its extension.

All the models derived above are for a single-dose radiation. In the next subsection, I will review variations of the LQ formula for the fractionated treatments and brachytherapy, as well as extensions to include regrowth into the LQ model.

2.2.3 Other Development of the LQ Models

Fractionated treatment does not give the total dose D to the patient at one time. It splits the dose D into n fractions of smaller dose d ($D = nd$) so that

the normal tissue will have a chance to repair during the intertreatment time. With the assumption that survival for each fraction is independent, (2.14) changes into

$$\sigma(D(n,d)) = \underbrace{\exp(-\alpha d - \beta d^2)\cdots\exp(-\alpha d - \beta d^2)}_{n} = \exp(-(\alpha + \beta d)D).$$

(2.44)

Equations (2.14) and (2.44) assume that there is no regrowth during treatment. However proliferation plays an important role when the treatment time is long compared to the tumor doubling time. Travis and Tucker [86] were the first to include a growth factor into the LQ model. By fitting mouse lung cancer data of Mah *et al* [57], they found the regrowth is exponential with parameter b, and the isoeffect curves E $(= -\ln S(D))$ are constant,

$$E = \beta D(\alpha/\beta + D/n) - bT,$$

(2.45)

where n is the number of fractions and T is the total treatment time. Some other scholars [56, 83, 98, 99] also study regrowth and they found there is a regrowth delay in clinical observations. Therefore by using a delay term in the exponent of the LQ model, we obtain an LQ model as a function of dose and time-delayed regrowth,

$$\sigma(D,t) = e^{-\alpha D - \beta D^2/n} e^{\frac{\ln(2)}{T_d}(t - t_k)}.$$

(2.46)

where $T_d = \ln(2)/b$ is the tumor doubling time and t_k is a time delay between the beginning of treatment and measurable re-growth of the tumor.

In brachytherapy, the model is modified using the Lea-Catcheside factor $G(t)$ [44]

$$\sigma(D) = e^{-\alpha D - \beta G(t) D^2}.$$

(2.47)

The Lea-Catchside factor describes the interaction of past radiation damage with the current damage. But the interaction probability decays exponentially with rate γ, the repair rate of the cells. The Lea-Catchside factor is usually written for time greater than end of the treatment time T $(t > T)$ as

$$G(t) = \frac{2}{D(t)^2} \int_{-\infty}^{\infty} \dot{D}(\tau) \int_{-\infty}^{\tau} e^{-\gamma(\tau - s)} \dot{D}(s)\, ds\, d\tau$$

or

$$G(t) = \frac{2}{D(t)^2} \int_{-\infty}^{t} \dot{D}(\tau) \int_{-\infty}^{\tau} e^{-\gamma(\tau - s)} \dot{D}(s) \, ds \, d\tau. \tag{2.48}$$

where $\dot{D}(t)$ is the dose rate, $D(t)$ is the cumulative dose. The Lea-Catchside factor has a clear physical derivation from the LPL model, where γ here is the linear repair rate ϵ_{BA} in the LPL model [19].

2.3 Hazard Function Related to LQ Models

This section is adapted from [31].

The number of cancer cells is normally modeled by differential equations. We can use the hazard function to represent the death caused by radiation in the differential equations. Based on the limitations of the target methods and the wide acceptance of the LQ model, here we only write down the hazard functions corresponding to the LQ models.

From the Survival Analysis in Statistic [3], the hazard function $h(t)$ describes the decay of survival fraction as

$$\begin{aligned} h(t) &= \lim_{\Delta t \to 0} \frac{Prob(\text{death in } [t, t + \Delta t])}{Prob(\text{survival in}[0, t])\Delta t} \\ &= \lim_{\Delta t \to 0} \frac{\sigma\left(D(t)\right) - \sigma\left(D(t + \Delta t)\right)}{\sigma\left(D(t)\right)\Delta t} = -\frac{1}{\sigma\left(D(t)\right)} \frac{d\sigma\left(D(t)\right)}{dt}. \end{aligned} \tag{2.49}$$

Therefore, the hazard function $h(t)$ has relation with the LQ survival fraction as

$$\frac{d\sigma(D(t))}{dt} = -h(t)\sigma(D(t)). \tag{2.50}$$

If the $\sigma(D)$ is given by the LQ model (2.14), the corresponding hazard function is

$$h_a(t) := (\alpha + 2\beta D(t))\dot{D}(t), \tag{2.51}$$

see also Zaider and Minerbo [101]. For the fractionated treatment, if we give n fractions of dose d, then total dose $D = nd$ and the hazard function corresponding to LQ model (2.44) should be

$$h_b(t) := (\alpha + \beta d)\dot{D}(t). \tag{2.52}$$

30

For the LQ model with Lea-Catchside factor, the hazard function will be

$$h_c(t) := \alpha \dot{D}(t) + \beta (G(t)D(t)^2)' = \left(\alpha + 2\beta \int_{-\infty}^{t} e^{-\gamma(t-s)} \dot{D}(s)ds \right) \dot{D}(t), \quad (2.53)$$

In [20], Dawson and Hillen derived a hazard function corresponding to their target model from first principles. It includes dose interaction within a window with width $\omega > 0$, that is $[t - \omega, t]$; we denote it as h_d:

$$h_d(t) := \left(\alpha + 2\beta \big(D(t) - D(t - \omega)\big) \right) \dot{D}(t), \quad (2.54)$$

The interaction window ω can be chosen as the time interval that DNA repair would happen. It is the reciprocal of the repair rate γ [84].

In more generality, we propose an effective interaction dose d_{eff}, which will include all the above hazard functions (2.51), (2.52),(2.53) and (2.54) into one framework:

$$h_{eff}(t) := (\alpha + \beta d_{eff}(t)) \, \dot{D}(t), \quad (2.55)$$

Therefore,

(a) $d_{eff}(t) = 2D(t)$ for Zaider-Minerbo's formula (2.51),

(b) $d_{eff}(t) = d$ for fractionated treatments (2.52),

(c) $d_{eff}(t) = 2 \int_{-\infty}^{t} e^{-\gamma(t-s)} \dot{D}(s)ds$ for the Lea-Catchside factor,

   and

(d) $d_{eff}(t) = 2(D(t) - D(t - \omega))$ for the finite interaction window.

The corresponding survival fractions to (2.55) are then

$$\sigma(D(t)) = \exp\left(-\int_0^t h_{eff}(s)ds \right) = \exp\left(-\alpha D(t) - \beta \int_0^t d_{eff}(s)\dot{D}(s))ds \right)$$
$$(2.56)$$

with each special case as

(a) $\sigma_a(D(t)) \; = \; \exp\left(-\alpha D(t) - \beta D^2(t) \right),$

(b) $\sigma_b(D(t)) \; = \; \exp\left(-(\alpha + \beta d)D(t) \right),$

(c) $\sigma_c(D(t)) \; = \; \exp\left(-\alpha D(t) - \beta G(t)D(t)^2 \right),$ with $G(t)$ from (2.48),

(d) $\sigma_d(D(t)) \; = \; \exp\left(-\alpha D(t) - \beta \int_0^t 2(D(s) - D(s - \omega))\dot{D}(s)ds \right).$

There are several interesting special cases:

Case 1 (c → a): If the repair rate γ in (2.55) (c) approaches 0, i.e. $\gamma \to 0$, then $d_{eff}(t) = 2D(t)$ and we obtain the Zaider-Minerbo formula as shown by (2.55) (a). We have the same approximation from (2.56) (c) to (2.56) (a) as $G(t) \to 1$ when $\gamma \to 0$.

This tells us that the approach (a) is useful if early lesions are not repaired and are always able to interact.

Case 2a (d → a): If the interaction window in (d) is large ($\omega \to \infty$), we have $D(t) - D(t - \omega) = D(t)$ using the fact that $D(-\infty) = 0$. Therefore d_{eff} is the same as that in (2.55) (a) and the survival fraction (2.56) (d) equals to (2.56) (a).

Hence once again we find that model (a) implicitly assumes that interactions of lesions induced by radiation are on a long time scale.

Case 2b (d → b): Let us compute (2.56) (d) for the fractionated treatment. We assume that the treatment length of each fraction is R_T and the interaction window $\omega = R_T$. Calculation tells us survival fraction σ_d is in agreement with the fractionated LQ model σ_b.

Denote $t_i, i = 1, \cdots, n$ as the beginning time of each fraction, therefore doses are delivered during the interval $[t_i, t_i + R_T], i = 1, \cdots, n$. We assume the dose d is given constantly in each fraction, that is, the dose rate is the step function as follows

$$\dot{D}(t) = \begin{cases} \frac{d}{R_T}, & t \in [t_i, t_i + R_T], \quad i = 1, \cdots, n \\ 0, & else \end{cases} \tag{2.57}$$

At a moment between the jth and the $j+1$th fraction, time t satisfies $t_j + R_T < t < t_{j+1}$ and the total dose is $D = jd$. Because of choice of $\dot{D}(t)$ in (2.57), the integral in the (2.56) (d) will equal to

$$\begin{aligned} \int_0^t 2\left(D(s) - D(s - \omega)\right) \dot{D}(s) ds &= 2 \sum_{i=1}^{j} \int_{t_i}^{t_i + R_T} \left(D(s) - D(s - \omega)\right) \frac{d}{R_T} ds \\ &= 2 \sum_{i=1}^{j} \int_{t_i}^{t_i + R_T} \frac{d}{R_T}(s - t_i) \frac{d}{R_T} ds \\ &= \left(\frac{d}{R_T}\right)^2 \sum_{i=1}^{j} R_T^2 = jd^2 = dD. \end{aligned} \tag{2.58}$$

Therefore, after the j-th fraction, the survival fraction σ_d equals to

$$\sigma_d(D(t)) = \exp\left(-\alpha D(t) - \beta dD\right) = \exp\left(-(\alpha + \beta d)D(t)\right)$$

which is the same as the survival fraction given by σ_b. That is to say, when the interaction window $\omega = R_T$ and the time t is not the moment to deliver the dose, the survival fraction σ_d is consistent to the σ_b.

However, formula (b) in (2.55) and (2.56) can only be used after finishing of a fractionated treatments. Formula (d) in (2.55) and (2.56) can also be used even within the process of dose delivery, i.e. $t \in [t_j, t_j + R_T]$. Denote $D_{j-1} = (j-1)d$ as the total dose after the first $j - 1$ fractions. When $t \in [t_j, t_j + R_T]$, besides the delivered dose in the first $j-1$ fractions, there is extra dose $\leq d$ in current j-th fraction. Let $D_{curr} = \frac{d}{R_T}(t - t_j)$ be the dose used in the jth fraction up to time t,

$$
\begin{aligned}
& \int_0^t 2\left(D(s) - D(s - \omega)\right)\dot{D}(s)ds \\
=\ & 2\sum_{i=1}^{j-1}\int_{t_i}^{t_i + R_T}\left(D(s) - D(s - \omega)\right)\frac{d}{R_T}ds + 2\int_{t_j}^t \left(D(s) - D(s - \omega)\right)\frac{d}{R_T}ds \\
=\ & \left(\frac{d}{R_T}\right)^2\sum_{i=1}^{j-1}R_T^2 + 2\int_{t_j}^t \frac{d}{R_T}(s - t_j)\frac{d}{R_T}ds \\
=\ & (j-1)d^2 + \left(\frac{d}{R_T}\right)^2(t - t_j)^2 \\
=\ & dD_{j-1} + D_{curr}^2. \tag{2.59}
\end{aligned}
$$

plugging into (2.56) (d), we find that during the dose delivery ($t \in [t_j, t_j + R_T]$), the cell survival is a combination of fractionated LQ model (2.44) and standard LQ model (2.14) as follows,

$$\sigma_d(D(t)) = \exp\left(-\alpha D_{j-1} - \beta dD_{j-1}\right)\exp\left(-(\alpha D_{curr} + \beta D_{curr}^2)\right)$$

Case 2c (d $\approx$ c): Notice that $D(t) = 0$ for $t < 0$, the effective dose (2.55) (c) could be calculated by integration by parts,

$$d_{eff}(t) = 2\,e^{-\gamma(t-s)}D(s)\big|_0^t - 2\gamma\int_0^t e^{-\gamma(t-s)}D(s)ds = 2D(t) - 2\gamma\int_0^t e^{-\gamma(t-s)}D(s)ds. \tag{2.60}$$

In [31], we proved that for brachytherapy, when the repair rate γ is the reciprocal of interaction interval ω, the difference between (2.55) (d) and (c) are negligible. Therefore, for brachytherapy, we could use the easier calculated form (2.55) (d) to calculate the hazard function.

In the following chapters, I will use the general hazard function (2.55) in my differential equations. In particular, d_{eff} (2.55) (a) and (b) will be used for d_{eff} in a single-dose treatment and fractionated treatment or brachytherapy, respectively. If the time is within the process of dose delivery, d_{eff} (d) will be used.

Chapter 3

Poisson TCP Models Based on Cell Population Models

The tumor control probability (TCP) is defined as the probability of zero tumor cells. In this chapter, we will give an extension of the Poissonian TCP (1.4) to include cell population dynamics. The cell population models are ordinary differential equations (ODE) describing the evolution of the mean number of surviving cells $N(t)$.

$$\frac{dN(t)}{dt} = [\mu - h(t)]\, N(t), \quad N(0) = N_0, \tag{3.1}$$

where μ is the net linear proliferation rate and $h(t)$ is the hazard function describing death due to the radiation, which is in the form of (2.56) and relates to the cell survival by $\sigma(D) = e^{-\int_0^t h(s)ds}$.

Using the mean number of cancer cells $N(t)$ as an estimator of the mean λ of a Poisson distribution (1.3), then we have the Poisson TCP as

$$TCP_P(t) = p(X = 0) = e^{-\lambda} = e^{-N(t)} = \exp\{-N_0\sigma(D)e^{\mu t}\}. \tag{3.2}$$

It is the original Poisson TCP (1.4) with regrowth factor $e^{\mu t}$. Equation (3.1) only considers the linear regrowth. Wheldon [95] and Usher [89] extended the Poisson TCP formula for two saturation growth models, the logistic model and the Gompertzian model. Their formulae are for uniform treatment schedules (time between two fractions of treatments are the same). In this chapter, we

generalize Wheldon's and Usher's method to non-uniform clinical treatments and obtain explicit formula for the TCP.

In what follows, I will first review the tumor regrowth model without radiation in Section 3.1 and Usher's TCP iterative derivation for uniform treatment in Subsection 3.2.1; In Subsection 3.2.2, I will prove that for a short dose delivery time per fraction, the explicit formula derived in Subsection 3.2.1 is the approximation of the TCP based on the cell population model. I derive an explicit TCP for non-uniform treatments by iterative derivation in Section 3.3 and in the last section I will compute TCP values for realistic clinical treatments.

3.1 Tumor Growth Laws

Suppose $N(t)$ denotes the mean number of tumor cells at time t. Three most often used ODEs for unirradiated tumor growth are the exponential, the Gompertzian and the logistic growth models.

- Exponential growth model

$$\frac{dN}{dt} = \mu N, \tag{3.3}$$

  where μ is the growth rate. This model is used when the nutrients and space for cancer cells are unlimited on the timescale of interest. This is an unbounded model. The model no longer applies if the clonogenic cell growth rate decreases as the tumour grows because of the limited resources or other growth inhibiting process.

  For large populations, the growth rate decreases to zero due to limited resources, and a parameter θ is used as carrying capacity of the environment. The following two models are self-limited, as we can see from Figure 3.1.

- Gompertzian growth model

$$\frac{dN}{dt} = -\mu N \ln(N/\theta). \tag{3.4}$$
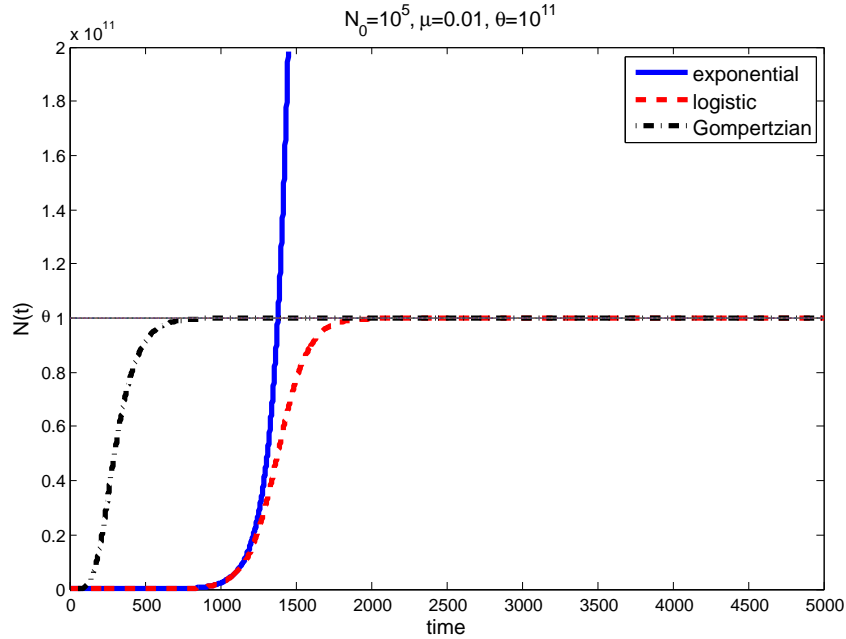
Figure 3.1: **Comparison of three growth models: exponential (solid), logistic (dashed) and Gompertzian (dash-dot line).** The number of tumor cells $N(t)$ is plotted as a function of time. The initial tumor cell number is $N_0 = 10^5$, the growth rate is $\mu = 0.01$ day^{-1} and the carrying capacity is $\theta = 10^{11}$.

- Verhulst (logistic) growth model

$$\frac{dN}{dt} = \mu N(1 - N/\theta). \tag{3.5}$$

In Figure 3.1, we show the number of tumor cells $N(t)$ plotted as a function of time for exponential (solid), logistic (dashed) and Gompertzian (dash-dot) growth. The initial tumor cell number is $N_0 = 10^5$, the growth rate is $\mu = 0.01$ day^{-1} and the carrying capacity is $\theta = 10^{11}$. We can see the exponential growth will grow unlimited, logistic and Gompertzian growth will be saturated by the environment (denoted by the carrying capacity θ in the model). Notice that initially the logistic model grows exponentially before going into saturation. The Gompertzian model, however, initially grows much quicker than the exponential growth.

The above three models are all special cases of a so called Richard'd differential equation or generalized logistic differential equation,

$$\frac{dN}{dt} = \frac{\mu N}{a}\left[1 - \left(\frac{N}{\theta}\right)^a\right]. \tag{3.6}$$

Where the parameters a (≥ 0), μ, θ (> 0) are determined from the growth characteristics of the cells. We can easily see that exponential growth model arises when $a \to 1$ and $\theta \to \infty$. The Gompertzian growth model follows when $a \to 0$ and the logistic growth model follows when $a \to 1$. Equation (3.6) is a Bernoulli Equation, its solution is

$$N(t) = \frac{N(0)}{\left[\left(\frac{N(0)}{\theta}\right)^a + e^{-\mu t}\left(1 - \left(\frac{N(0)}{\theta}\right)^a\right)\right]^{1/a}}. \tag{3.7}$$

We will use formula (3.7) to derive the TCP formula for uniform and non-uniform treatment in the following subsections.

3.2 Poisson TCP Model for Uniform Treatment

3.2.1 Iterative Derivation for Uniform Treatment [89]

Uniform treatments refer to those fractionated treatments with constant intertreatment time T (days). We write a uniform treatment as the tuple (d, T, n), meaning n fractions of treatments with dose d are separated by a time interval T. Let us review the model of Usher [89] in this subsection. Usher split time into two parts: the treatment time and the intertreatment time. He assumed that the treatment time is so small compared to the intertreatment time T that the regrowth during treatment is not important. Therefore, he considered a series of uncoupled events with period of 2: radiation, growth, radiation, growth, $\cdots$, radiation.

Denote by N_i, N_i' the number of cancer cells before and after the i-th radiation, respectively. For convenience, he assumed $N(0) = N_1$. After n fractions, the

number of cancer cell changes as:

$$N_1 \xrightarrow[rad]{\sigma} N_1' \xrightarrow[growth]{T} N_2 \xrightarrow[rad]{\sigma} N_2' \xrightarrow[growth]{T} \quad \cdots \quad \xrightarrow[growth]{T} N_n \xrightarrow[rad]{\sigma} N_n'$$

The 'rad' below the arrow stands for radiation and σ above the arrow is the corresponding survival fraction. The 'growth' is for regrowth and T for the growth time between fractions. From Chapter 2, we know

$$N_i' = \sigma(d)N_i, \qquad i = 1, 2, \cdots, n. \tag{3.8}$$

where $\sigma(d)$ is the survival fraction model introduced in Chapter 2. One example for the surviving fraction is the linear quadratic (LQ) model in (2.14).

Lemma 3.2.1. N_{i+1} and N_i have the following relations

1.

$$N_{i+1} = \frac{N_i'}{\left[\left(\frac{N_i'}{\theta}\right)^a + e^{-\mu T}\left(1 - \left(\frac{N_i'}{\theta}\right)^a\right)\right]^{1/a}}, \qquad i = 1, 2, \cdots, n. \tag{3.9}$$

2.

$$N_{i+1} = \frac{N_i}{(AN_i^a + B)^{1/a}}, \qquad i = 1, 2, \cdots, N \tag{3.10}$$

where $A = \left(1 - e^{-\mu T}\right)/\theta^a, B = e^{-\mu T}/\sigma^a$. According to Usher, $\sigma = \sigma(d)$ is in the form of Multitarget Single-hit (MTSH) model (2.11) or the LQ model (2.44).

Proof. 1. N_{i+1} is the i-th T days growth with initial cell number N_i', (3.9) is a direct result from formula (3.7).

2. From formula (3.8) and (3.9), we have

$$\begin{aligned}
N_{i+1} &= \frac{N_i'}{\left[\left(\frac{N_i'}{\theta}\right)^a + e^{-\mu T}\left(1 - \left(\frac{N_i'}{\theta}\right)^a\right)\right]^{1/a}} \\
&= \frac{\sigma N_i}{\left[\left(\frac{\sigma N_i}{\theta}\right)^a + e^{-\mu T}\left(1 - \left(\frac{\sigma N_i}{\theta}\right)^a\right)\right]^{1/a}} \\
&= \frac{N_i}{(AN_i^a + B)^{1/a}}.
\end{aligned}$$

where $A = (1 - e^{-\mu T})/\theta^a, B = e^{-\mu T}/\sigma^a$. $\qquad\square$

Then by induction, we find the number of cancer cells just before the $n - th$ treatment as follows

$$
\begin{aligned}
N_n &= \frac{N_{n-1}}{(AN_{n-1}^a + B)^{1/a}} = \frac{N_{n-2}}{\left[(A + AB)N_{n-2}^a + B^2\right]^{1/a}} \\
&= \cdots = \\
&= \frac{N_1}{\left[A\frac{1-B^{n-1}}{1-B}N_1^a + B^{n-1}\right]^{1/a}}
\end{aligned}
\tag{3.11}
$$

So after n fractions of radiation, the mean tumor cell number and the Poisson TCP will be

$$
N_n' = \sigma(d) * N_n, \quad TCP_p = e^{-N_n'}.
\tag{3.12}
$$

The Poisson TCP formula could be very complicated, in order to simplify our formula, we instead think of another measurement of the effect of each treatment schedule, the *total survival fraction* (TSF)

$$
TSF_n = N_n'/N_1.
\tag{3.13}
$$

The TSF is related to the Poisson TCP as

$$
TCP_P = e^{-N_1 * TSF_n}.
\tag{3.14}
$$

The smaller the total survival fraction, the larger the Poison TCP (3.14) is and therefore the better the treatment.

Theorem 3.2.2. *(see Usher [89]) The total survival fraction of cancer cells after the $n - th$ treatment for the three growth laws are*

$$
\begin{aligned}
TSF_{n,e}(d,T,n) &= \sigma^n e^{\mu(n-1)T}, \tag{3.15} \\
TSF_{n,g}(d,T,n) &= N_1^{-1} \exp\left\{ \ln(\sigma)\frac{1 - e^{-\mu nT}}{1 - e^{\mu T}} + \ln(\theta)(1 - e^{-\mu(n-1)T}) \right. \\
&\qquad\qquad \left. + \ln(N_1)e^{-\mu(n-1)T} \right\}, \tag{3.16} \\
TSF_{n,l}(d,T,n) &= \frac{\sigma}{A\frac{1-B^{n-1}}{1-B}N_1 + B^{n-1}}, \tag{3.17}
\end{aligned}
$$

where $A = \frac{1-e^{-\mu T}}{\theta}, B = \frac{e^{-\mu T}}{\sigma}$ and we use the additional subscript index e, g, l to denote the exponential, Gompertzian and logistic growth, respectively. Dose per fraction d is included in cell survival model σ, Usher considered both MTSH (2.11) and LQ survival model (2.44).

Proof. Formula (3.13) can be obtained by (3.11) and (3.8), then (3.15)-(3.17) can be received by taking different limits on a and θ. □
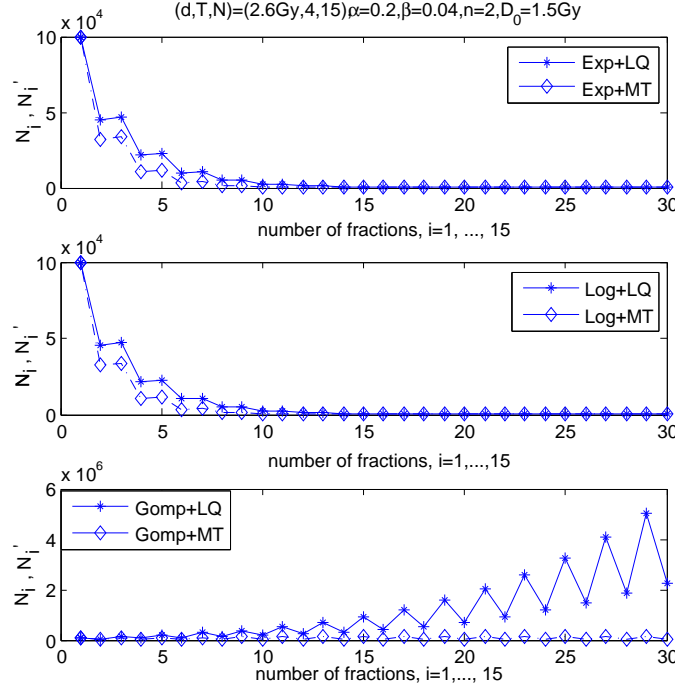
Figure 3.2: **Sequences of Number of cancer cells N_i, N_i' under one treatment.** The treatment schedule is $(d,\ T,\ n)$=(2.6 Gy, 4 days, 15 frs). Parameters for regrowth are: $\mu = 0.01$ day^{-1}, $N_0 = 10^5, \theta = N_0 * e^{28.5}$ and for cell survival model are $n = 2, D_0 = 1.5Gy, \alpha = 0.2Gy^{-1}, \beta = 0.04Gy^{-2}$. The top, middle and bottom graphs show the number of cancer cells as function of time for exponential, logistic and Gompertzian growth, respectively. In each graph, the dashed line with stars are for LQ surviving fraction and the solid lines with diamonds are for MTSH survival fraction (MT in the graph).

In Figure 3.2 we plot the sequence of $N_1, N_1', \cdots, N_n, N_n'$ by choosing the growth law parameters as $\mu = 0.01$ day^{-1}, $N_0 = 10^5, \theta = N_0 \times e^{28.5}$. The schedule is chosen as $(d,\ T,\ n)$=(2.6 Gy, 4 days, 15 frs). We find that numbers of tumor cells with the exponential growth and logistic growth decrease quickly for this schedule, but for the Gompertzian growth with the MTSH cell survival, the number of cancer cells increases rather than decreases.

We can find an explanation for the behavior of the Gompertzian model by looking at the mathematical properties of equation (3.4). The right hand side of equation (3.4) is not Lipschitz continuous at 0. Hence the cancer growth rate is over proportionally large for N close to 0, leading to instantaneous tumor regrowth. It should be noted that the Gompertzian model has been derived in the context of tumor growth experiments and it is quite successful in predicting tumor sizes [94],[81]. However, the model was not designed for small tumors, where the singularity at 0 becomes dominating. Since we are interested in small tumor cell numbers as a result of radiation treatment, we are skeptical in using the Gompertzian model. We believe that it overestimates the growth rate close to 0. Therefore, for the following content, we will just focus on exponential and logistic growth laws.

3.2.2 Poisson TCP Derived from Continuous Population Models

The above derivation gives an explicit formula, however, time was split into two separate series of intervals: radiation and regrowth time. In this subsection, we are going to think of the time as a continuous variable.

With radiation included, the number of tumor cells can be governed by

$$\frac{d\tilde{N}(t)}{dt} = \left[\frac{\mu}{a}\left(1 - (\frac{\tilde{N}}{\theta})^a\right) - h(t)\right]\tilde{N}(t), \quad \tilde{N}(0) = N_0. \tag{3.18}$$

where μ, a, θ are parameters for the growth law and $h(t)$ is the hazard function describing death due to radiation, which is normally related to cell survival model $\sigma(D)$ by

$$\sigma(D(t)) = \exp\left(-\int_0^t h(s)ds\right). \tag{3.19}$$

Equation (3.18) is still a Bernoulli type differential equation $\frac{dy}{dt} + p(t)y = q(t)y^n$ with $p(t) = h(t) - \frac{\mu}{a}$, $q(t) = -\frac{\mu}{a\theta^a}$ and $n = a + 1$. Its solution is

$$\tilde{N}(t) = \left[\frac{N_0^a e^{a\int_0^t \frac{\mu}{a} - h(s)ds}}{1 + N_0^a \frac{\mu}{\theta^a}\int_0^t e^{a\int_0^\tau \frac{\mu}{a} - h(s)ds}d\tau}\right]^{1/a}. \tag{3.20}$$

Theorem 3.2.3. *Assume there are n fractions of dose d with the intertreatment time T. Death in each fraction is independent of the other fractions. Let R_T denote the time that radiation is applied in a single fraction.*

*(1). (**Exponential growth**) For exponential growth tumor, i.e., $a = 1, \theta \to \infty$ in (3.18), when taking the limit of $R_T \to 0$, we have $t = (n-1)(R_T + T) \to (n-1)T$ and the continuous formula (3.20) coincides with the discrete case from Subsection 3.2.1 and*

$$\frac{\tilde{N}(t)}{N_0} \xrightarrow{R_T \to 0} TSF_{n,e} \quad from \quad (3.15),$$

*(2). (**Logistic growth**) For logistic growth tumor, i.e., $a \to 1$, when taking the limit of $R_T \to 0$, the discrete and continuous formulas coincide and*

$$\frac{\tilde{N}(t)}{N_0} \xrightarrow{R_T \to 0} TSF_{n,l} \quad in \quad (3.17). \tag{3.21}$$

Proof. (1). By taking limit of $a \to 1, \theta \to \infty$ in (3.20), we have

$$\tilde{N}(t) = N_0 e^{\int_0^t \mu - h(s)ds} = N_0 e^{\mu t} \sigma(D), \tag{3.22}$$

where we use (3.19) in the last equality. Because death in each fraction is independent of the other fractions, we could use fractionated LQ model (2.44) for our cell survival, i.e.,

$$\sigma(D) = \sigma(d)^n := \sigma^n. \tag{3.23}$$

Plugging (3.23) into (3.22) and divide N_0 on both side, we have (3.15) when $t \to (n-1)T$.

(2). When $a \to 1$, (3.20) is

$$\tilde{N}(t) = \frac{N_0 e^{\int_0^t \mu - h(s)ds}}{1 + N_0 \frac{\mu}{\theta} \int_0^t e^{\int_0^\tau \mu - h(s)ds} d\tau} = \frac{N_0 e^{\mu t} \sigma(D(t))}{1 + N_0 \frac{\mu}{\theta} \int_0^t e^{\mu \tau} \sigma(D(\tau)) d\tau}. \tag{3.24}$$

Let $N_0 = N_1$, by using (3.17) we have

$$N(t) = TSF_{n,l} * N_0 = \frac{N_0 \sigma}{A \frac{1-B^{n-1}}{1-B} N_0 + B^{n-1}} = \frac{N_0 \sigma^n e^{\mu(n-1)T}}{1 + \frac{e^{\mu T}-1}{\theta} \frac{e^{\mu(n-1)T \sigma^n}-\sigma}{\sigma e^{\mu T}-\sigma} N_0}. \tag{3.25}$$

When $t = (n-1)(T + R_T) \to (n-1)T$, $\sigma(D) = \sigma^n$, (3.24) and (3.25) have the same numerator, but (3.24) differs from (3.25) by the integral term in the denominator.

Assume each treatment happened at $T_i, i = 1, 2, \cdots, n$, i.e., $T_i = (i-1)(R_T + T)$. Therefore if we split the time into treatment time and intertreatment time, the integral in (3.24) would be written as

$$\int_0^t e^{\mu\tau}\sigma(D(\tau))d\tau = \underbrace{\sum_{i=1}^n \int_{T_i}^{T_i+R_T} e^{\mu\tau}\sigma(D(\tau))d\tau}_{\mathcal{A}} + \underbrace{\sum_{i=1}^{n-1} \int_{T_i+R_T}^{T_{i+1}} e^{\mu\tau}\sigma(D(\tau))d\tau}_{\mathcal{B}}.$$

$$(3.26)$$

Notice that when $\tau \in [T_i + R_T, T_{i+1}]$, $\sigma(D(\tau)) = \sigma^i$, therefore part $\mathcal{B}$ can be calculated by

$$
\begin{aligned}
\sum_{i=1}^{n-1} \int_{T_i+R_T}^{T_{i+1}} e^{\mu\tau}\sigma(D(\tau))d\tau &= \sum_{i=1}^{n-1}\sigma^i \int_{T_i+R_T}^{T_{i+1}} e^{\mu\tau}d\tau \\
&= \frac{1}{\mu}\sum_{i=1}^{n-1}\sigma^i \left(e^{\mu(T_{i+1})} - e^{\mu(T_i+R_T)}\right) \\
&= \frac{1}{\mu}\sum_{i=1}^{n-1}\sigma^i \left(e^{\mu i(T+R_T)} - e^{\mu(i-1)(T+R_T)+\mu R_T}\right) \\
&= \frac{1}{\mu}\sum_{i=1}^{n-1}\sigma^i e^{\mu(i-1)(T+R_T)}e^{\mu R_T}\left(e^{\mu T} - 1\right) \\
&= \frac{(e^{\mu T}-1)e^{\mu R_T}\sigma}{\mu}\sum_{i=1}^{n-1}\sigma^{i-1}\left(e^{\mu(i-1)(T+R_T)}\right) \\
&= \frac{(e^{\mu T}-1)e^{\mu R_T}\sigma}{\mu}\frac{1-\left(\sigma e^{\mu(T+R_T)}\right)^{n-1}}{1-\sigma e^{\mu(T+R_T)}}
\end{aligned}
$$

When $R_T \to 0$ as what we assumed in the derivation of (3.17), the above equation has the following approximation

$$\sum_{i=1}^{n-1} \int_{T_i+R_T}^{T_{i+1}} e^{\mu\tau}\sigma(D(\tau))d\tau \to \frac{(e^{\mu T}-1)\sigma}{\mu}\frac{1-(\sigma e^{\mu T})^{n-1}}{1-\sigma e^{\mu T}}. \qquad (3.27)$$

The integrand in the part $\mathcal{A}$ of (3.26) is bounded, because $\sigma^i \leq \sigma(D(\tau)) \leq 1$ when $\tau \in [T_i, T_i + R_T]$, we have

$$e^{\mu\tau}\sigma^i \leq e^{\mu\tau}\sigma(D(\tau)) \leq e^{\mu\tau}.$$

Therefore when $R_T \to 0$, each integrand approaches 0 and thereafter part $\mathcal{A}$ of (3.26) approaches 0 as well. Hence, (3.24) changes into the following when $R_T \to 0$

$$\tilde{N}(t) \to \frac{N_0 e^{\mu(n-1)T}\sigma^n}{1 + N_0 \frac{\mu}{\theta}\frac{(e^{\mu T}-1)\sigma}{\mu}\frac{1-(\sigma e^{\mu T})^{n-1}}{1-\sigma e^{\mu T}}} = \frac{N_0^a e^{\mu(n-1)T}\sigma^n}{1 + N_0\frac{(e^{\mu T}-1)}{\theta}\frac{\sigma^n e^{\mu(n-1)T}-\sigma}{\sigma e^{\mu T}-1}}.$$

$$(3.28)$$

which is exactly the same as (3.25).

$\square$

That is to say, when the dose delivery time R_T for a single fraction is small, we could use the iterative method to derive the Poisson TCP models. Therefore, I will use the iterative method to derive the Poisson TCP model for non-uniform treatments.

3.3 TCP Formula for Non-uniform treatment

In clinical practice, radiotherapy schedules normally have a break during the weekend. Yurtseven [100] summarized ten clinical treatment schedules in her thesis, where she extended or cut some treatments to make the total dose uniform to 72 Gy. Here we update her table by newly reported protocols with no extension or truncation in Table 3.1. The schedules labeled by capital letters from 'A' to 'E' are known as *standard treatments*, given one fraction per day, while the lower case letters from 'a' to 'e' are the corresponding *hyperfractionated schedules*, given half the radiation dose twice per day with a 6 hour break in between.

Obviously the schedules have different intertreatment times for weekdays and weekends. Suppose we have p days with radiation each week. For standard treatment, there are two values for intertreatment time, i.e, $T = (T_1, T_2)$, where $T_1 = 1$ day for weekdays and $T_2 = 7 - p + 1$ for weekends. For hyperfractionation treatment, we have $T = (T_1, T_2, T_3)$ with $T_1 = 1/4, T_2 = 3/4$ for weekdays and $T_3 = 7 - p + 3/4$ for weekends. In this section, we extend the previous TSF calculations to non-uniform treatments.

Protocol	Reference	Dose/fx.(Gy)	days/week	T-days	fx./day	T-dose
A	[74]	2	5	53	once	78
B	[28]	2	5	47	once	70
C	[1]	3	5	26	once	60
D	Corresponding to 'd'	2.4	5	44	once	76.8
E	[50]	4.3	5	16	once	51.6
a	Corresponding to 'A'	1	5	53	twice	78
b	Corresponding to 'B'	1	5	47	twice	70
c	Corresponding to 'C'	1.5	5	26	twice	60
d	[90]	1.2	5	44	twice	76.8
e	Corresponding to 'E'	2.15	5	16	twice	51.6

Table 3.1: **Ten treatment schedules.** The protocols labeled by capital letters are known as *standard treatment*, given once per day; the protocols labeled by lower case letters are *hyperfractionated*, i.e. given twice per day. The only change we made from the cited report is the hyperfractionation protocol 'd' and its corresponding standard treatment 'D'[90]. The paper mentioned a total dose exceeded 72 Gray are applied, here we choose total dose of 76.8 Gray. 'T-'in columns 'T-day' and 'T-dose' means total, 'fx' in columns 'Dose/fx.(Gy)' and 'fx./day' means fraction.

Note that we do not apply radiation every day. The day on which the i-th radiation is given is not the same as the i-th day since the beginning of the treatment. Here we are tracking the days that doses are delivered. Because there are p days with radiation each week, the i-th radiation can be written as

$$i = kp + q, \quad 1 \leq q \leq p, \quad k = 0, 1, 2 \cdots$$

that means it is the q-th treatment in week $k+1$. Once again we denote N_i, N_i' the number of cancer cells before and after the $i - th$ radiation, respectively. In what follows we study standard treatment '$A - E$' with one treatment per day on weekdays in detail. Denote N_1 the initial number of cancer cells before the first treatment, N_{kp+1} the number of cancer cells before the first treatment of week $k + 1$, and N_{kp}' the number of cancer cells after the last treatment of k-th week. Their relations are

$$N_1 \xrightarrow[1^{st} \ week]{\sigma, T_1} N'_p \xrightarrow[growth]{T_2} N_{p+1} \xrightarrow[2^{nd} \ week]{\sigma, T_1} N'_{2p} \xrightarrow[\cdots]{\sigma, T_1, T_2} N_{kp+1} \xrightarrow[last \ week]{\sigma, T_1} N'_{kp+q}$$

Lemma 3.3.1. *1. Denote $A_1 = (1 - e^{-\mu T_1})/\theta^a$, $B_1 = e^{-\mu T_1}/\sigma^a$, the number of cancer cells on days in the same week have the following equation*

$$N_{kp+q} = \frac{N_{kp+1}}{\left[A_1 \frac{1 - B_1^{q-1}}{1 - B1} N_{kp+1}^a + B_1^{q-1} \right]^{1/a}}, 1 < q \le p. \qquad (3.29)$$

2. Denote $A_2 = (1 - e^{-\mu T_2})/\theta^a$, $B_2 = e^{-\mu T_2}/\sigma^a$ and $C = A_2 + A_1 B_2 \frac{1 - B_1^{p-1}}{1 - B_1}$, $\Gamma = B_1^{p-1} B_2$, the number of cancer cells on days that cross the weekend have the following relation

$$N_{kp+1} = \frac{N_{kp}}{\left[A_2 N_{kp}^a + B_2 \right]^{1/a}} = \frac{N_{(k-1)p+1}}{\left[C N_{(k-1)p+1}^a + \Gamma \right]^{1/a}}. \qquad (3.30)$$

3. The first day of the last week has relation with the initial tumor cell number as

$$N_{kp+1} = \frac{N_1}{\left[C \frac{1 - \Gamma^k}{1 - \Gamma} N_1^a + \Gamma^k \right]^{1/a}}. \qquad (3.31)$$

where C, Γ are the same as that in case 2.

4. Before the last fraction ($i = kp + q$), the tumor cells number N_i has relation with N_1

$$N_{kp+q} = \frac{N_1}{\left[(A_1 \frac{1 - B_1^{q-1}}{1 - B_1} + C B_1^{q-1} \frac{1 - \Gamma^k}{1 - \Gamma}) N_1^a + \Gamma^k B_1^{q-1} \right]^{1/a}}. \qquad (3.32)$$

where $A_i, B_i, i = 1, 2$ and C, Γ are the same as that in case 1 and 2.

Proof. 1. During the weekdays of one week, the intertreatment time remains the same as T_1, so (3.29) can be obtained by using (3.11) with intertreatment time T_1.

2. The first equation in (3.30) can be obtained by using (3.10) directly,

$$
\begin{aligned}
N_{kp+1} &= \frac{N_{kp}}{\left[A_2 N_{kp}^a + B_2\right]^{1/a}} = \frac{N_{(k-1)p+p}}{\left[A_2 N_{(k-1)p+p}^a + B_2\right]^{1/a}} \\[2mm]
&= \frac{\dfrac{N_{(k-1)p+1}}{\left[A_1 \frac{1-B_1^{p-1}}{1-B_1} N_{(k-1)p+1}^a + B_1^{p-1}\right]^{1/a}}}{\left[\dfrac{A_2 N_{(k-1)p+1}^a}{A_1 \frac{1-B_1^{p-1}}{1-B_1} N_{(k-1)p+1}^a + B_1^{p-1}} + B_2\right]^{1/a}} \\[2mm]
&= \frac{N_{(k-1)p+1}}{\left[A_2 N_{(k-1)p+1}^a + B_2\left(A_1 \frac{1-B_1^{p-1}}{1-B_1} N_{(k-1)p+1}^a + B_1^{p-1}\right)\right]^{1/a}} \\[2mm]
&= \frac{N_{(k-1)p+1}}{\left[C N_{(k-1)p+1}^a + \Gamma\right]^{1/a}}.
\end{aligned}
$$

where in the second row we use equation (3.29) and $C = A_2 + A_1 B_2 \frac{1-B_1^{p-1}}{1-B_1}$ and $\Gamma = B_1^{p-1} B_2$.

3. By induction and (3.30), we have

$$
\begin{aligned}
N_{kp+1} &= \frac{N_{(k-1)p+1}}{\left[C N_{(k-1)p+1}^a + \Gamma\right]^{1/a}} \\[2mm]
&= \frac{N_{(k-2)p+1}}{\left[(C + C\Gamma) N_{(k-2)p+1}^a + \Gamma^2\right]^{1/a}} \\[2mm]
&= \cdots = \frac{N_1}{\left[C \frac{1-\Gamma^k}{1-\Gamma} N_1^a + \Gamma^k\right]^{1/a}}.
\end{aligned}
$$

4. Equation (3.32) can be easily obtained by (3.29) and (3.31)

$$
\begin{aligned}
N_{kp+q} &= \frac{N_{kp+1}}{\left[A_1 \frac{1-B_1^{q-1}}{1-B_1} N_{kp+1}^a + B_1^{q-1}\right]^{1/a}} \\[2mm]
&= \frac{N_1}{\left[(A_1 \frac{1-B_1^{q-1}}{1-B_1} + C B_1^{q-1} \frac{1-\Gamma^k}{1-\Gamma}) N_1^a + \Gamma^k B_1^{q-1}\right]^{1/a}}.
\end{aligned}
$$

where we use (3.29) in the first equation and (3.31) in the second one. $\qquad\square$

Similar to the case of uniform treatment, the total survival fraction can be calculated explicitly

Theorem 3.3.2. *For a standard treatment given by $(d, (T_1, T_2), i)$ $(i = kp+q)$, the total survival fraction for exponential and logistic growth models are*

$$TSF_{i,\,e}(d, T, i) \;=\; \sigma^i e^{\mu((i-k-1)T_1 + kT_2)}, \tag{3.33}$$

$$TSF_{i,\,l}(d, T, i) \;=\; \sigma \left[A_1 \frac{1 - B_1^{q-1}}{1 - B_1} N_1 + \left(A_2 + A_1 B_2 \frac{1 - B_1^{p-1}}{1 - B_1} \right) B_1^{q-1} \right.$$
$$\left. \frac{1 - (B_1^{p-1} B_2)^k}{1 - B_1^{p-1} B_2} N_1 + B_1^{i-k-1} B_2^k \right]^{-1}, \tag{3.34}$$

where $A_i = (1 - e^{-\mu T_i})/\theta$, $B_i = e^{-\mu T_i}/\sigma$, $i = 1, 2$.

It is obvious that when $T_1 = T_2 = T$, (3.33) goes back to (3.15) if $i = n$. For (3.34), it is not hard to verify that it is the same as (3.17) when $T_1 = T_2 = T$.

$$A_1 \frac{1 - B_1^{q-1}}{1 - B_1} + \left(A_2 + A_1 B_2 \frac{1 - B_1^{p-1}}{1 - B_1} \right) B_1^{q-1} \frac{1 - (B_1^{p-1} B_2)^k}{1 - B_1^{p-1} B_2}$$
$$= A_1 \frac{1 - B_1^{q-1}}{1 - B_1} + \left(A_1 + A_1 B_1 \frac{1 - B_1^{p-1}}{1 - B_1} \right) B_1^{q-1} \frac{1 - (B_1^{p-1} B_1)^k}{1 - B_1^{p-1} B_1}$$
$$= A_1 \frac{1 - B_1^{q-1}}{1 - B_1} + A_1 \left(1 + B_1 \frac{1 - B_1^{p-1}}{1 - B_1} \right) B_1^{q-1} \frac{1 - B_1^{pk}}{1 - B_1^p}$$
$$= A_1 \frac{1 - B_1^{q-1}}{1 - B_1} + A_1 \frac{1 - B_1 + B_1 - B_1^p}{1 - B_1} B_1^{q-1} \frac{1 - B_1^{pk}}{1 - B_1^p}$$
$$= A_1 \frac{1 - B_1^{q-1}}{1 - B_1} + A_1 \frac{B_1^{q-1} - B_1^{pk+q-1}}{1 - B_1}$$
$$= A_1 \frac{1 - B_1^{i-1}}{1 - B_1}$$

For hyperfractionation treatment, we use a similar construction and have the following result.

Theorem 3.3.3. *Given hyperfractionated treatment schedule $(d, (T_1, T_2, T_3), 2i)$, the total survival fraction for exponential and logistic growth laws are*

$$TSF_{2i,\,e}(d, T, 2i) \;=\; \sigma^{2i} e^{\mu(iT_1 + (i-k-1)T_2 + kT_3)}, \tag{3.35}$$

$$TSF_{2i,\,l}(d, T, 2i) \;=\; \sigma \left[\left(A_1 + F_{12} B_1 \frac{1 - B_{12}^{q-1}}{1 - B_{12}} \right) N_1 + B_{12}^{q-1} B_1 \frac{1 - (B_{12}^{p-1} B_{13})^k}{1 - B_{12}^{p-1} B_{13}} \right.$$
$$\left. \left(F_{13} + F_{12} B_{13} \frac{1 - B_{12}^{p-1}}{1 - B_{12}} \right) N_1 + B_1^i B_2^{i-k-1} B_3^k \right]^{-1}, \tag{3.36}$$

49

Figure 3.3: **The total survival fraction (TSF) as a function of time.** Here we only use the linear quadratic survival model. For the radiosensitivity parameters α, β, we use two sets of values - one from Usher [89]: $\alpha = 0.2 Gy^{-1}, \beta = 0.04 Gy^{-2}$ (left) and those from Nahum *et al* [62]: $\alpha = 0.26 Gy^{-1}, \beta = 0.031 Gy^{-2}$ (right).

where $A_i = (1 - e^{-\mu T_i})/\theta, B_i = e^{-\mu T_i}/\sigma, i = 1, 2, 3$ *and* $B_{1j} = B_1 B_j, F_{1j} = A_j + A_1 B_j, j = 2, 3.$

When $T_1 = T_2$, formulae (3.35) and (3.36) go back to (3.33) and (3.34), respectively.

3.4 Results for Prostate Cancer Treatments

For the ten protocols in Table 3.1, we compute their total survival fraction (TSF) through formulae (3.33)-(3.36) in a logarithmic plot. As a first quality measure, we look at the final TSF at the end of treatment and report them in Table 3.2. We calculate the TSF for two groups of radiosensitive parameters:

one from Usher [89] and one from Nahum *et al* [62]. Although values of TSF for these two groups of parameters are different, they both tell us that the higher the dose per fraction d is, the more effective a treatment to kill cancer. For example: the treatment labeled as 'D' has smaller TSF value in Table 3.2 than other treatments in both columns.

Protocols	$\alpha/\beta = 5$ (E-07)	$\alpha/\beta = 8.387$ (E-08)
A	0.006	0.002
B	0.049	0.026
C	0.059	0.081
D	0.002	0.001
E	0.054	0.178
a	0.127	0.024
b	0.815	0.230
c	2.177	1.337
d	0.084	0.019
e	4.563	5.602

Table 3.2: **TSF values for the ten protocols in Table 3.1.** Two choices of α/β-ratios used for tumor are $\alpha/\beta = 5$ Gy^{-1} from Usher [89] and $\alpha/\beta = 8.387$ Gy^{-1} from Nahum *et al* [62]. Values in brackets beside the α/β values (E-07 and E-08) are the order of each number in that column.

Figure 3.3 and 3.4 plot the total survival fraction (TSF) and tumor control probability (TCP) as a function of time, respectively. Both Figure 3.3 and 3.4 tell us the same as Table 3.2 about the higher the dose per fraction d is, the more effective a treatment to kill cancer. Also, we find that the *standard treatments* kill more cancer cells than their corresponding *hyperfractionated treatments*. However, we can not apply too high dose rate in practice because of the normal tissue complication. In Chapter 4, we will maximize the Poisson TCP in this chapter to find the optimal treatment schedules, under the constraint of a normal tissue complication model- Cumulative Radiation Effect (CRE). The CRE values for the above ten treatment schedules also tells us the standard treatments kill more cancer cells at the risk of more normal

tissues damage.
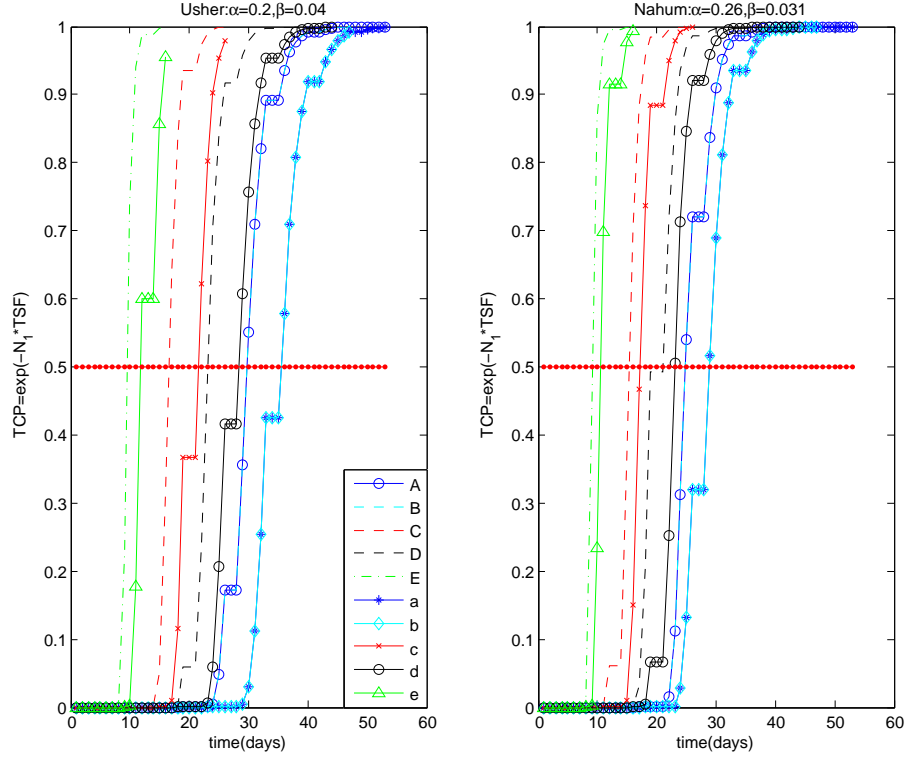
Figure 3.4: **The tumor control probability (TCP) as a function of time.** We use formula (3.14) to calculate the TCP values. In Figure 3.3, we only use the linear quadratic survival model. The values for α, β are $\alpha = 0.2 Gy^{-1}, \beta = 0.04 Gy^{-2}$ (left) and $\alpha = 0.26 Gy^{-1}, \beta = 0.031 Gy^{-2}$ (right).

Chapter 4

Optimization Based on TCP and Cumulative Radiation Effect

Usher [89] tried to find optimal treatment schedules based on his *total survival fraction* (TSF) formulae (3.15-3.17) and the cumulative radiation effect (CRE) model (1.6). But his work has two shortcomings: *i*) his treatments are all uniform; *ii*) his results are not global optima as he did optimization coordinate by coordinate. I extended his formula for clinically used non-uniform treatments in Table 3.1 in Chapter 3. In this chapter, I will first extend the CRE formula for non-uniform treatments in Section 4.1 and briefly introduce a numerical algorithm - *genetic algorithm* - which I will use for optimization in Section 4.2. Then I do optimization in two ways: one is to find the critical points of the TCP formula, the other is to do optimization by the genetic algorithm. I will compare results with Usher's in Section 4.3 and report some optimization results on treatment schedules simulated within reliable intervals. Finally, combined the TCP and CRE calculation, we found that higher dose treatments result in quicker tumor killing at a risk of more normal tissue complication; the hyperfractionated treatments have effective reduction on the normal tissue complication compared to their standard treatments.

4.1 Cumulative Radiation Effect Model

So far the CRE model $CRE = \frac{n^c d}{T^b}$ defined in (1.6) has only been developed for uniform treatment, i.e., T is constant.

We find that the components b, c of the number of fraction n and intertreatment time T is the sensitivity of CRE with respect to n or T. Recall that the sensitivity of a model $f(x)$ with respect to variable x is defined as

$$S(f, x) = \frac{\frac{df(x)}{dx}}{\frac{f(x)}{x}}, \tag{4.1}$$

Therefore,

$$S(CRE, n) = \frac{\frac{dCRE(d,T,n)}{dn}}{\frac{CRE(d,T,n)}{n}} = \frac{\frac{cn^{c-1}d}{T^b}}{\frac{n^c dT^{-b}}{n}} = c. \tag{4.2}$$

Similarly, $S(CRE, T) = b$.

As mentioned in Introduction, the units of CRE are arbitrary units denoted by *reu*, which stands for *radiation effect unit*. Fowler [28] criticized the CRE model with these components b and c as they only depend on the type of radiation. He suggested the CRE model should no longer be used, because it does not include accelerated re-growth during treatment, it underestimates the time factor for acute reacting tissues and overestimates the time factor for late reacting tissue, such as healthy tissue. We agree with Fowler and we are well aware of these shortcomings. However, we are not ready to dismiss the idea of a CRE entirely. Based on the above interpretation we suggest to write the CRE as a general power law of the form:

$$CRE = d^{a_1} T^{a_2} n^{a_3} \tag{4.3}$$

where $a_1 = S(CRE, d), a_2 = S(CRE, T)$ and $a_3 = S(CRE, n)$ are the sensitivities of the CRE with respect to the treatment variable (d, T, n), respectively. More detailed data are needed to estimate the above sensitivities.

Here, in order to compare our results to Usher's results, we still use the CRE model with exponents $a_1 = b, a_2 = 1$ and $a_3 = c$ and extend it for nonuniform treatment (d, T, n), where T is a vector for the intertreatment times. We introduce an index i to the CRE-value, indicating the number of fraction:

$$CRE_i = \frac{i^c d}{T^b}. \tag{4.4}$$

For uniform treatment, the difference of the CRE between two consecutive fractions $i - 1$ and i is

$$\Delta CRE_i = CRE_i - CRE_{i-1} = \frac{i^c d}{T^b} - \frac{(i-1)^c d}{T^b} =: f(i)\frac{d}{T^b} \qquad (4.5)$$

where, $f(i) = i^c - (i-1)^c$ has the following properties:

- $f(1) = 1$. This means that the first radiation will contribute a damage value of d/T^b,

- $f(i)$ is a decreasing function of i for $c < 1$. Hence each newly added fractionation has a slightly reduced effect and the newly added contribution to the CRE is less than d/T^b.

The observation that the CRE increment is decreasing during the progression of treatment is plausible for the following reasons:

1) The healthy normal tissue will be reduced due to the damage made by the former radiations, so less normal tissue is available for further damage;

2) Even if the newly produced damage is the same for each time, the damage caused by the former radiation will have some repair during the time between $(i-1)$-th and i-th fraction. This will make the increment from CRE_{i-1} to CRE_i less than d/T^b.

We use this incremental interpretation to define the CRE for non-uniform treatments.

Definition 4.1.1. *The CRE for non-uniform treatment with variable inter-treatment time T is given by:*

$$CRE_1 = \frac{d}{T_1^b}, \quad CRE_i = CRE_{i-1} + f(i)\frac{d}{T_i^b}, \quad i = 2, \cdots, n. \qquad (4.6)$$

where $f(i) = i^c - (i-1)^c$ and T_i denotes the time between fraction $i - 1$ and fraction i.

If $T_i = T$ constant, then (4.6) goes back to model (1.6).

Additionally, Fowler [28] warned that if we had to use CRE, it should not be used solely, as its significance is questionable. To make up for the shortcomings of the CRE model, we compute the normal tissue complication by the Biological Effective Dose (BED) (1.2) as well.

Usher's optimization methods are quite *ad hoc* and do not necessarily lead to the global optimum (see Section 4.3). We are going to use genetic algorithm to do the optimization properly.

4.2 Genetic Algorithm (GA)

Genetic Algorithm is a generic population-based heuristic optimization algorithm [61]. A Genetic Algorithm uses some mechanisms inspired from biological evolution: reproduction, mutation, recombination (or crossover), natural selection and survival of the fittest. Typical crossover acts on two selected DNA (called parents) to get one or two new candidates (see Figure 4.1 (a)), while mutation usually acts on only one parent as shown in Figure 4.2 (a)-(d). These operators will create a set of new candidates which are called offsprings. Mathematically, each candidate solution consists of all the variables of a problem. Compared to the biological terminology, all the variables of a candidate solution are considered as the DNA, each variable is thought as genes of that DNA, for example, a vector $(d,\ T,\ n)$ to indicate the treatment schedule. There is also an objective function, also called fitness function to determine which solution will survive during the selection.

Usually, a randomly generated population forms the first population and we will keep the size of the population as a constant number. Reproduction is applied to the current population based on their fitness: individuals with higher fitness have a bias to be chosen as parents for crossover and mutation. As the size of the population is constant, offsprings compete with the existing individuals for their places in the next generation based on the principle of the survival of the fittest. The algorithm will end when some satisfactory candidates for the problem are found.

Typical crossover in genetic algorithm are shown in Figure 4.1 (1) and (2).

Parents:

Children:

(a)

$X_1 = (1.2, 3.4, 5.7)$ $X_1' = (1.2, 3.4, \underline{9.9})$

$X_2 = (3.1, 5.9, 9.9)$ $X_2' = (3.1, 5.9, \underline{5.7})$

(1)

$X_1 = (1.2, 3.4, 5.7)$ $X_1' = aX_1 + (1-\alpha)X_2$

$X_2 = (3.1, 5.9, 9.9)$ $0 < a < 1$

(2)
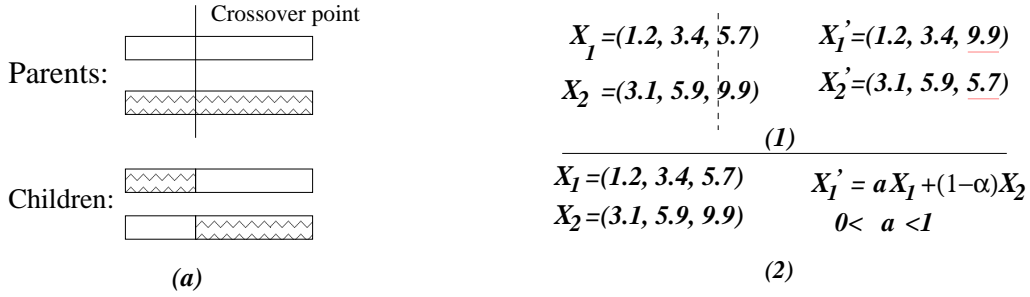
Figure 4.1: **Crossover in Biology and genetic algorithm.** In Biology, crossover needs two parents to generate new individuals. The top two rectangles in (a) represent the DNA of two parents, once a crossover point is chosen, they will interchange part of their DNA to generate two offsprings as shown in (a). The two candidates solution in Genetic Algorithm could also generate two new candidates by crossover as shown in (1). In addition, the crossover can also be extended by linear combination of two parents to generate new children by changing the weight α in front of one parent.

Figure 4.1 (1) is also called single point crossover. It is analog to crossover in biology: once a crossover point is chosen, genes on one side of the crossover point will interchange to generate two new DNAs. Figure 4.1 (2) is called arithmetic crossover. Geometrically, given two parents X_1, X_2, we know the children from the arithmetic crossover $\alpha X_1 + (1 - \alpha)X_2$ are all situated on the line connecting X_1 and X_2. In our algorithm here, we use the extended crossover operator proposed by T. Gao et. al. [33], which is called GT algorithm. It is a multi-parents crossover, extending the search area from a line to a polygonal area with M vertices. Suppose we have M parents X_i, $i = 1, \cdots , M$, then the children are formed by:

$$C = \sum_{i=1}^{M} \alpha_i X_i, \quad \alpha_i \in [0, 1], i = 1, \cdots , M. \tag{4.7}$$

The mutation is shown in Figure 4.2. Compared to the crossover, mutation could happen based on one single individual. The four types of mutation based on one DNA are deletion, duplication, inversion and transition as shown from (a) - (d). However, deletion and duplication will change the length of the DNA, therefore we mainly use the mutation corresponding to inversion and

$$X_1 = (1.2, 3.4, 5.7) \qquad X_1^{'} = (1.2, 5.7, 3.4)$$

(3)

$$X_1 = (1.2, 3.4, 5.7) \qquad X_1^{'} = (1.2, 3.5, 5.7)$$

(4)
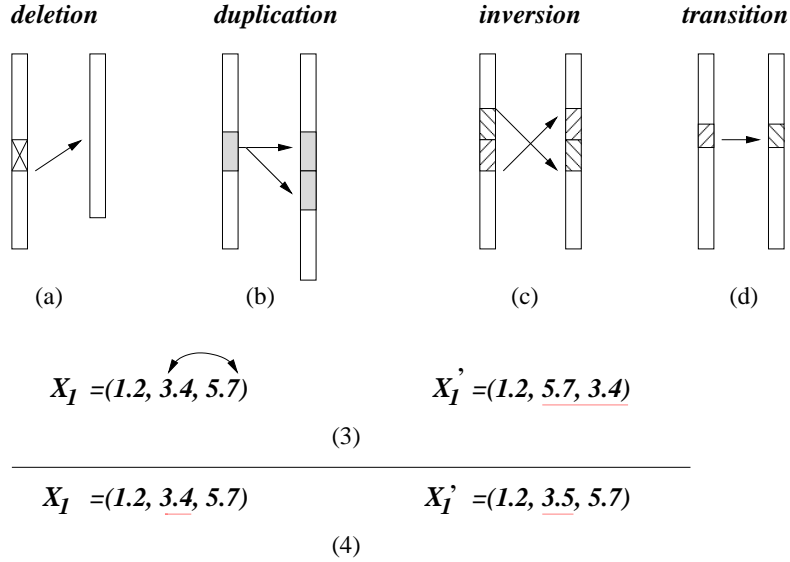
Figure 4.2: **Mutation in Biology and genetic algorithm.** The top row show four different kinds of mutation based on one parent in Biology: depletion (a), duplication (b), inversion (c) and transition (d). Deletion and duplication will change the length of the DNA, which is not suitable for our problem here. Inversion is applicable when all the variables have the same unit for the numbers which is not the case of our problem. Therefore, I only use the mutation corresponding to transition in my simulation as shown in (4): I randomly choose a variable, generate a small perturbation to it to obtain a new candidate.

transition in the genetic algorithm. In Figure 4.2 (3), two genes are inversed to generate a new DNA. This mutation method is eligible when all the genes have the same unit of numbers. In Figure 4.2 (4), a perturbation is given to a randomly chosen gene. Because we have integers for the number of treatments n and real numbers for dose d in our problem, they have different units. It is not proper to use mutation (3). Therefore, I only use mutation (4): give a small perturbation to a randomly chosen variable for this problem.

4.3 Optimization of Poisson TCP with the Constrain of CRE

Wheldon and his coworkers [96, 97] gave some optimal schedules for exponential tumor growth by only minimizing the total survival fraction (TSF). Usher [89] found that the CRE values for their results are greater than 1800 *reu*, the recommended maximal value of the CRE. Usher [89] therefore improved the results for exponential and Gompertzian tumor growth by limiting CRE=1800 *reu*. However Usher's schedules are not necessarily the global optimal solutions, as he did optimization coordinate by coordinate.

In the following section, we will derive optimal schedules by two different methods: one is to find the critical points of the function $TSF(d, T, n)$. The other is to minimize the three-variable function $TSF(d, T, n)$ under the constraint $CRE_n = n^c d/T^b \leq 1800$ *reu* by a genetic algorithm. We find that these two methods arrive at the same optimal schedules. To compare with Usher's results, we also run the genetic algorithm by restricting n to be an integer. We find that Usher's results are close to the optima. Finally, we also simulate our algorithm within a realistic domain for $(d,\ T,\ n)$.

4.3.1 Results for Uniform Treatment

Case 1: Exponential Growth with MTSH Survival

The constant growth rate μ of the exponential growth model can be related to the tumor doubling time τ by

$$\mu = \ln(2)/\tau.$$

Usher [89] uses doubling time τ rather than the growth rate μ to calculate TSF, hence we rewrite the TSF_e (3.15) in terms of tumor doubling time as

$$TSF_e(d, T, n) = \sigma(d)^n e^{\frac{\ln(2)}{\tau}(n-1)T} \tag{4.8}$$

where $\sigma(d)$, is now given through the multitarget singlehit (MTSH) model (2.11). We find that the optimal solution depends on the doubling time τ. The

results for exponential growth with MTSH survival are presented in Table 4.1. The parameters for MTSH survival fraction models are the same as Usher's [89]: $n = 2, D_0 = 1.5$ Gy. The columns labeled by (1) refer to the results of Usher [89], columns labeled by (2) are the optimization results of a genetic algorithm with integer constraint on the number of treatment n. We also search for the critical point of $TSF_e(d, T, n)$ without integer constraints on n. These are quite close to those of column (2) and are not shown in Table 4.1. For implementation of the genetic algorithm, we restrict the domain for the three treatment variables as follows: dose $d \in [0.01, 5]$ Gy, inter-treatment time $T \in [1, 300]$ days and the number of fractions $n \in [4, 60]$. The number of fractions is restricted in $[4, 60]$ because the CRE is well documented for treatment fractions only in this interval [89].

We can see from Table 4.1 that the results from the two methods are quite close to each other because our global maximal schedules also make the CRE equal to the maximal allowed value, i.e. $CRE = 1800$ *reu*. Furthermore, noticing the TSF values in both columns share the same order as shown in column (2), we find that the longer the doubling time of cells, the smaller the total survival fraction. This is consistent with common sense: the more time needed for cancer cell number doubling, the slower the cells grow between treatments resulting in a smaller survival fraction after n fractions.

Moreover, we find the optimal dose d^* per fraction is independent of the doubling time and lies at around 3.5 Gy. But the inter-treatment time becomes quite large for a slowly growing tumor. For example, the inter-treatment time T^* is more than 40 days for a doubling time of 110 days. In fact it appears that the optimal inter-treatment time is about 1/3 of the tumor doubling time.

Case 2: Expential Growth with LQ Survival

Here, we use TSF for exponential growth formula (4.8) but now with LQ surviving fraction (2.14). We set our domain for the three variables according to Usher's choices as $d \in [0.01, 20]$ Gy, $T \in [1, 800]$ days and the number of fractions $n \in [4, 60]$. The radiosensitivity parameters are the same as Usher's: $\alpha = 0.2$ Gy$^{-1}, \beta = 0.04$ Gy$^{-2}, \alpha/\beta = 5$ Gy^{-1}. The results are reported in Table

doubling	Optimal Result							
time τ	dose d^* (Gy)		intertreatment time T^* (days)		fx. n^*		TSF^*	
(days)	(1)	(2)	(1)	(2)	(1)	(2)	(1)	(2)
10	3.59	3.59	3.84	3.88	15	15	1.7310	1.7308E-10
30	3.60	3.60	11.57	11.52	18	18	1.8509	1.8509E-12
50	3.55	3.55	18.99	18.77	20	20	1.6539	1.6535E-13
70	3.57	3.57	26.66	26.38	21	21	2.9933	2.9926E-14
90	3.55	3.55	33.34	33.72	22	22	7.8248	7.8230E-15
110	3.53	3.53	41.19	40.75	23	23	2.5714	2.5708E-15

Table 4.1: **Results for exponential growth with MTSH survival fraction.** The columns labeled by (1) refer to the results of Usher [89], columns labeled by (2) are the results of genetic algorithm with integer restriction on n. The two columns for TSF have the same order as shown in the second column. The parameters for MTSH survival fraction models are: $n = 2, D_0 = 1.5$ Gy.

4.2. Once again, we find the two columns (1) for Usher, (2) for the genetic algorithm, are close to each other. We observe that the optimal number of fractions n^* is always on the boundary of the domain we preset ($n^* = 4$), and the optimal doses d^* are very high, almost all above 10 Gy. The optimal dose d^* and inter-treatment time T^* increase as the doubling time increases. However, some of these results are impractical, as they suggest, for example, that treatment of 14.92 Gy is given every other year for the doubling time $\tau = 150$ days. We study more realistic scenarios in Section 4.3.2.

Case 3: Logistic Growth with MTSH or LQ Survival

Usher did not study the logistic growth model in his paper [89], but he used the Gompertzian law. As mentioned in Chapter 3, Gompertzian law is not applicable for the tumor eradication. To stay close to Usher's results we choose his carrying capacity θ for the logistic model.

$$\theta = N_1 e^{28.5}.$$

We do not have Usher's results for comparison, so we present our results in Table 4.3 for logistic growth with MTSH survival model in column (1) and

doubling	Optimal Result							
time τ	dose d^* (Gy)		intertreatment time T^* (days)		fx. n^*		TSF^*	
(days)	(1)	(2)	(1)	(2)	(1)	(2)	(1)	(2)
1	7.51	7.51	1.28	1.27	4	4	4.22E-06	4.22E-06
10	10.28	10.28	22.18	22.25	4	4	1.23E-09	1.23E-09
30	11.96	11.96	87.82	87.82	4	4	3.54E-12	3.54E-12
70	13.44	13.44	253.65	253.90	4	4	1.22E-14	1.13E-14
100	14.12	14.12	397.28	397.23	4	4	6.73E-16	16.73E-16
150	14.92	14.93	659.67	661.04	4	4	1.97E-17	1.97E-17

Table 4.2: **Results for exponential growth with LQ survival fraction.** (d, T, n) describe the uniform treatment schedule, TSF stands for the total survival fraction. The columns labeled by (1) refer to the results of Usher [89], columns labeled by (2) are our results of genetic algorithm. The parameters for linear quadratic survival fraction models are: $\alpha = 0.2$ Gy^{-1}, $\beta = 0.04$ Gy^{-2}.

logistic growth with LQ survival model in column (2). We set the domain of the three variables as dose per fraction $d \in [0.01, 15]$ Gy, inter-treatment time $T \in [0.002, 1000]$ days and the number of fractions $n \in [4, 60]$. All the results make the CRE to be the maximal allowed value of $CRE = 1800 \ reu$. It is interesting to observe that for the MTSH cell survival, the optimal dose d^* is independent of the growth rate (around 3.5 Gy). The inter-treatment time and the total survival fraction show the same trend as for the exponential cases (actually also the same as for Gompertzian growth, see [89]): the smaller the growth rate μ (or the bigger the doubling time τ), the larger the optimal inter-treatment time and the tumor control probability (smaller of the total survival fraction).

For linear quadratic survival fraction, the optimal number of fractions n^* always arrives at the boundary of the domain which we preset for the genetic algorithm, i.e. $n^* = 4$, and the optimal dose per fraction d^* are much higher than that for MTSH cell survival.

Many of the above protocols are impractical. Therefore, we try to find some more practical potentially suboptimal uniform treatment protocols.

Growth		Optimal Result for Logistic Growth							
growth	doubling	dose d^* (Gy)		time T^* (days)		fx. n^*		TSF^*	
rate μ	time τ	(1)	(2)	(1)	(2)	(1)	(2)	(1)	(2)
0.001	693	3.55	15	256.17	688.33	31	4	1.314E-20	1.124E-20
0.005	139	3.52	14.77	51.24	598.70	24	4	6.795E-16	4.036E-17
0.01	69	3.56	13.42	26.09	250.79	21	4	3.150E-14	1.212E-14
0.05	14	3.57	10.76	5.31	33.456	16	4	4.898E-11	2.538E-10
0.1	7	3.62	9.78	2.72	14.090	14	4	6.578E-10	6.201E-9

Table 4.3: **Results for logistic growth.** The columns labeled by (1) are for logistic growth with MTSH survival and the columns labeled by (2) are for logistic growth with LQ survival. The values in the 'doubling time' have units of 'days'.

4.3.2   Realistic Optimal Uniform Treatments

In this section we restrict our schedule variables (d, T, n) to realistic intervals as follows: dose per fraction $d \in [1, 4]$ Gy, the number of fractions $n \in [1, 100]$ and inter-treatment time $T \in [1/2, 7]$ days. To be able to include hyperfractionation, the increment of our T is $1/2$ day from $1/2$ to 7 days.

Above we saw that the predictions between MTSH model and LQ model are quite different. The LQ model is a well established model and it is the standard model for cell survival. Many experimentalists have measured α and β sensitivities for various cell lines. Hence we choose the LQ surviving fraction from now on (and do not study the MTSH survival fraction any further).

Usher studied prostate cancer, hence we use it here as well. For the linear-quadratic model, we choose radio-sensitivity parameters as measured by Chapman's group [62]: $\alpha/\beta = 8.373$ Gy^{-1} with $\alpha = 0.26$ $Gy^{-1}, \beta = 0.031$ Gy^{-2}. At the same time, we keep Usher's parameters for comparison, whose radio-sensitivity ratio is $\alpha/\beta = 5$ Gy^{-1} with $\alpha = 0.2$ $Gy^{-1}, \beta = 0.04$ Gy^{-2}. It is worthy to note that there are reports about an α/β ratio for prostate cancer less than 3 [18]. But whether the ratio is really less than 3 or not is still under debate since the reported low values have very wide confidence intervals so that high α/β ratio values cannot be excluded. We assume the parameters

for growth laws are $N_1 = 10^5, \theta = N_1 e^{28.5}$ and study various growth rates. We find that the optimization results for exponential and logistic growth with linear-quadratic survival fraction, as reported in Table 4.4, are identical. This arises due to the very large carrying capacity. All these schedules in Table 4.4 maximize $CRE = 1800$ *reu.*

Growth	Nahum $\alpha, \beta, \alpha/\beta = 8.387Gy^{-1}$				Usher $\alpha, \beta, \alpha/\beta = 5Gy^{-1}$			
doubling	dose/fx.	time T^*	fx.		dose/fx.	time T^*	fx.	
time τ	d^* (Gy)	(days)	N^*	TSF^*	d^* (Gy)	day	N^*	TSF^*
693	1.117	7	100	1.00E-14	1.117	7	100	2.66E-12
139	1.117	7	100	1.61E-13	1.117	7	100	4.26E-11
69	1.051	4	100	2.34E-12	1.018	3	100	4.44E-10
14	1.003	1	85	1.13E-9	1.008	0.5	75	8.22E-8
7	1.008	0.5	75	1.11E-8	1.008	0.5	75	5.23E-7
1.4	3.998	0.5	9	7.38E-6	4.000	0.5	9	1.75E-5

Table 4.4: **Exponential growth with LQ model within reasonable domain.** The radiosensitivity parameters are $\alpha = 0.26$ Gy$^{-1}, \beta = 0.031$ Gy^{-2} given by Nahum *et al* [62] and $\alpha = 0.2$ Gy$^{-1}, \beta = 0.04$ Gy^{-2} by Usher. Values in the column of doubling time have the unit of days. For logistic growth, quite close results are obtained.

f

Table 4.4 suggests that, for both choices of α/β ratios, low-frequency low dose treatments are recommended for a slow growing cancer; high frequency (up to hyperfractionated) treatments with low dose per fraction are required for moderately growing cancer and hyperfractionation with high dose per fraction treatments are good for fast growing cancer.

The optimal treatment schedule for $\mu = 0.1$ is a hyperfractionation of 1 Gy, twice per day for 75 fractions, which is already quite close to the realistic schedules which reported in Table 3.1. Schedule 'a' in Table 3.1 uses hyperfractionation of 1 Gy twice per day with weekend off for a total of 78 fractions and schedule 'b' uses hyperfractionation of 1 Gy, twice per day during week days with weekends off and a total of 70 fractions.

4.4 Optimization of Nonuniform Treatment for Prostate Cancer

To study optimization of non-uniform treatments, we consider the 10 realistic treatments of Table 3.1 and compute the TCP, TSF, BED and CRE at the end of treatment.

4.4.1 Tumor Control Probability

In Figures 3.3 and 3.4, we presented the TSF (3.33, 3.35) and their corresponding TCP (3.14) for an exponentially growing tumor as a function of time in a logarithmic plot, respectively. In Table 4.5, besides the TSF values that we already reported in Table 3.2, we also calculated the CRE (4.6) and BED (1.2) values for both groups of α/β ratios. Only based on TSF values, we find the ranking:

$$D > A > B > E > C > d > a > b > c > e. \tag{4.9}$$

for Usher's α/β value and

$$D > A > d > a > B > C > E > b > c > e. \tag{4.10}$$

for Nahum's α/β value.

These rankings just mean that schedule 'D' with 32 fractions of 2.4 Gy will kill more tumor cells than schedule 'A' with 39 fractions of 2 Gy etc. If we look at the ordering of only standard or only hyperfractionation treatment, they basically coincide, i.e.

$$D > A > B > C > E, \quad \text{and} \quad d > a > b > c > e. \tag{4.11}$$

The switch of 'C' and 'E' in (4.9) is insignificant as we can see from Figure 3.3 and Table 4.5 since the TSF values are very close.

The interesting thing is that the hyperfractionated protocols 'd' and 'a' are more efficient for larger α/β-ratio ($\alpha/\beta = 8.387$) than standard treatments 'B' and 'C', which favors the lower-dose treatments. The TSF graphs and rankings for logistic growth are identical and are not shown here.

The TCP for the ten protocols give the same relative order for the ten treatments, since the TCP is a monotonic transformation of the TSF

$$TCP = e^{-TSF*N_1}.$$

The TCP basically tells us that the higher the dose per fraction is, the quicker the treatments show the killing effect (from TCP=0 to TCP=1), but the final tumor killing results also depend on the total dose.

The *Biological Effect Dose* can also be used to measure the effect of protocols. We calculate the BED values for our two α/β-ratios in the two columns named 'BED' of Table 4.5.

	tumor				normal tissue
	$\alpha/\beta = 5$ (Usher)		$\alpha/\beta = 8.387$ (Nahum)		
Protocols	TSF (E-07)	BED$_5$	TSF (E-08)	BED$_{8.387}$	CRE
A	0.006	109.20	0.002	96.60	2125
B	0.049	98.00	0.026	86.69	1982
C	0.059	96.00	0.081	81.46	2072
D	0.002	113.66	0.001	98.78	2242
E	0.054	95.98	0.178	78.05	2131
a	0.127	93.60	0.024	87.30	1831
b	0.815	84.00	0.230	78.35	1709
c	2.177	78.00	1.337	70.73	1789
d	0.084	95.23	0.019	87.79	1932
e	4.563	73.79	5.602	64.83	1841

Table 4.5: **TSF, BED and CRE values for the ten protocols in Table 3.1.** Two choices of α/β-ratios used for tumor are $\alpha/\beta = 5 \ Gy^{-1}$ from Usher [89] and $\alpha/\beta = 8.387 \ Gy^{-1}$ from Nahum *et al* [62]. Values in brackets in two 'TSF' columns (E-07 and E-08) are the order of each number in that column. Parameter used in CRE are $c = 0.65, b = 0.11$.

We can also use these BED values to make a ranking for efficiency. The BED rankings show the same tendency as the TSF ranking with an insignificant switch from '$C > E$' for $\alpha/\beta = 5$ Gy^{-1} and '$b > E$' for $\alpha/\beta = 8.387$ Gy^{-1}. This is a bit surprising, since the BED is based on a simple formula (1.2), which only depends on d, D and n, but does not include re-growth between
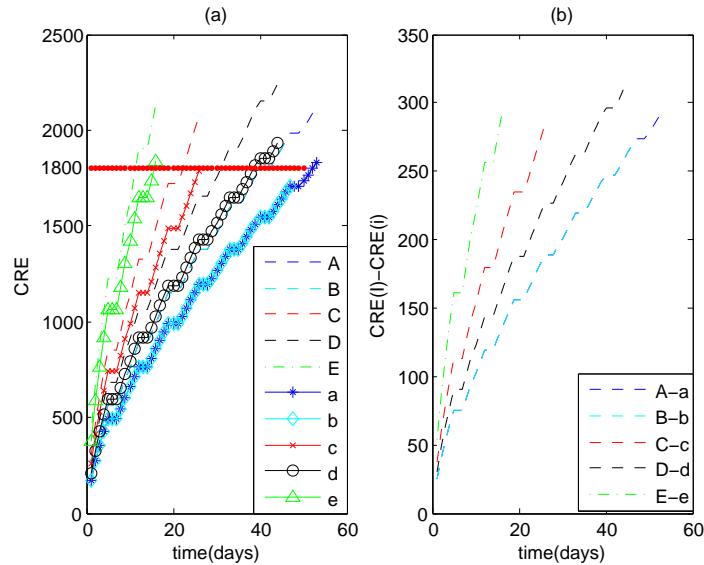
Figure 4.3: **CRE for the ten protocols (X-ray).** (a) CRE as function of time for the ten protocols, for X-ray radiation, i.e. c=0.65, b=0.11. The horizontal line denotes the threshold of CRE = 1800 reu. (b) shows the difference CRE(I)-CRE(i) between standard fractionation $I \in \{A, B, C, D, E\}$ and hyperfractionation $i \in \{a, b, c, d, e\}$.

treatment and inter-treatment times. It somehow confirms why the BED has been so useful in treatment planning.

4.4.2 Late Effects on Normal Tissue

To estimate the late effects on normal tissue, we calculate the final CRE values for the ten treatment protocols and present them in the last column of Table 4.5. The left panel in Figure 4.3 shows the CRE as function of time for the ten treatment protocols, where we used the parameters for X-ray radiation, i.e. c=0.65, b=0.11. The right panel shows the difference between standard treatments and their corresponding hyperfractionations. Most protocols have $CRE > 1800$ reu, only hyperfractionated treatments come close to 1800 reu where treatments 'b' and 'c' are the only two below the threshold. Furthermore, the differences between the standard and hyperfractionated

treatments in CRE values are always about 250-300 reu, hence hyperfraction-ation is clearly beneficial to reduce late effects.
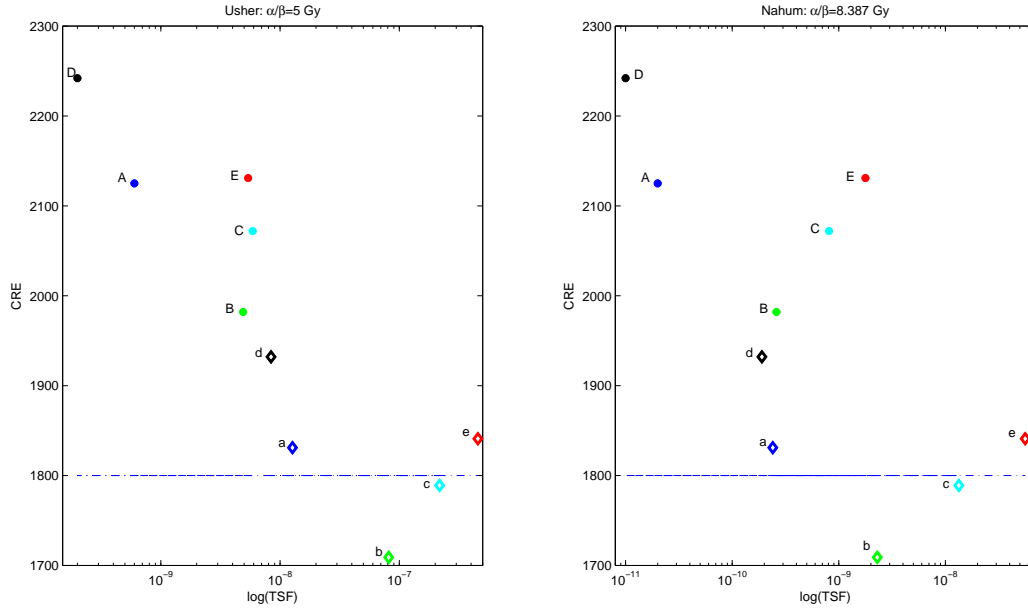
Figure 4.4: **CRE as function of $\log$(TSF) at the end of treatment.** The horizontal line denotes the threshold of CRE = 1800 reu. Left: $\alpha/\beta = 5$ Gy, right: $\alpha/\beta = 8.387$ Gy.

In Figure 4.4 we plot the log(TSF) and the CRE at the end of treatment into one graph. It is clear to see that smaller values of TSF have higher CRE values and does not seem to depend much on the α/β ratio. It is exciting that for the protocols labeled by 'b' and 'c', their CRE values are always less than 1800 reu. That gives us an explanation why in clinic, oncologists discuss hyperfractionated treatments as a way to reduce normal tissue complication.

4.5 Conclusion

In this Chapter, we optimize the Poisson TCP with the constraint of CRE value smaller than 1800 reu. The work in this Chapter tells us that the higher dose

treatments can kill tumor cells quicker at the risk of more normal tissue late effects; and that the hyperfractionated treatments have effective reduction on normal tissue damage compared to their standard treatments. These positive results motivate me to explore more sophisticated models for the TCP and models to measure normal tissue complications.

Chapter 5

Stochastic TCP Models Derived from a Birth-Death Process

The use of differential equation models is appropriate for large numbers of cells. However, only a small number of cells exist at the end of a successful treatment. In this case, stochastic effects dominate and deterministic models become inappropriate for predicting the number of surviving cells. In this chapter, we first briefly review two existent TCP models derived from birth-death processes: a one-compartment model derived by Zaider and Minerbo [101] and a two-compartment model with cell cycle by Dawson and Hillen [20]. Then we introduce the detailed steps to derive a generalized TCP model which incorporates the stochastic effect, with the first two models as special cases. Furthermore, we adapted this approach to derive a TCP model under the assumption of tumor stem cells, where one compartment is cancer stem cells with unlimited growth potential and no death, the other are transient or differentiated cancer cells with limited growth potential and death.

5.1 Zaider-Minerbo TCP Derived from a Birth-Death Process

Instead of thinking about the mean number of tumor cells, Zaider and Minerbo [101] considered the probability P_i of i tumour cells surviving at time t. The

changes of the tumor cells are shown in the following diagram in Figure 5.1.
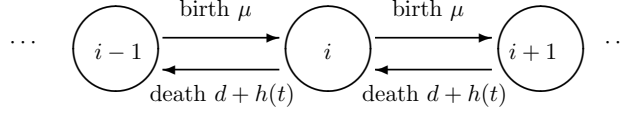
Figure 5.1: **The diagram of the state change for the Zaider-Minerbo TCP model.** During a small time interval, the number of cells can jump to its neighboring number.

where μ is the growth rate, d is the natural death rate and $h(t)$ is the hazard function corresponding to the cell survival model, which is in the form of (2.51) as we discussed in Section 2.3. Based on the diagram in Figure 5.1, the master equation to describe the probabilities $P_i(t), i = 0, 1, \cdots$ are

$$\frac{dP_0(t)}{dt} = (d + h(t)) P_1(t)$$

$$\frac{dP_i(t)}{dt} = (i-1)\mu P_{i-1}(t) - i\big(\mu + d + h(t)\big)P_i(t) + (i+1)\big(d + h(t)\big)P_{i+1}(t), \forall i.$$

(5.1)

It is easy to check that the expected number of tumor cells $N(t) = \sum_{i=0}^{\infty} iP_i(t)$ satisfies the mean field equation

$$\frac{dN}{dt} = \big(\mu - d - h(t)\big)N, \quad N(0) = N_0,$$

(5.2)

provided that the sum $\sum_{i=0}^{\infty} iP_i(t)$ converges. As we mentioned above, the mean-field description (5.2) of tumour cell evolution is a reasonable approach when the number of cells is large. However, for a relatively small cell-population (e.g., at the end of the treatment), the average behavior is no longer appropriate as probabilistic or stochastic noise becomes dominant. That is our motivation to introduce system (5.1).

A generating function $A(s, t)$ has been introduced to solve system (5.1), which is defined as

$$A(s, t) = \sum_{i=0}^{\infty} P_i(t)s^i.$$

(5.3)

Again, we assume that the series converges for $0 \leq s \leq 1$. According to Zaider and Minerbo [101], the generating function $A(s, t)$ satisfies the following

71

hyperbolic equation

$$\frac{\partial}{\partial t} A(s,t) = (\mu s - d - h)(s - 1)\frac{\partial}{\partial s} A(s,t), \quad A(s,0) = s^{N_0}. \tag{5.4}$$

which is solved by the method of characteristics. Then, they obtained an explicit expression for the TCP,

$$TCP_{ZM}(t) = P_0(t) = A(0,t) = \left[1 - \frac{S_h(t)e^{\mu t}}{1 + \mu S_h(t)e^{\mu t} \int_0^t \frac{dr}{S_h(r)e^{\mu r}}} \right]^{N_0}, \tag{5.5}$$

where

$$S_h(t) = \exp\left(- \int_0^t d + h(r)\, dr \right) \tag{5.6}$$

is the probability of cell survival for a given hazard function $h(t)$ and natural death rate d. In [20], Dawson and Hillen simplified (5.5) into

$$TCP_{ZM}(t) = \left[1 - \frac{N(t)}{N_0 + \mu N_0 N(t) \int_0^t \frac{dr}{N(r)}} \right]^{N_0}, \tag{5.7}$$

where $N(t)$ solves the mean field equation (5.2). Note that when $\mu = 0$, the Zaider-Minerbo TCP reduces to the binomial TCP. For simplicity, we will refer this TCP formula as ZM TCP later.

5.2 Dawson-Hillen TCP including Cell Cycle

Dawson and Hillen [20] extended the model of Zaider and Minerbo by including cell cycle dynamics. Their idea is based on the fact that a typical tumour consists of cells which are actively proliferating (cells in the G_1, S, G_2, or M phase) and cells which are quiescent (cells in the G_0-phase). Since actively proliferating cells are more sensitive to radiation than the quiescent cells [71], one must keep track of these two subpopulations separately to predict the total cell population. The two compartments are called active and quiescent compartment, respectively, which is shown in Figure 1.2.

Cells in the active compartment will divide once they finish the cell cycle $G_1 \to S \to G_2 \to M$ phases. In [20], it was assumed that all newly generated daughter cells directly enter the quiescent compartment. Quiescent cells

cannot duplicate themselves, but may come back to the active compartment to enter the cell cycle process as denoted in Figure 1.2. Let $a(t)$ denote the population of active cells and $q(t)$ the population of quiescent cells. The two-compartmental mean field population model is governed by

$$\frac{d}{dt}a = -\mu a + \gamma q - h_a(t)a, \quad a(0) = a_0, \tag{5.8}$$

$$\frac{d}{dt}q = 2\mu a - \gamma q - h_q(t)q, \quad q(0) = q_0, \tag{5.9}$$

where the parameter $\mu > 0$ denotes a constant per-capita birth rate. Note that the population of active cells divides at a rate of μa, giving rise to $2\mu a$ daughter cells, which all move into the quiescent compartment (the first term in (5.9)). With birth, there is the loss of the mother cells, represented by the term $-\mu a$ in (5.8). The parameter $\gamma > 0$ denotes the rate at which quiescent cells become active. $h_a(t)$ and $h_q(t)$ are the hazard functions due to radiation treatment for active and quiescent cells with natural death term d_a, d_q, respectively, given by

$$h_a(t) = d_a + \alpha_a \dot{D}(t) + 2\beta_a \dot{D}(t)(D(t) - D(t - \omega)), \tag{5.10}$$

$$h_q(t) = d_q + \alpha_q \dot{D}(t) + 2\beta_q \dot{D}(t)(D(t) - D(t - \omega)), \tag{5.11}$$

as proposed by Dawson and Hillen in [20]. The parameters α_a, β_a and α_q, β_q are the radiosensitivities for active and quiescent cells, respectively. As mentioned in Chapter 2, the parameter ω represents the mean repair time of DSB. In the limit as $\omega \to \infty$, the hazard functions have the same form as that given by Zaider and Minerbo, with natural death rate included.

Denote $P_i(t)$ and $Q_j(t)$ as the probabilities that i active cells and j quiescent cells are present at time t, respectively. The state changes of tumor cells are described in Figure 5.2, and the corresponding master equations are

$$\frac{dP_i(t)}{dt} = (\mu + h_a)(i + 1)P_{i+1} + \gamma \sum_{j=0}^{\infty} jQ_j P_{i-1} - (\mu + h_a)iP_i - \gamma \sum_{j=0}^{\infty} jQ_j P_i, \tag{5.12}$$

$$\frac{dQ_j(t)}{dt} = (\gamma + h_q)(j + 1)Q_{j+1} + \mu \sum_{i=0}^{\infty} iP_i Q_{j-2} - (\gamma + h_q)jQ_j - \mu \sum_{i=0}^{\infty} iP_i Q_j, \tag{5.13}$$

whose mean field equations are (5.8, 5.9).
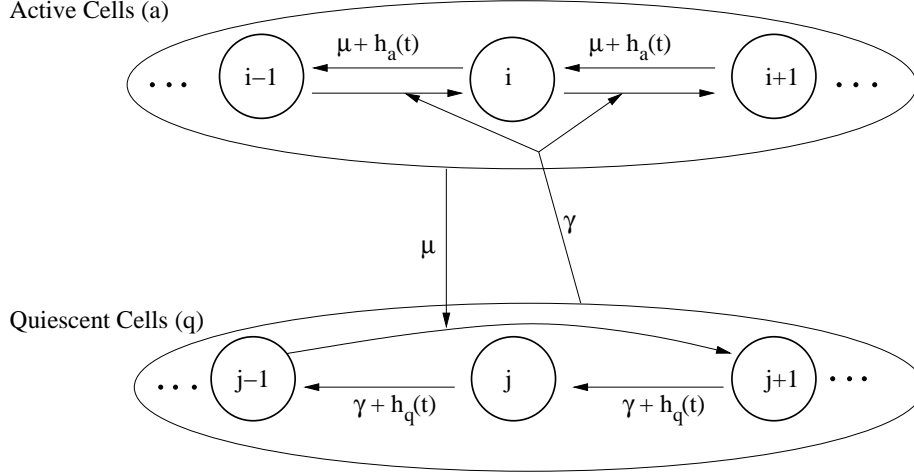
Figure 5.2: **Diagram of the state change for the Dawson-Hillen TCP model.** The two compartments are active cells (a) and quiescent cells (q), respectively. During a really small time interval, the number of cells in the active compartment can change to its neighboring number. However, in the quiescent compartment, the number of cells will reduce by one from a higher number because of the death, but it increases by two each time because two new born cells transfer into the quiescent compartment.

Similarly, the generating functions

$$X(s,t) = \sum_{i=0}^{\infty} P_i(t)s^i, \quad Z(s,t) = \sum_{j=0}^{\infty} Q_j(t)s^j$$

satisfy

$$\frac{\partial}{\partial t}X(s,t) + (\mu + h_a(t))(s-1)\frac{\partial}{\partial s}X(s,t) = \gamma q(t)(s-1)X, \qquad (5.14)$$

$$\frac{\partial}{\partial t}Z(s,t) + (\gamma + h_q(t))(s-1)\frac{\partial}{\partial s}Z(s,t) = \mu a(t)(s^2-1)Z, \qquad (5.15)$$

with initial conditions $X(s,0) = s^{a_0}, Z(s,0) = s^{q_0}$. After solving the equations by the method of characteristics, the TCP is

$$
\begin{aligned}
TCP_{DH} &= P_0(t)Q_0(t) = X(0,t)Z(0,t) \\
&= \left(1 - \frac{1}{\Lambda_a(t)}\right)^{a_0}\left(1 - \frac{1}{\Lambda_q(t)}\right)^{q_0}\exp\left\{-\gamma\int_0^t q(z)\frac{\Lambda_a(z)}{\Lambda_a(t)}dz + \right. \\
&\qquad \left. \mu\left[\int_0^t a(z)\frac{\Lambda_q(z)^2}{\Lambda_q(t)^2}dz - 2\int_0^t a(z)\frac{\Lambda_q(z)}{\Lambda_q(t)}dz\right]\right\},
\end{aligned}
\qquad (5.16)
$$

where

$$\Lambda_a(t) = e^{\int_0^t (\mu + h_a(z))dz} \quad \text{and} \quad \Lambda_q(t) = e^{\int_0^t (\gamma + h_q(z))dz}. \tag{5.17}$$

We will refer to this TCP formula as DH TCP from now on. In the next section, we are going to explain in detail how to derive the TCP model from the mean field equations.

5.3 Generalized TCP Model Derived from a Birth-Death Process

This section is adapted from the published paper Hillen *et al* [37], where the results of this section were derived by myself.

DH TCP assumes that all daughter cells enter into the quiescent compartment, whereas ZM TCP can be considered that all daughter cells stay in the active compartment and no quiescent compartment exists. If we loosen the assumption and allow the newly generated cells to become either active or quiescent, the assumption of the above two TCPs are the special cases of the more general assumption. As shown in Figure 5.3, we assume a fraction of f newly born cells remain in the active compartment, the other $1 - f$ fraction newly generated daughter cells transfer into the quiescent compartment. To make it comparative with DH TCP, we again include the natural death terms in the hazard function as (5.10, 5.11).

Denote again $a(t)$, $q(t)$ by the population of the active cells and quiescent cells, respectively. We will have the cell population model given by [37]

$$\frac{d}{dt}a = 2\mu f a - \mu a + \gamma q - h_a(t)a, \tag{5.18}$$

$$\frac{d}{dt}q = 2\mu(1 - f)a - \gamma q - h_q(t)q, \tag{5.19}$$

where the parameters $\mu, \gamma, h_a(t), h_q(t)$ have the same meaning as the ones in (5.8, 5.9). Notice that compared to (5.8, 5.9), the new system has an extra term $2\mu f$ in (5.18), and an extra fraction $1 - f$ in the first term of (5.19). In particular, system (5.18, 5.19) reduce to (5.8, 5.9) when $f = 0$; equation (5.18) is the same as (5.2) when $f = 1$ and $q = 0$.

Figure 5.3: **Relation between Generalized TCP, ZM TCP and DH TCP.** In the generalized TCP, only $1 - f$ fraction of newly born cells transfer to the quiescent compartment, the other f fraction of newly born cells remain in the active compartment. Therefore, the generalized TCP arrives at the DH TCP when $f = 0$, and reduces to the ZM TCP when $f = 1$, with additional assumption that the number of quiescent cells is zero.

As we can see from the two earlier subsections, in order to incorporate the stochastic effect, we need to do the following

- Find the master equations corresponding to the mean field equations (5.18, 5.19),

- Formulate the generating functions for these master equations,

- Solving the hyperbolic system of these generating functions,

- Find the TCP formula.

In the mean time, we need to verify that the two special cases arrive in each step for $f = 1$ and $f = 0$, respectively.

In order to verify the two special cases in each step, we re-arrange the first two terms in equation (5.18), and rewrite (5.18, 5.19) as follows:

$$\frac{d}{dt}a = \mu f a - \mu(1-f)a + \gamma q - h_a(t)a \tag{5.20}$$

$$\frac{d}{dt}q = \mu(1-f)a + \mu(1-f)a - \gamma q - h_q(t)q. \tag{5.21}$$

The proliferation terms in (5.18, 5.19) can be understood as a loss term $-\mu a$ in (5.18) for the mother cells which undergo mitosis, and two gain terms $+2\mu f a$ in (5.18) and $+2\mu(1-f)a$ in (5.19) for new daughter cells which choose active or quiescent compartment, respectively. The birth terms in (the equivalent) system (5.20, 5.21) allow a different interpretation: here a mother cell is only discarded from the active compartment, if it switches to the quiescent state, expressed through $-\mu(1-f)a$ in equation (5.20) and one component of $+\mu(1-f)a$ in (5.21). The additional daughter cell has the choice between active and quiescent compartment, which is modeled through $+\mu f a$ in (5.20) and $+\mu(1-f)a$ in (5.21). Formulation (5.18, 5.19) allows us to systematically derive the corresponding birth-death process in a consistent way.

In what follows I will derive the TCP formula step by step.

Step 1: Master equations corresponding to (5.20, 5.21).

Once again, let $P_i(t)$ and $Q_j(t)$ denote the probabilities that i active cancer cells and j quiescent cells are present at time t, respectively. We assume that initially we have a_0 active cells and q_0 quiescent cells, and $P_i(t) = 0, Q_j(t) = 0$ for $i, j < 0$, i.e.

$$P_{a_0}(0) = 1, \quad P_i(0) = 0 \text{ for } i \neq a_0, \tag{5.22}$$

$$Q_{q_0}(0) = 1, \quad Q_j(0) = 0 \text{ for } j \neq q_0. \tag{5.23}$$

The master equations describing the dynamics of these probabilities are

$$\frac{dP_i(t)}{dt} = \left(\mu(1-f) + h_a\right)(i+1)P_{i+1} + \mu f(i-1)P_{i-1} + \gamma \sum_{j=0}^{\infty} jQ_j P_{i-1}$$

$$- \left(\mu(1-f) + h_a\right)iP_i - \mu f i P_i - \gamma \sum_{j=0}^{\infty} jQ_j P_i. \tag{5.24}$$

$$\frac{dQ_j(t)}{dt} = (\gamma + h_q)(j+1)Q_{j+1} + \mu(1-f)\sum_{i=0}^{\infty} iP_i Q_{j-2}$$

$$-(\gamma + h_q)jQ_j - \mu(1-f)\sum_{i=0}^{\infty} iP_i Q_j. \tag{5.25}$$

When $f = 1$ and $Q_j = 0, j = 0, 1, \cdots$, then the above system coincides with (5.1) given by Zaider-Minerbo. On the other hand, when $f = 0$, (5.24, 5.25) go back to the master equation (5.12, 5.13) given by Dawson-Hillen, as expected. We can also verify by direct computation that the expected values

$$a(t) = \sum_{i=0}^{\infty} iP_i(t), \quad q(t) = \sum_{j=0}^{\infty} jQ_j(t). \tag{5.26}$$

satisfy equations (5.20) and (5.21) provided the series converge. Hence (5.20, 5.21) is the system of mean field equations for the above birth-death process.

Step 2: Formulating the generating functions.
The birth-death process in (5.24, 5.25) can be solved using the generating functions. We assume the generating functions

$$V(s,t) = \sum_{i=0}^{\infty} s^i P_i(t), \qquad W(s,t) = \sum_{j=0}^{\infty} s^j Q_j(t). \tag{5.27}$$

exist for $0 \leq s \leq 1$. To derive the differential equations of $V(s,t)$, $W(s,t)$, denote

$$b = \mu f, \qquad \delta = \mu(1-f) + h_a(t). \tag{5.28}$$

Equation for function V. Notice

$$\frac{\partial V(s,t)}{\partial s} = \sum_{i=0}^{\infty} s^{i-1} iP_i = \sum_{i=1}^{\infty} s^{i-1} iP_i. \tag{5.29}$$

The partial derivative of $V(s,t)$ with respect to t can be obtain by using (5.24)

$$
\begin{aligned}
\frac{\partial V(s,t)}{\partial t} &= \sum_{i=0}^{\infty} s^i \frac{dP_i(t)}{dt} \\
&= \sum_{i=0}^{\infty} s^i \Bigg[\delta(i+1)P_{i+1} + b(i-1)P_{i-1} + \gamma \sum_{j=0}^{\infty} jQ_j P_{i-1} \\
&\qquad\qquad - \delta i P_i - bi P_i - \gamma \sum_{j=0}^{\infty} jQ_j P_i \Bigg] \\
&= \delta \sum_{i=0}^{\infty} s^i (i+1)P_{i+1} + bs^2 \sum_{i=0}^{\infty} s^{i-2}(i-1)P_{i-1} + \gamma q(t)s \sum_{i=0}^{\infty} s^{i-1} P_{i-1} \\
&\qquad - \delta s \sum_{i=0}^{\infty} s^{i-1} i P_i + bs \sum_{i=0}^{\infty} s^{i-1} i P_i - \gamma q(t) \sum_{i=0}^{\infty} s^i P_i \\
&= \delta \frac{\partial V}{\partial s} + bs^2 \frac{\partial V}{\partial s} + \gamma q(t)sV - \delta s \frac{\partial V}{\partial s} + bs \frac{\partial V}{\partial s} - \gamma q(t)V, \qquad (5.30)
\end{aligned}
$$

where we use the index shifting in the last equation. Therefore, after reorganizing the terms, we obtain the hyperbolic equation for $V(s,t)$,

$$
\frac{\partial V}{\partial t} + (s-1)(\delta - bs)\frac{\partial V}{\partial s} = \gamma q(t)(s-1)V, V(s,0) = s^{a_0}. \qquad (5.31)
$$

Equation for function W. The derivation of the equation for $W(s,t)$ is similar. Following the above process, we obtain a hyperbolic partial differential equations for W as well,

$$
\frac{\partial W}{\partial t} + (\gamma + h_q(t))(s-1)\frac{\partial W}{\partial s} = \mu(1-f)a(t)(s^2-1)W, W(s,0) = s^{q_0}. \qquad (5.32)
$$

These equations for the generating functions coincide with those in Zaider and Minerbo [101] when $f = 1$, $q(t) = \sum_{j=0}^{\infty} jQ_j = 0$, and with those in Dawson and Hillen [20] when $f = 0$.

Step 3: Solving the system of generating functions.
We will use the method of characteristics to solve the above system, first for V and then for W.

Solution of function V. The equation (5.31) has the characteristic

equations

$$\frac{ds}{dt} = (1 - s)(bs - \delta), \qquad s(0) = s_0, \tag{5.33}$$

$$\frac{dV}{dt} = \gamma q(s - 1)V, \qquad V(s_0, 0) = s_0^{a_0}. \tag{5.34}$$

We introduce $y(t) = \frac{1}{1-s}$ to transform equation (5.33) into a linear equation for $y(t)$:

$$\frac{dy}{dt} = \frac{1}{(1-s)^2}\frac{ds}{dt} = (b - \delta)y(t) - b, \quad y(0) = \frac{1}{1 - s_0}. \tag{5.35}$$

The solution is

$$y(t) = \Lambda_a^{-1}(t)\left(y(0) - b\int_0^t \Lambda_a(y)dy\right),$$

where

$$\Lambda_a(t) = e^{-\int_0^t (b - \delta(z))dz}. \tag{5.36}$$

Therefore,

$$\frac{1}{1 - s(t)} = \Lambda_a^{-1}(t)\left(\frac{1}{1 - s_0} - b\int_0^t \Lambda_a(y)dy\right). \tag{5.37}$$

Consequently,

$$s_0 = 1 - \frac{1}{\frac{\Lambda_a(t)}{1-s(t)} + b\int_0^t \Lambda_a(y)dy}. \tag{5.38}$$

Equation (5.34) is linear in V and can be solved directly

$$V(s(t), t) = s_0^{a_0} \exp\left(\gamma\int_0^t q(z)\Big(s(z) - 1\Big)dz\right). \tag{5.39}$$

Since the right-hand side depends on the full characteristic path $s(z)$, we need to replace $s(z)$ through the end point $s(t)$. To do this, we observe from (5.38) that

$$s_0 = 1 - \frac{1}{\frac{\Lambda_a(t)}{1-s(t)} + b\int_0^t \Lambda_a(y)dy} = 1 - \frac{1}{\frac{\Lambda_a(z)}{1-s(z)} + b\int_0^z \Lambda_a(y)dy}. \tag{5.40}$$

Hence

$$s(z) - 1 = -\frac{\Lambda_a(z)}{\frac{\Lambda_a(t)}{1-s(t)} + b\int_z^t \Lambda_a(y)dy}. \tag{5.41}$$

Using this expression in (5.39), we get an explicit solution for V, namely

$$V(s, t) = \left(1 - \frac{1}{\frac{\Lambda_a(t)}{1-s} + b\int_0^t \Lambda_a(y)dy}\right)^{a_0} \exp\left(-\gamma\int_0^t q(z)\frac{\Lambda_a(z)}{\frac{\Lambda_a(t)}{1-s} + b\int_z^t \Lambda_a(y)dy}dz\right). \tag{5.42}$$

Again, we confirm that for $f = 1$, we have $b = \mu$, $\delta = h_a(t)$, when $q = 0$, $V(s,t)$ is consistent with the results of $A(s,t)$ in Zaider and Minerbo [101]. Similarly, for $f = 0$, we obtain $b = 0$, $\delta = \mu + h_a$, $V(s,t)$ is the same as the generating function $X(s,t)$ for $P_i(t)$ found in Dawson and Hillen [20].

Solution of function W. For solving W, we notice that equation (5.32) has the characteristic equations

$$\frac{ds}{dt} = (s-1)(\gamma + h_q(t)), \qquad s(0) = s_0, \tag{5.43}$$

$$\frac{dW}{dt} = \mu(1-f)a(s^2-1)W, \qquad W(s_0, 0) = s_0^{q_0}. \tag{5.44}$$

Therefore, by using the integrating factor method to the second equation, W has solution

$$W(s(t), t) = s_0^{q_0} \exp\{\int_0^t \mu(1-f)a(y)(s(y)^2 - 1)dy\}. \tag{5.45}$$

The initial condition s_0 can be expressed by $s(t)$ as

$$s_0 = 1 + (s-1)e^{-\int_0^t (\gamma + h_q(z))dz}. \tag{5.46}$$

If we let

$$\Lambda_q(t) = e^{\int_0^t (\gamma + h_q(z))dz}, \tag{5.47}$$

then $s_0 = 1 - \frac{1-s(t)}{\Lambda_q(t)}$. Therefore $W(s(t), t)$ can be expressed as

$$W(s(t), t) = \left(1 - \frac{1-s(t)}{\Lambda_q(t)}\right)^{q_0} \exp\{\int_0^t \mu(1-f)a(y)(s(y)^2 - 1)dy\}. \tag{5.48}$$

Here we use the fact that $s_0 = 1 - \frac{1-s(t)}{\Lambda_q(t)} = 1 - \frac{1-s(y)}{\Lambda_q(y)}$, and obtain the relations

$$s(y) - 1 = \frac{(s(t)-1)\Lambda_q(y)}{\Lambda_q(t)}, \tag{5.49}$$

$$s(y)^2 - 1 = \frac{(s(t)-1)^2\Lambda_q^2(y)}{\Lambda_q^2(t)} + 2\frac{(s(t)-1)\Lambda_q(y)}{\Lambda_q(t)}. \tag{5.50}$$

Then $W(s,t)$ can be expressed as

$$\begin{aligned} W(s,t) &= \left(1 - \frac{1-s}{\Lambda_q(t)}\right)^{q_0} \exp\left\{\mu(1-f)\int_0^t a(y)\frac{(s-1)^2\Lambda_q^2(y)}{\Lambda_q^2(t)}dy \right. \\ &\qquad \left. + 2\mu(1-f)\int_0^t a(y)\frac{(s-1)\Lambda_q(y)}{\Lambda_q(t)}dy\right\}. \end{aligned} \tag{5.51}$$

When $f = 0$, this solution is the same as the solution of $Z(s,t)$ found by Dawson and Hillen [20].

Step 4: TCP Formula.

Based on the explicit solution formulas for V in (5.42) and W in (5.51), the TCP is

$$
\begin{aligned}
TCP &= P_0(t)Q_0(t) = V(0,t) \cdot W(0,t) \\
&= \left(1 - \frac{1}{\Lambda_a(t) + \mu f \int_0^t \Lambda_a(z)dz}\right)^{a_0} \left(1 - \frac{1}{\Lambda_q(t)}\right)^{q_0} \cdot \\
&\quad \exp\left\{-\gamma \int_0^t q(z) \frac{\Lambda_a(z)}{\Lambda_a(t) + \mu f \int_z^t \Lambda_a(y)dy} dz + (1-f) \right. \\
&\quad \left. \left[\mu \int_0^t a(z)\frac{\Lambda_q(z)^2}{\Lambda_q(t)^2}dz - 2\mu \int_0^t a(z)\frac{\Lambda_q(z)}{\Lambda_q(t)}dz\right]\right\}, \quad (5.52)
\end{aligned}
$$

where Λ_a is given by (5.36) and Λ_q by (5.47). When $f = 1$, $q = 0$ we recover the TCP formula given by Zaider and Minerbo [101], as stated in equation (5.5). Similarly, when $f = 0$, we recover the TCP formula of Dawson and Hillen [20], namely (5.16).

5.4 TCP Formula for Cancer with Stem Cells

The traditional theory on cancer growth is that all the cancer cells have uncontrolled proliferation capability and are able to invade to neighboring tissues. Therefore, cancer treatment is based on the idea that cancer will be controlled by killing as many cancer cells as possible. However, it is now understood that not all the cells in a tumor function equally. In many cancers there exists a small population of cells which initiate and control the tumor. These cells are known as cancer stem cells (CSC). So far there is much evidence of the existence of CSC in leukaemias [9], brain cancer [78], prostate [15], liver [54] and other cancers.

Stem cells in normal tissue develop into differentiated cells through cell lineages, which begins at a self-renewing stem cell, progresses through transient and progenitor cells until finally producing fully differentiated cells. Cancer

stem cells are similar and they produce progenitor and transient cells which, in the case of cancer, will not fully differentiated into functioning tissue cells. For our modelling purpose we denote the cancer stem cells by CSC and the following lineage as TC (transient cancer cells). The cancer stem cell hypothesis [14] says that a small subpopulation of cells in a tumor consist of the cancer stem cells. Compared to the transient cancer cells (TC) with limited proliferation property, the cancer stem cells have infinite potential to self-renewal and differentiated into the heterogeneous cancer cells which consist of the bulk of the tumor. It is assumed that the stem cells can divide either symmetrically into two CSCs or two TC, or asymmetrically into one CSC and one TC. As proved by Hillen *et al* [39], this is mathematically equivalent to the assumption that a fraction f of daughter cells are stem cells and the other fraction $1 - f$ of daughter cells are TC.

Evidence showed the CSC can arise from the mutations of normal stem cells. There are several stages for the early progenitors of the CSC to undergo mutation until their progeny mature and form a tumor. Several researchers have studied this process by mathematical models, for example Ganguly and Puri [29], Marciniak-Czochra *et al* [58], Lo *et al* [51]. To simplify, Enderling *et al* [25] used an agent-based computer model to study the tumor with stem cells, they divided all the tumor cells into two compartments: one is CSC without death and the other is differentiated cancer cells with death. They found that the increased death rate of the differentiated cancer cells will result in the bigger tumor cluster, which is named as paradox of the tumor growth. Hillen *et al* [38] uses a pair of integro-differential equations to explain this paradox. Here, we consider a simplified two-compartment CSC model: one compartment for the CSC and the other for transient cancer cells (TC). The CSC can grow infinite times with rate μ and no natural death, while TC only have limited growth capability with rate ν and have death rate ρ. We assume that the CSC have self-renew fraction f, i.e., after each mitosis, a fraction f of daughter cells will stay in the CSC compartment and the other fraction $1 - f$ of daughter cells are differentiated into TC. Denote $a(t), q(t)$ as the population of CSC and

TC, the mean field equations for these two compartments are

$$\frac{da(t)}{dt} = 2f\mu a - \mu a \tag{5.53}$$

$$\frac{dq(t)}{dt} = 2(1-f)\mu a + \nu q - \rho q \tag{5.54}$$

When radiation treatment is applied to this tumor bulk, the mean field equations for this system are

$$\frac{da(t)}{dt} = 2f\mu a - \mu a - h_a(t)a \tag{5.55}$$

$$\frac{dq(t)}{dt} = 2(1-f)\mu a + \nu q - \tilde{h}_q(t)q \tag{5.56}$$

where $\tilde{h}_q$ is defined as (5.11) with natural death rate $d_q = \rho$ and h_a is defined as (5.10) with $d_a = 0$.

We will now derive a TCP formula following the steps we have done in Section 5.3. Let $P_i(t)$ and $Q_j(t)$ denote the probabilities that i CSC and j TC are present at time t, and their initial sizes are a_0 and q_0, respectively. The master equations describing the dynamics of these probabilities are

$$\frac{dP_i(t)}{dt} = (\mu(1-f) + h_a)(i+1)P_{i+1} + \mu f(i-1)P_{i-1}$$
$$- (\mu(1-f) + h_a)iP_i - \mu f iP_i, \tag{5.57}$$

$$\frac{dQ_j(t)}{dt} = \tilde{h}_q(j+1)Q_{j+1} + \nu(j-1)Q_{j-1} + \mu(1-f)\sum_{i=0}^{\infty} iP_iQ_{j-2}$$
$$-(\tilde{h}_q + \nu)jQ_j - \mu(1-f)\sum_{i=0}^{\infty} iP_iQ_j. \tag{5.58}$$

It is easy to verify by direct computation that the expected values

$$a(t) = \sum_{i=0}^{\infty} iP_i(t) \quad \text{and} \quad q(t) = \sum_{j=0}^{\infty} jQ_j(t) \tag{5.59}$$

satisfy equations (5.55) and (5.56) provided the series converge.

Notice (5.57) is a special case of (5.24) with $\gamma = 0$. Assume generating function $V(s,t) = \sum_{i=0}^{\infty} s^i P_i(t)$ exists for $0 \le s \le 1$, by results of steps 2 and step 3 in

Section 5.3, $V(s,t)$ satisfies

$$\frac{\partial V}{\partial t} + (s-1)\left(\mu(1-f) + h_a(t) - \mu f s\right)\frac{\partial V}{\partial s} = 0, \quad V(s,0) = s^{a_0}. \tag{5.60}$$

with solution

$$V(s,t) = \left(1 - \frac{1}{\frac{\Lambda_a(t)}{1-s} + \mu f \int_0^t \Lambda_a(y)dy}\right)^{a_0} \tag{5.61}$$

where

$$\Lambda_a(t) = e^{-\int_0^t (\mu f - (\mu(1-f) + h_a(z)))dz}. \tag{5.62}$$

As for the generating function for $Q_j(t)$, assume $W(s,t) = \sum_{j=0}^{\infty} s^j Q_j(t)$ exists for $0 \leq s \leq 1$. Similar mathematical calculation as in Section 5.3 tell us that $W(s,t)$ satisfies

$$\frac{\partial W}{\partial t} + \left(\tilde{h}_q - \nu s\right)(s-1)\frac{\partial W}{\partial s} = \mu(1-f)a(t)(s^2-1)W, \tag{5.63}$$

with initial condition $W(s,0) = s^{q_0}$. Notice that equation (5.63) differs from (5.32), since we have an additional birth term in (5.56) which is not present in (5.19).

Equation (5.63) has characteristic equation as

$$\frac{ds}{dt} = (1-s)(\nu - \tilde{h}_q) - \nu(1-s)^2, \quad s(0) = s_0, \tag{5.64}$$

$$\frac{dW}{dt} = \mu(1-f)a(t)(s^2-1)W, \quad W(s_0,0) = s_0^{q_0}. \tag{5.65}$$

The equation (5.64) is the same as (5.33) for $\nu = b, \tilde{h}_q = \delta$. Therefore, using the result of (5.38) from the previous section, we have

$$s_0 = 1 - \frac{1}{\frac{\Lambda_q(t)}{1-s(t)} + \nu \int_0^t \Lambda_q(y)dy}, \tag{5.66}$$

where

$$\Lambda_q(t) = e^{-\int_0^t \nu - \tilde{h}_q(z)dz}. \tag{5.67}$$

Equation (5.65) has the solution

$$W(s(t),t) = s_0^{q_0} \exp\left\{\int_0^t \mu(1-f)a(y)(s(y)^2-1)dy\right\}. \tag{5.68}$$

The term $s(y)$ in the integral depends on the values in the middle of the path which we do not know. Using the same trick as in Section 5.3, we rewrite $s(y) - 1$ and $(s(y) - 1)^2$ as

$$s(y) - 1 = -\frac{\Lambda_q(y)}{\frac{\Lambda_q(t)}{1-s(t)} + \nu \int_y^t \Lambda_q(z)dz}, \tag{5.69}$$

$$s(y)^2 - 1 = \left(\frac{\Lambda_q(y)}{\frac{\Lambda_q(t)}{1-s(t)} + \nu \int_y^t \Lambda_q(z)dz}\right)^2 - 2\frac{\Lambda_q(y)}{\frac{\Lambda_q(t)}{1-s(t)} + \nu \int_y^t \Lambda_q(z)dz}. \tag{5.70}$$

Then $W(s, t)$ can be expressed as

$$\begin{aligned}
W(s,t) = {} & \left(1 - \frac{1}{\frac{\Lambda_q(t)}{1-s(t)} + \nu \int_0^t \Lambda_q(z)dz}\right)^{q_0} \\
& \exp\left\{\mu(1-f)\int_0^t a(y)\left(\frac{\Lambda_q(y)}{\frac{\Lambda_q(t)}{1-s(t)} + \nu \int_y^t \Lambda_q(z)dz}\right)^2\right. \\
& \left. - 2\mu(1-f)\int_0^t a(y)\frac{\Lambda_q(y)}{\frac{\Lambda_q(t)}{1-s(t)} + \nu \int_y^t \Lambda_q(z)dz}dy\right\}. \tag{5.71}
\end{aligned}$$

Based on the explicit solution formulas for V in (5.61) and W in (5.71), the TCP for cancer with stem cells is

$$\begin{aligned}
TCP_{stem} = {} & P_0(t)Q_0(t) = V(0,t) \cdot W(0,t) \\
= {} & \left(1 - \frac{1}{\Lambda_a(t) + \mu f \int_0^t \Lambda_a(z)dz}\right)^{a_0} \left(1 - \frac{1}{\Lambda_q(t) + \nu \int_0^t \Lambda_q(z)dz}\right)^{q_0} \cdot \\
& \exp\left\{\mu(1-f)\left[\int_0^t a(y)\left(\frac{\Lambda_q(y)}{\Lambda_q(t) + \nu \int_y^t \Lambda_q(z)dz}\right)^2\right.\right. \\
& \left.\left. - 2\int_0^t a(y)\frac{\Lambda_q(y)}{\Lambda_q(t) + \nu \int_y^t \Lambda_q(z)dz}\right]dy\right\}, \tag{5.72}
\end{aligned}$$

where Λ_a, Λ_q are defined as in (5.62) and (5.67), respectively. We will show simulations in Section 5.5.2.

Model	Cell-Cycle Model		CSC model	
	Active	Quiescent	CSC	TC
Init.$M_1 = 10^6$	$a_0 + q_0 = M_1$		$a_0 + q_0 = M_1$	
Radio-sensitivity $\alpha(\text{Gy}^{-1})$	$\alpha_a = 0.145$	$\alpha_q = 0.159$	$\alpha_a = 0.159$	$\alpha_q = 0.145$
$\beta(\text{Gy}^{-2})$	$\beta_a = 0.0353$	$\beta_q = 0$	$\beta_a = 0$	$\beta_q = 0.0353$
Growth rate (day^{-1})	$\mu = 0.0655$	$\gamma = 0.0476$ (transition rate)	$\mu = 0.0476$	$\nu = 0.0655$

Table 5.1: **Parameters for simulation.** 'Cell-Cycle Model' is the generalized TCP model and 'CSC model' stands for the model with CSC. We switch the radiosensitivity parameter of the active and quiescent compartments to obtain those of CSC and TC compartments.

5.5 Numerical Simulations

5.5.1 Simulation for the Generalized Cell Cycle Model

In [20], Dawson and Hillen calculated the DH TCP with the choices of values for radiosensitive parameters: $\alpha_a = 0.145$ Gy^{-1}, $\beta_a = 0.070646/2$ Gy^{-2} for active cells and $\alpha_q = 0.159$ Gy$^{-1}, \beta_q = 0$ for quiescent cells. In addition, the growth rate is $\mu = 0.0655$ day^{-1} and transition rate $\gamma = 0.0467$ day^{-1}.

As we mentioned earlier, the cells in the quiescent compartment are less sensitive to the radiation, we expect that after the same treatment protocol, more cells will be left if more quiescent cells exist. When $f = 1$, all the cells are active, the TCP values should be bigger than those for other values of f, if the other parameters are the same. The smaller the values of f is, the smaller the TCP value should be.

To see this, we calculate the TCP for $f = 0$, 0.5 and 1 for fractionated treatment A and C in Table 3.1, where the doses delivered to the patient in each fraction are $d = 2$ Gy and $d = 3$ Gy, respectively. We run our simulation until Day 100. The simulations do match our expectations, as shown in Figure 5.4. Here we only show the graph for $d = 3$ Gy, similar results are obtained for $d = 2$ Gy.

However, this is not the case for the hyperfractionated treatment. We simulate
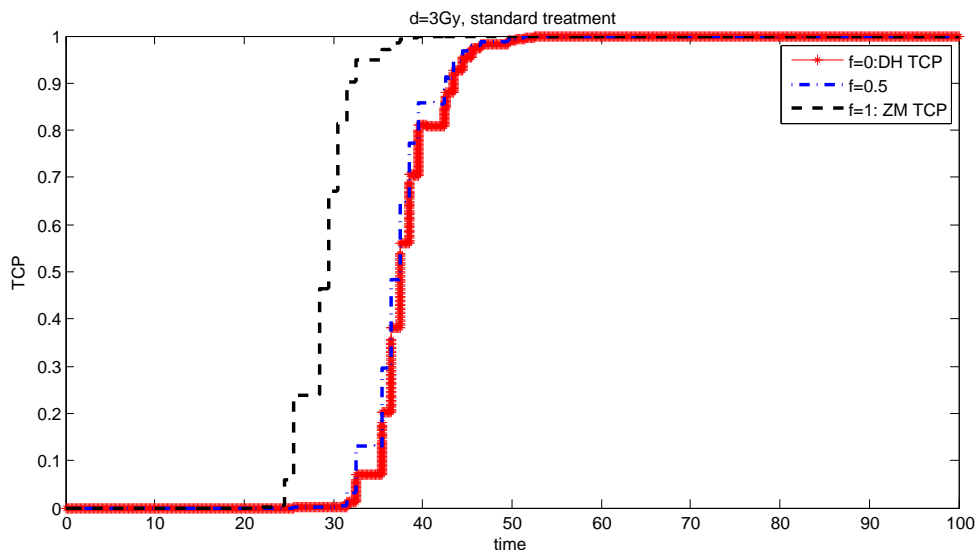
Figure 5.4: **TCP calculation for standard treatment 'C' in Table 3.1 ($d = 3$ Gy).** We calculate the values for $f = 0$ (DH TCP), $f = 0.5$ and $f = 1$ (ZM TCP) until Day 100. All the simulations have the same parameters: $\alpha_a = 0.145$ Gy^{-1}, $\beta_a = 0.070646/2$ Gy^{-2} for active cells and $\alpha_q = 0.159$ Gy^{-1}, $\beta_q = 0$ for quiescent cells. The birth rate for active cells is $\mu = 0.0655$ day^{-1} and transition rate for quiescent cells is $\gamma = 0.0467$ day^{-1}. The initial number of total cells $M_1 = 10^6$: for $f = 1, a_0 = M_1, q_0 = 0$, the other two fs have $a_0 = \frac{\gamma}{\mu+\gamma}M_1$ and $q_0 = \frac{\mu}{\mu+\gamma}M_1$. The other choices of fraction of the $a_0 + q_0 = M_1$ have similar results.

the hyperfractionated treatment d (d=1.2 Gy) and represent the results in Figure 5.5. A similar graph is obtained for treatment c ($d = 1.5$ Gy). We find that $f = 0$ (DH TCP), $f = 0.5$ and $f = 1$ (ZM TCP) have quite a similar TCP prediction.

Therefore, ZM TCP will overestimate the tumor killing when the dose per fraction is high (like 2Gy and 3Gy), but for a lower dose or proper choice of parameters, the three TCP models are equivalent.

In Hillen *et al* [37], we also compared the ZM TCP and DH TCP, we found that the ZM TCP model has a much bigger TCP value after the same treat-
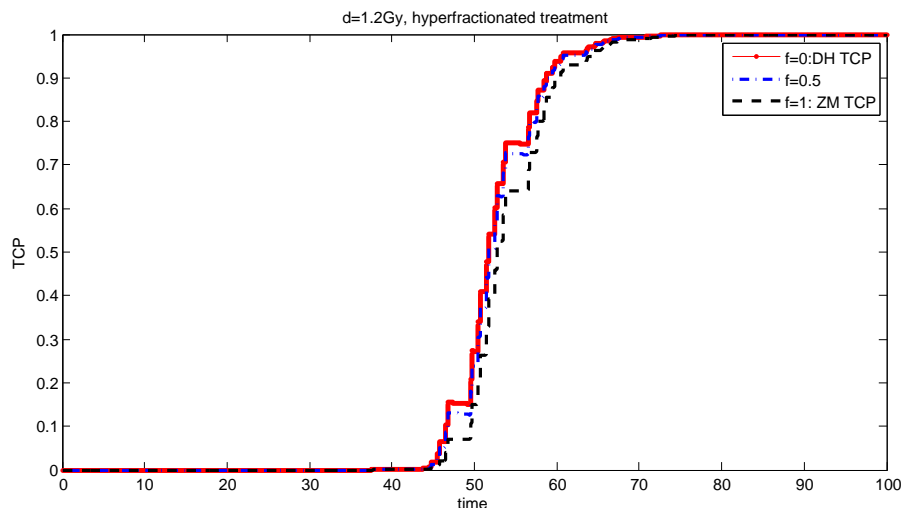
Figure 5.5: **TCP calculation for hyperfractionated treamtment 'd' in Table 3.1** ($d = 1.2$ **Gy**). We calculate the values for $f = 0$ DH TCP, $f = 0.5$ and $f = 1$ ZM TCP. All the parameters are chosen the same as those used in Figure 5.4.

ment, this happens because we have different choices of hazard function in our simulation, where we use hazard function (2.51) for ZM TCP and (2.52) for DH TCP.

In Gong *et al* [31], we summarized the hazard function in one framework and also simulated the ZM TCP with a weighted growth rate based on the mean time that a cell spends in active compartment $1/\mu$ or $1/\gamma$ in quiescent compartment (see Thieme [84] for the mean time derivation). Similar results as Figure 5.5 are obtained: ZM TCP has the same result as DH TCP if cells in ZM model take the weighted growth rate and radiosensitivity parameters.

5.5.2   Simulation for Cancer with Stem Cells

In this subsection, we simulate the TCP for cancers with stem cells. Cancer stem cells are less sensitive to radiation than the transient cancer cells. Therefore, we switch the radiosensitive parameters of the active cells and quiescent compartments to obtain those for CSC and TC (see Table 5.1): $\alpha_a = 0.159$
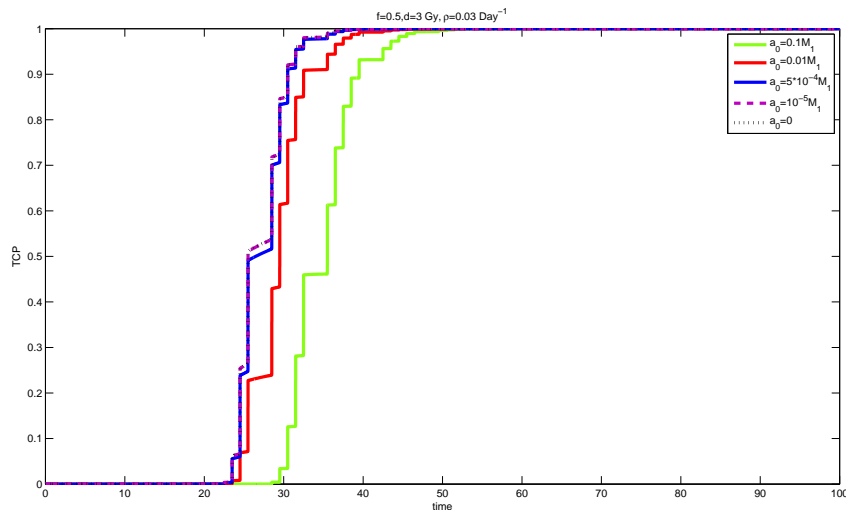
Figure 5.6: **TCP calculation for various initial fraction of CSC within** 10^6 **cells.** We calculate five initial fractions of CSC in a tumor cluster with 10^6 cells: from right to left, we have $a_0 = p * M_1$ for $p = 0.1$ (green solid), 0.001 (red solid), $5 \cdot 10^{-4}$ (blue solid) and 10^{-5} (purple dashed) and 0 (black dash-dot). Parameters chosen here are: self-renewal fraction is $f = 0.5$, birth rate and radiosensitive parameter are listed in Table 5.1. This is for the result for the standard treatment 'C' ($d = 3$ Gy) in Table 3.1. For the other treatments, we have similar graphs.

Gy^{-1}, $\beta_a = 0$ for CSC and $\alpha_q = 0.145$ Gy^{-1}, $\beta_q = 0.0353$ Gy^{-2} for TC. Villadsen *et al* [91] showed, through the study of adult human breast, the cancer stem cell in ducts are essentially quiescent while the progenitor cells in the lobules divide more actively. Here, we choose the growth rate as $\mu = 0.0467$ day^{-1} and $\nu = 0.0655$ day^{-1}, respectively.

Enderling *et al* [25] found the inclusion of CSC is necessary for the tumor cluster to grow. Therefore, we first study the effect of varying initial fraction of CSC in the tumor cluster consisting of $M_1 = 10^6$ cells in Figure 5.6. For the same initial tumor size, we find that the smaller numbers of CSC in the tumor, the easier the tumor can be treated. Figure 5.6 is for standard treatment 'C'($d = 3$ Gy) in Table 3.1. We have similar results for other treatment schedules.
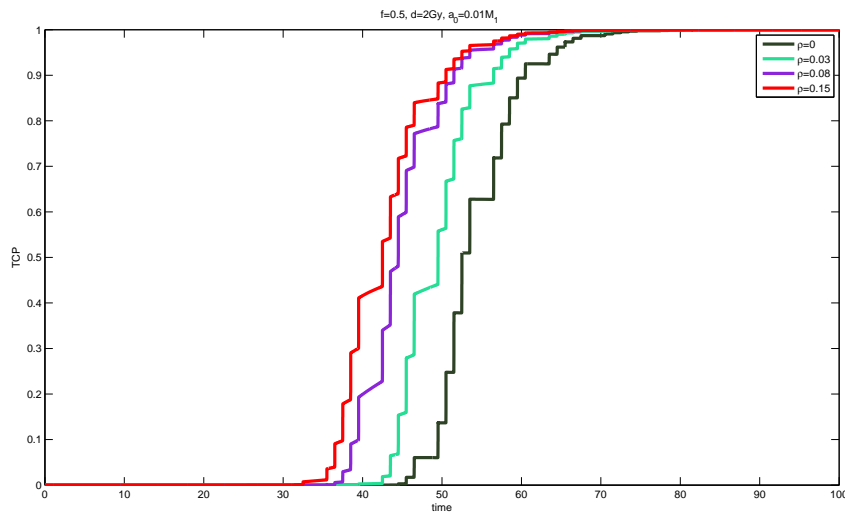
Figure 5.7: **TCP calculation of CSC for various death rate for treatment 'B' in Table 3.1 ($d = 2$ Gy).** From right to left, we calculate the death rates $\rho = 0$, 0.03, 0.08, 0.15 day $^{-1}$. Parameters chosen are the same as those in Figure 5.6 except $f = 0.5, a_0 = 0.01M_1$.

Enderling *et al* [25] also found a paradox of tumor growth: a larger death rate of transient cancer cells will result in a bigger tumor cluster. The effect of the death rate in our simulations is reported in Figure 5.7. Here we choose the same parameters as the Figure 5.6, except we fix the initial fraction of CSC as 0.01 and consider variable death rates. A higher death rate of TC makes the tumor easy to be killed. This effect is less pronounced when the dose per fraction is high as shown in Figure 5.8. We do not observe the same paradox as Endering *et al* [25] reported, since the tumor growth paradox arises as a result of competition for space in a fully populated tumor. Through radiation treatment the tumor density is small and space-restrictions are no longer relevant. Hence the tumor growth paradox is not observed here.

Figure 5.9 and 5.10 report the effect of the self-renewal fraction f of CSC to the calculation of TCP for standard treatment 'C' ($d = 3$ Gy) and hyperfractionated treatment 'd' ($d = 1.2$ Gy) in Table 3.1, respectively. Here we fix the initial CSC $a_0 = 0.01M_1$, the death rate of TC is $\rho = 0.03$ day^{-1}. We can see from Figure 5.9 that a smaller self-renewal fraction f of CSC makes
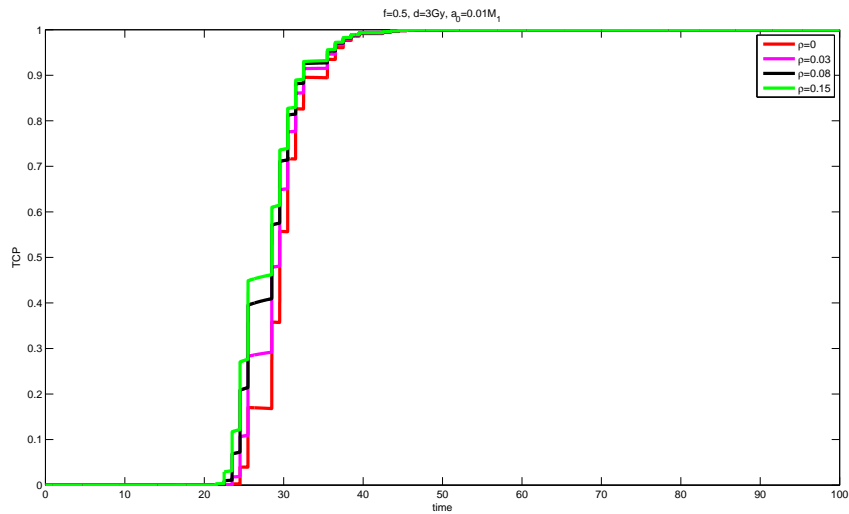
Figure 5.8: **TCP calculation of CSC for various death rate for treatment 'C' in Table 3.1 ($d = 3$ Gy).** From right to left, we calculate the death rates $\rho = 0$, 0.03, 0.08, 0.15 day $^{-1}$. Parameters chosen are the same as those in Figure 5.6 except $f = 0.5, a_0 = 0.01M_1$.

it easier to control the cancer for treatment 'C'. The similar graph is found for treatments 'A, B' (d=2 Gy)in Table 3.1. However, for hyperfractionated treatment 'd' with $d = 1.2$ Gy, the different self-renewal fractions f have no effect on the TCP values, as we can see in Figure 5.10. That is, the effect of the differentiation of cancer cells becomes dominant for large dose per fraction. These simulations confirm the general trend that was found for the cell cycle model: the inclusion of quiescent cells leads to different simulations for large dose per fraction.
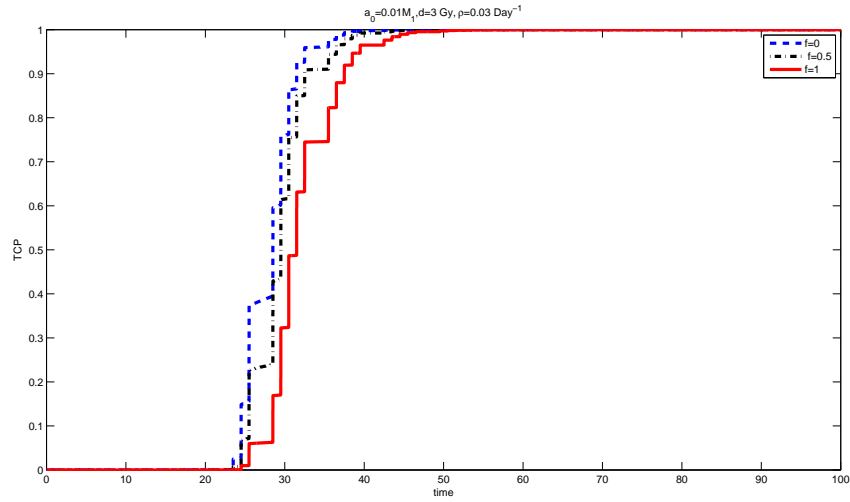
Figure 5.9: **TCP calculation of CSC for various self-renewal fraction for standard treatment 'C' in Table 3.1 ($d = 3$ Gy).** From left to right, we calculate the self-renewal fractions $f = 0$, 0.5, 1, respectively. Parameters chosen are the same as those in Figure 5.6 except $a_0 = 0.01M_1$.
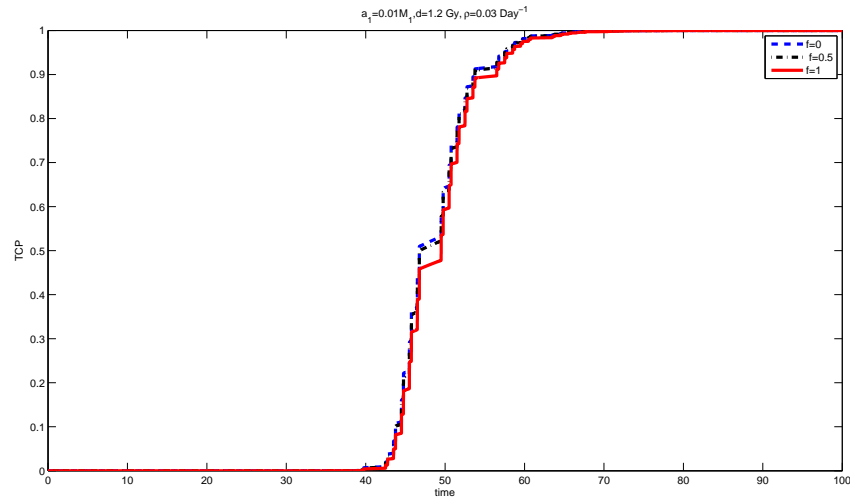
Figure 5.10: **TCP calculation of CSC for various self-renewal fractions for hyperfractonated treatment 'd' in Table 3.1 ($d = 1.2$ Gy).** From left to right, we calculate the self-renewal fraction $f = 0$, 0.5, 1, respectively. Parameters chosen are the same as those in Figure 5.6 except $a_0 = 0.01M_1$.

Chapter 6

Normal Tissue Complication Probability Model

Generally speaking, normal tissues will inevitably be damaged during the tumor external beam radiotherapy. Oncologists need to quantify the normal tissue complication of a treatment to make sure those complications are bearable for the patients. The cumulative radiation effect (CRE) model has been suggested by Fowler [28] not to be used any more. Another kind of model to measure the complication is the normal tissue complication probability (NTCP), which is defined as the probability that normal tissues cannot function properly after radiation exposure. The existent NTCP models are quite few. In this chapter, I will first review two existent NTCP models in Section 6.1 and 6.2. Then, in Section 6.3, I use a birth-death process to derive a NTCP model characterized by logistic growth. The calculation of NTCP will also provide an alternative proof to the formula proposed by Hanin [36] to compute the probability distribution $P_i(t)$ of tumor cell amount from the generating function $A(s, t)$. Simulations are given in Section 6.4.

6.1   Lyman NTCP Model

The simplest NTCP model is Lyman NTCP proposed by Lyman in 1985 [53], in which it describes a sigmoidal dose-response curve of normal tissue as a

function of given dose D delivered on a fractional volume v,

$$NTCP_{\text{Lyman}}(D) = \frac{1}{\sqrt{2\pi}} \int_{-\infty}^{z} e^{-s^2/2} ds, \tag{6.1}$$

where the upper limit z is determined by

$$z = \frac{D - TD_{50}(v)}{m \cdot TD_{50}(v)}, \tag{6.2}$$

Here $TD_{50}(v)$ is the tolerance dose for a given partial volume (v) so that the $NTCP = 0.5$, it relates the tolerance dose for whole organ $TD_{50}(1)$ as

$$TD_{50}(v) = TD_{50}(1)v^{-n}, \quad 0 < n \leq 1. \tag{6.3}$$

m, n are two parameters depending on the type of tissues. Equation (6.3) comes from the power law of the isoeffect dose [76]: the multiplication of the n-th power of the radiated fractional volume v and the dose delivered on it D_v remains constant. If $D_{v_1}, D_{v_2}, D_{\text{whole}}$ are delivered to a partial volume of v_1, v_2 and the whole organ, respectively, this power law says,

$$v_1^n D_{v_1} = v_2^n D_{v_2} = D_{\text{whole}} 1^n. \tag{6.4}$$

Equation (6.1) can also be written as an integral over the normal distribution with mean value TD_{50} and standard derivation $m \cdot TD_{50}$,

$$NTCP_{\text{Lyman}}(D) = \frac{1}{\sqrt{2\pi}m \cdot TD_{50}} \int_{-\infty}^{D} e^{-\frac{1}{2}\left(\frac{D' - TD_{50}}{m \cdot TD_{50}}\right)} dD'. \tag{6.5}$$

This allows an interpretation of m as the ratio of the standard derivation and mean-value.

This NTCP model is only applicable for a uniformly distributed treatment, that is the dose D is uniformly delivered to the volume fraction of v. However, in daily practice, three dimensional (3D) CT scanned images are used in computerized treatment planning systems to generate a 3D non-uniformly distributed dose. In order to make the 3D image easy to read, the dose-volume histogram (DVH) is used to reduce the 3D treatment planning dose distributions into a one dimensional graph of dose D, which is a function of fractional

volume v against delivery dose D, representing that fractional volume v receives total dose D.

The DVH can be represented in two ways: differential DVH or cumulative DVH. In both DVH graphs, the x-axis denotes the dose delivered and the y-axis denotes fraction of volume, but the meanings of the y-coordinate are different: in the differential DVH, the height of each point shows the fraction of volume that receives the particular dose denoted by the x-coordinate; while in the cumulative DVH, each height represents the fraction of volume which receives greater than or equal to a dose given by the x-coordinate. The cumulative DVH is more often used and a typical cumulative DVH is displayed in Figure 6.1.
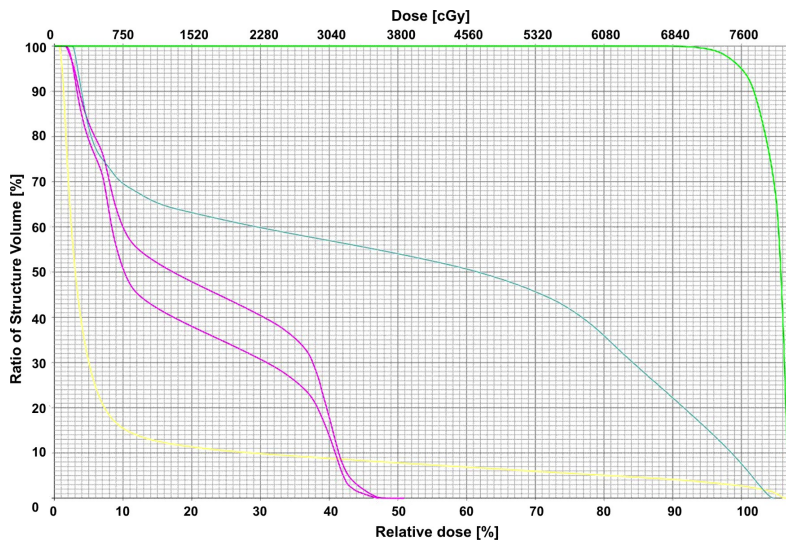
Figure 6.1: **An example of dose-volume histogram (DVH) for prostate.** The green line is planning target volume, blue line is for rectum, brown is for bladder and the purple lines are for right and left femurs. The bottom x-axis is relative dose and the top x-axis is the total dose (cGy). This figure is generously provided by Dr. Colin Field and Prof. Matthew Parliament from Cross Cancer Institute at University of Alberta.

In order to reduce the nonuniform dose distribution into an equivalent uniform dose, several methods exist and one widely used method is proposed by Kutcher and Burman [47]. They first approximated the irregular shaped DVH

graph by some step functions (see Figure 6.2). The area underneath the step functions could be divided into several rectangles with height Δv_i and length D_i (see area shaded by back slashes). The longest rectangle has length $D_{\max}$, the maximal dose in the DVH graph (e.g. 7600 cGy in Figure 6.1), it is also called the reference dose. For each rectangle with height Δv_i, it is equivalent to the treatment of delivering $D_{\max}$ uniformly onto a fractional volume of $\Delta v_{i\text{eff}}$ (shaded by forward slashes in Figure 6.2),

$$\Delta v_{i\text{eff}} = \Delta v_i \left(\frac{D_i}{D_{\max}} \right)^{1/n}, \tag{6.6}$$

that means, delivering dose D_i to a fraction volume of Δv_i has the same dose effect as the treatment of delivering dose $D_{\max}$ to a fraction volume of $\Delta v_{i\text{eff}}$. The total effective treatment volume is given by the summation of all these $\Delta v_{i\text{eff}}$,
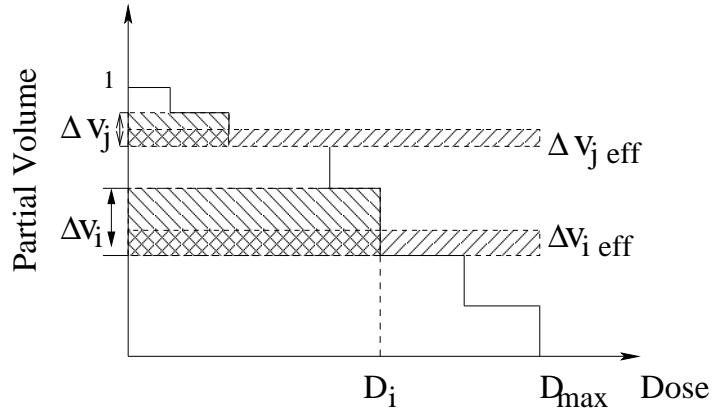
Figure 6.2: **DVH approximation by step function and calculation of effective volume.** The step functions are first used to approximate the DVH graph. As denoted above, areas below the step functions can be divided into rectangles with height Δv_i and length D_i (area shaded by back slashes). The treatment denoted by rectangle with height Δv_i can be reduced to an equivalent treatment of delivering $D_{\max}$ onto fractional volume of $\Delta v_{i\text{eff}}$ (shaded by forward slashes). The summation of these fractional volumes results in v_{eff}. Graph redrawn from [47].

97

$$v_{\text{eff}} = \sum_i^M \Delta v_{i\text{eff}} = \sum_i^M \Delta v_i \left(\frac{D_i}{D_{\max}}\right)^{1/n} = \int_{v_{min}}^{v_{max}} \left(\frac{d(v)}{D_{\max}}\right)^{1/n} dv. \qquad (6.7)$$

where in the last equation, we give a mathematical calculation for v_{eff} which does not need all these step functions. This can be easily done by data fitting to obtain the function of dose against fraction volume $d(v)$ and then integrate at interval $[v_{min}, v_{max}]$.

Using this method, the dose distribution represented by the DVH graph has been switched to an equivalent uniform treatment of delivering $D_{\max}$ into a partial volume v_{eff}. The upper limit z in (6.1) can now be determined from the DVH as

$$t = \frac{D_{\max} - TD_{50}(v_{\text{eff}})}{m \cdot TD_{50}(v_{\text{eff}})}, \qquad (6.8)$$

where $D_{\max}$ are given from the DVH graph and v_{eff} is calculated by (6.7) from the DVH graph and $TD_{50}(v_{\text{eff}}) = TD_{50}(1) \cdot v_{\text{eff}}^{-n}$, $0 < n \le 1$. This model is also referred as Lyman-Kutcher-Burman NTCP model. Besides this method, Niemierko [64] proposed the idea of reducing DVH dose distribution into an uniform treatment of delivering the *equivalent uniform dose* (EUD) to the whole organ. But whether to choose $D_{\max}$ delivered onto effective volume v_{eff}, or EUD onto the whole organ, or any other combination of dose and volume, it does not matter because Luxton *et al* [52] proved that the result of the Kutcher-Burman reduction is independent of the choice of the reference dose. This model is simple, only three parameters m, n and $TD_{50}(1)$ need to be determined. These three parameters have been estimated for a number of organs in Burman *et al* [10] by fitting data summarized by Emami *et al* [24]. One main criticism of these parameters is that many data in Emami *et al* [24] are based on the clinical prediction or experience, rather than experimental or clinical data. Afterwards, people continue to work on the parameter fitting based on clinical data, examples are Semenenko *et al* [77] for pneumonitis and xerostomia, Peeters *et al* for prostate cancer [69], Dawson *et al* for liver [20]. However, recently Daly *et al* [17] pointed out that it cannot be used for the spinal cord.

Figure 6.3: **The steps for the organ to be damage.**

6.2 Critical Volume NTCP Model

Compared to the Lyman NTCP, the critical volume NTCP model is more mechanistic because it includes the tissue structure in the model. The spatial distributions of normal tissues are divided into two categories: parallel or serial [11]. A parallel structure organ consists of cells that simultaneously maintain their function. Therefore, the organ can still function correctly after a significant fraction of the organ is damaged. Instead, a small damage to serial structural organ will result in losing its functions [11].

The critical volume NTCP considers the parallel organ structure in its model derivation [40, 65]. The basic assumption of this model is that organs are composed of functional subunits (FSU), the smallest tissue element capable of performing biological function. Examples of FSUs are renal tubules in kidney and lobules in liver. Therefore, any damage to an organ has a three-level hierarchy as shown in Figure 6.3.

To simplify the model, authors in [40, 65] further assumed that

(1). An organ is damaged only when a critical number of such FSUs is damaged. We denote this number as L.

(2). The probability of damaging one FSU after applied dose D is $P_{FSU}(D)$.

(3). FSU could be regenerated from a single surviving cell, therefore to make an FSU lose its function, all the cells in the FSU need to be inactivated.

(4). FSUs are identical and uniformly distributed through the organ.

Based on the assumption (2) to (4), if we use LQ survival fraction for each cell, and assume each FSU is composed of N_0 independent cells, then the P_{FSU} has the form of

$$P_{FSU}(D) = (1 - e^{-\alpha D - \beta D^2})^{N_0}. \tag{6.9}$$

99

where α, β are the radiosensitivities of the healthy organ cells.

The critical volume NTCP model is determined by survival number of FSUs. Take a homogeneous tissue with N numbers of such FSU for example, assume that the probability of the damaged numbers of FSU obeys a Binomial distribution, then the probability that M FSUs are damaged are

$$P(M) = \binom{N}{M} P_{FSU}(D)^M (1 - P_{FSU}(D))^{N-M}. \tag{6.10}$$

Based on the assumption (1), the probability of complication to the organ is

$$NTCP_{cv} = \sum_{M=L}^{N} P(M). \tag{6.11}$$

If the total number of FSU in the tissue, N, is quite large, we can use Normal distribution to approximate binomial distribution by the central limit theorem, i.e.,

$$NTCP_{cv} = \sum_{M=L}^{N} P(M) \approx \int_{L}^{\infty} P_{norm}(M) dM, \tag{6.12}$$

where

$$P_{norm}(M) = \frac{1}{\sqrt{2\pi} \, \text{var}(M)} \exp\left(\frac{-(M - \overline{M})^2}{2 \, \text{var}(M)^2}\right),$$

with $\overline{M} = N P_{FSU}(D)$ and $\text{var}(M)^2 = N P_{FSU}(D)(1 - P_{FSU}(D))$. The critical volume NTCP has the same form as Lyman $NTCP$ after rescaling of $t = \frac{M - \overline{M}}{\text{var}(M)}$.

$$NTCP_{cv} = \frac{1}{\sqrt{2\pi}} \int_{\frac{L-\overline{M}}{\text{var}(M)}}^{\infty} e^{-t^2/2} dt = \frac{1}{\sqrt{2\pi}} \int_{-\infty}^{\frac{\overline{M}-L}{\text{var}(M)}} e^{-t^2/2} dt = \Phi\left(\frac{\overline{M} - L}{\text{var}(M)}\right). \tag{6.13}$$

If an organ survives only when all the FSUs function properly, that is a serial structural organ and $L = 1$, the model is called critical element NTCP,

$$NTCP_{ce} = \sum_{M=1}^{N} P(M) = 1 - P(0) = 1 - (1 - P_{FSU})^N. \tag{6.14}$$

Stavrev *et al* [79] generalized the critical volume model, critical element model and the tumor control probability into one frame work.

In addition, Kallman *et al* [42] derived an NTCP model to consider the normal tissue as a combination of serial and parallel structures. In their model, an organ consists of n parallel structures, each parallel structure is a m-subunit serial structure. A parameter 'relative seriality' $s = \frac{m}{m*n} = \frac{1}{n}$ is used to describe the volume dependence of the normal tissue. For more details, I refer to the original paper [42].

6.3 NTCP Model Derived From a Birth-Death Process

Here we use the idea from Chapter 5 to derived a NTCP model from a birth death process. We assume all the cells are identical and independent, an organ works properly if more than L cells exists. Denote $P_i(t)$ the probability of i normal cells at time t, the normal tissue complication is defined as a probability

$$NTCP(t) = \sum_{i=0}^{L} P_i(t) \tag{6.15}$$

By the first principle, the master equation that describes the change of normal cells is

$$\frac{dP_0}{dt} = h(t)P_1, \tag{6.16}$$

$$\frac{dP_i}{dt} = \mu_{i-1}(i-1)P_{i-1} - (\mu_i + h(t))iP_i + h(t)(i+1)P_{i+1}, i \geq 1, \tag{6.17}$$

with $\mu_i, i \geq 1$ are birth rate depending on the states of the normal tissue and $h(t)$ is death rate chosen the same as (5.10) including both natural death and death induced by radiation.

It should be noted that here we model the regrowth of a population of healthy cell using one compartment only. In future studies we can include stem cells, differentiated cells and other cells of the corresponding cell lineage.

6.3.1 Birth Rate μ_i

Cell growth will decrease as the population increases because of depletion of growth factors and space limitation. Here, we choose the birth rate μ_i as a

decreasing function of state i,

$$\mu_i = \begin{cases} \mu(1 - \frac{i}{M}), & i = 1, 2, \cdots, M \\ 0, & otherwise. \end{cases} \tag{6.18}$$

where M is the carrying capacity and μ is a constant maximal growth rate. This choice of μ_i will make the number of the normal tissue cells stay below or equal to the carrying capacity M.

Lemma 6.3.1. *Assume μ_i is given by (6.18). If $P_i(0) = 0, i \geq M + 1$, then $P_i(t) = 0, i \geq M + 1, \forall t > 0$.*

Proof. Define $R_j(t) = \sum_{i=j}^{\infty} P_i(t), j \geq M + 1$. Then $R_j(0) = 0, j \geq M + 1$.

$$\frac{dR_{M+1}(t)}{dt} = \sum_{i=M+1}^{\infty} \frac{dP_i}{dt} = \mu_M M P_M - h(t)(M+1)P_{M+1}(t) \leq 0.$$

therefore $R_{M+1}(t) \leq 0$ but $R_{M+1}(t) \geq 0$ as the sum of probability, so $R_{M+1}(t) = 0$. Similarly, $R_j(t) = 0, j > M + 1$.

$$P_j(t) = R_j(t) - R_{j+1}(t) = 0, j \geq M + 1.$$

$\square$

This choice of μ_i can be considered as the nonlinear extension of those in Chapter 5, where the linear birth rate results in the mean field function satisfying exponential growth. We can prove that this μ_i will make the mean field function obeys logistic growth under certain assumption.

Theorem 6.3.2. *Assume μ_i is given by (6.18). Provided the series*

$$N(t) = \sum_{i=0}^{\infty} i P_i(t).$$

converges, then $N(t)$ is the mean field function of system (6.16, 6.17) and satisfies a differential equation:

$$\frac{dN(t)}{dt} = \mu N(t) \left(1 - \frac{N(t)}{M}\right) - h(t)N(t) + \frac{\mu}{M} \cdot Var(X). \tag{6.19}$$

where $Var(X)$ is the variance of normal tissues defined by $Var(X) = E\left((X - N(t))^2\right)$.

Proof. Taking derivative of $N(t)$ with respective to time t, we have

$$
\begin{aligned}
\frac{dN}{dt} &= \sum_{i=0}^{\infty} i \frac{P_i(t)}{dt} \\
&= \sum_{i=0}^{\infty} \left[\mu_{i-1} i(i-1) P_{i-1} - (\mu_i + h(t)) i^2 P_i(t) + h(t) i(i+1) P_{i+1}(t) \right] \\
&= \sum_{i=0}^{\infty} (i+1) i \mu_i P_i(t) - \sum_{i=0}^{\infty} (\mu_i + h(t)) i^2 P_i(t) + \sum_{i=0}^{\infty} h(t) i(i-1) P_i(t) \\
&= \sum_{i=0}^{\infty} (\mu_i - h(t)) i P_i(t) \\
&= \sum_{i=0}^{\infty} \left(\mu(1 - \frac{i}{M}) - h(t) \right) i P_i(t) \\
&= \mu N(t) - h(t) N(t) - \frac{\mu}{M} \sum_{i=0}^{\infty} i^2 P_i(t) \\
&= \mu \left(1 - \frac{N(t)}{M} \right) N(t) - h(t) N(t) + \frac{\mu}{M} \cdot \text{Var}(X),
\end{aligned}
$$

where in the last equation, we use the identity $\text{Var}(X) = E(X^2) - E(X)^2$.
Note: For $\text{Var}(X) \to 0$, we formally obtain the mean field logistic equation.

$\square$

6.3.2 Numerical Solution for Finite Dimensional System

We proved our choice of birth rate will guarantee a finite number of normal tissue cells. Let $P(t) = (P_0(t), P_1(t), \cdots, P_M(t))^T$, then the system (6.16, 6.17) can be written as:

$$\frac{dP}{dt} = AP. \tag{6.20}$$

where matrix A is given by

$$
A = \begin{pmatrix}
0 & h(t) & 0 & \cdots & 0 & 0 \\
0 & -(\mu_1 + h(t)) & 2h(t) & \cdots & 0 & 0 \\
0 & \mu_1 & -2(\mu_2 + h(t)) & \cdots & 0 & 0 \\
\vdots & \vdots & \vdots & \ddots & \vdots & \vdots \\
0 & 0 & 0 & \cdots & -(M-1)(\mu_{M-1} + h(t)) & Mh(t) \\
0 & 0 & 0 & \cdots & (M-1)\mu_{M-1} & -M(\mu_M + h(t))
\end{pmatrix} \tag{6.21}
$$
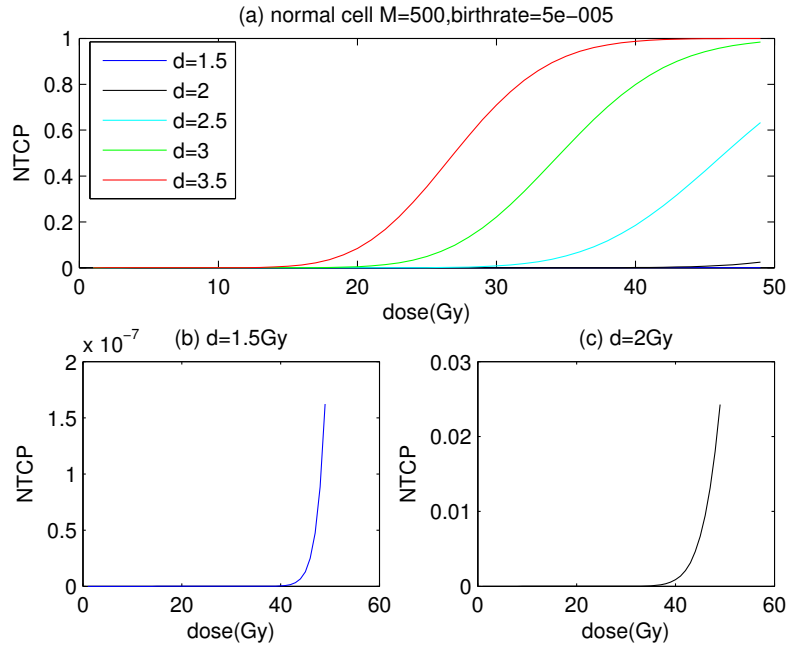
Figure 6.4: **NTCP as a function of dose.** NTCP is calculated by (6.15) and $P_i(t)$ are solution of system (6.20). (a) is NTCP figures for five different dose per fraction $d = 1.5, 2, 2.5, 3, 3.5$ Gy, respectively, (b) and (c) are for the two dose $d = 1.5$ and $d = 2$ Gy in (a) which we cannot see clearly. We choose radiosensitivity parameters $\alpha/\beta = 3$ for normal tissue with $\alpha = 0.06$, threshold of normal tissue complication as 5% of carrying capacity, i.e. $L = 5\%M$, the maximal birth rate $\mu = 5E - 005$ day^{-1} and the carrying capacity is $M = 500$.

We can see from matrix A that 0 is an absorbing state. when we have radiation, $h(t)$ includes both natural death rate and death induced by radiation, the same as (5.10) whereas $h(t)$ only contains natural death if no radiation is given to patients.

We solve this system numerically, and draw the $NTCP$ with respect to dose. The results are reported in Figure 6.4.

Restricted by the performance of the computer, we could only simulate NTCP for small number of carrying capacity M. In the next subsection, we will find a way to approximately calculate NTCP for large value of M.

6.3.3 Analytical Solution of $P_i(t)$

The system of (6.16, 6.17) can be solved analytically by introducing the generation function

$$A(s,t) = \sum_{i=0}^{\infty} P_i(t)s^i,$$

which satisfies the following equation,

$$\frac{\partial A}{\partial t} = \mu\left(1 - \frac{1}{M}\right)s(s-1)\frac{\partial A}{\partial s} + (1-s)h(t)\frac{\partial A}{\partial s} + \frac{\mu s^2}{M}(1-s)\frac{\partial^2 A}{\partial s^2},$$

$$(6.22)$$

When $M \to \infty$, we have the approximation

$$\frac{\partial A}{\partial t} = \mu s(s-1)\frac{\partial A}{\partial s} + (1-s)h(t)\frac{\partial A}{\partial s}, \qquad (6.23)$$

which is the same type of equation as that in (5.31) in Chapter 5 with $\gamma = 0, \mu = b$ and $h(t) = \delta$. It has a solution

$$A(s,t) = \left[1 - \frac{1}{\frac{\Lambda(t)}{1-s} + \mu \int_0^t \Lambda(y)dy}\right]^{N_0} = \left[\frac{\Lambda(t) + \mu(1-s)\int_0^t \Lambda(y)dy - 1 + s}{\Lambda(t) + \mu(1-s)\int_0^t \Lambda(y)dy}\right]^{N_0}.$$

$$(6.24)$$

where $\Lambda(t) = \exp\left(-\int_0^t (\mu - h(y))dy\right)$ and $N_0 = N(0)$ is the initial number of normal cells. In Chapter 5, we only calculate $P_0(t) = A(0,t)$ for tumor control probability. Here, in order to find NTCP, we need to find the distribution of $P_i(t), 0 \le i \le L$, which can be derived from $A(s,t)$ as well by

$$P_i(t) = \frac{1}{i!}\frac{\partial^i A(s,t)}{\partial s^i}\bigg|_{s=0}, i = 0, 1, \cdots. \qquad (6.25)$$

Therefore $NTCP(t)$ is

$$NTCP(t) = \sum_{i=0}^{L} P_i(t). \qquad (6.26)$$

Before we write down the formula for $P_i(t)$, we rewrite the (6.24) as follows

$$A(s,t) = \left[\frac{a(t) - b(t)s}{c(t) - d(t)s}\right]^{N_0}. \qquad (6.27)$$

where

$$a(t) = \Lambda(t) + \mu \int_0^t \Lambda(y)dy - 1, \tag{6.28}$$

$$b(t) = \mu \int_0^t \Lambda(y)dy - 1, \tag{6.29}$$

$$c(t) = \Lambda(t) + \mu \int_0^t \Lambda(y)dy, \tag{6.30}$$

$$d(t) = \mu \int_0^t \Lambda(y)dy. \tag{6.31}$$

In the following, we will use a, b, c, d to denote $a(t), b(t), c(t), d(t)$ for short. Reorganizing $A(s,t)$ as follows for further computation of $P_i(t)$,

$$A(s,t) = \left[\frac{a - bs}{c - ds}\right]^{N_0} = \left[\frac{b}{d} + \frac{ad - bc}{d}(c - ds)^{-1}\right]^{N_0} = \left[r + \delta(c - ds)^{-1}\right]^{N_0}.$$

where $r = \frac{b}{d}$ and $\delta = \frac{ad - bc}{d}$.

Lemma 6.3.3. $\forall k \geq 1$, the k-th derivative of $A(s,t)$ with respect to s is

$$\frac{\partial^k A}{k! \, \partial s^k} = \left[r + \delta(c - ds)^{-1}\right]^{N_0 - k} d^k \sum_{j=0}^{k-1} \binom{N_0}{k - j}\binom{k - 1}{j}\delta^{k-j}$$
$$(c - ds)^{-2k+j}\left[r + \delta(c - ds)^{-1}\right]^j. \tag{6.32}$$

Proof. First it is easy to check that (6.32) is right for $k = 1$.

$$\frac{\partial A}{\partial s} = N_0 \left[r + \delta(c - ds)^{-1}\right]^{N_0 - 1} \delta(-1)(c - ds)^{-2}(-d)$$
$$= \left[r + \delta(c - ds)^{-1}\right]^{N_0 - 1} d \sum_{j=0}^{0} \binom{N_0}{1}\binom{0}{0}\delta(c - ds)^{-2}.$$

Suppose (6.32) holds for $k = m$, that is

$$\frac{\partial^m A}{m! \, \partial s^m} = \left[r + \delta(c - ds)^{-1}\right]^{N_0 - m} d^m \sum_{j=0}^{m-1} \binom{N_0}{m - j}\binom{m - 1}{j}$$
$$\delta^{m-j}(c - ds)^{-2m+j}\left[r + \delta(c - ds)^{-1}\right]^j, \tag{6.33}$$

Taking derivative on both sides of (6.33), we have,

$$\frac{\partial^{m+1}A}{m!\,\partial s^{m+1}}$$

$$= (N_0 - m)\left[r + \delta(c - ds)^{-1}\right]^{N_0-m-1}\delta d(c - ds)^{-2}d^m$$

$$\sum_{j=0}^{m-1}\binom{N_0}{m-j}\binom{m-1}{j}\delta^{m-j}(c - ds)^{-2m+j}\left[r + \delta(c - ds)^{-1}\right]^j$$

$$+ \left[r + \delta(c - ds)^{-1}\right]^{N_0-m}d^m\sum_{j=0}^{m-1}\binom{N_0}{m-j}\binom{m-1}{j}\delta^{m-j}$$

$$\left[(-2m + j)(c - ds)^{-2m+j-1}(-d)\left(r + \delta(c - ds)^{-1}\right)^j\right.$$

$$\left.+(c - ds)^{-2m+j}j\left(r + \delta(c - ds)^{-1}\right)^{j-1}\delta d(c - ds)^{-2}\right]$$

$$= \left[r + \delta(c - ds)^{-1}\right]^{N_0-(m+1)}d^{m+1}$$

$$\left[\underbrace{\sum_{j=0}^{m-1}\binom{N_0}{m-j}\binom{m-1}{j}(N_0 - m)\delta^{m+1-j}(c - ds)^{-2m-2+j}\left[r + \delta(c - ds)^{-1}\right]^j}_{A}\right.$$

$$+\underbrace{\sum_{j=0}^{m-1}\binom{N_0}{m-j}\binom{m-1}{j}(2m - j)\delta^{m-j}(c - ds)^{-2m+j-1}\left(r + \delta(c - ds)^{-1}\right)^{j+1}}_{B}$$

$$\left.+\underbrace{\sum_{j=0}^{m-1}\binom{N_0}{m-j}\binom{m-1}{j}j\delta^{m+1-j}(c - ds)^{-2m+j-2}\left(r + \delta(c - ds)^{-1}\right)^j}_{C}\right]$$

Combining Part A and part C, we have

$$\sum_{j=0}^{m-1}\binom{N_0}{m-j}\binom{m-1}{j}(N_0-m+j)\delta^{m+1-j}(c-ds)^{-2m-2+j}\left[r + \delta(c - ds)^{-1}\right]^j \quad (6.34)$$

After shifting the index, part B changes into

$$\sum_{j=1}^{m}\binom{N_0}{m-j+1}\binom{m-1}{j-1}(2m - j + 1)\delta^{m+1-j}(c - ds)^{-2m-2+j}\left[r + \delta(c - ds)^{-1}\right]^j$$

$$(6.35)$$

Equations (6.34) and (6.35) both contain term

$$\delta^{(m+1)-j}(c - ds)^{-2(m+1)+j}\left[r + \delta(c - ds)^{-1}\right]^j,$$

only the coefficients and index are different. Now we check the coefficients for $j = 0, j = m$ and $1 \le j \le m$ separately.

When $j = 0$, the coefficient of $\frac{\partial^{m+1} A}{m! \, \partial s^{m+1}}$ only comes from equation (6.34) and can be rewrite as

$$
\begin{aligned}
\binom{N_0}{m-0}\binom{m-1}{0}(N_0 - m + 0) &= \binom{N_0}{m}(N_0 - m) \\
&= \binom{N_0}{m+1}(m+1),
\end{aligned}
$$

which is the binomial coefficients $\binom{N_0}{k-j}\binom{k-1}{j}$ in (6.32) for $k = m+1$ and $j = 0$, multiplied by a factor of $m + 1$.

For $j = m$, (6.35) contributes the coefficient of $\frac{\partial^{m+1} A}{m! \, \partial s^{m+1}}$ as

$$
\binom{N_0}{m-m+1}\binom{m-1}{m-1}(2m - m + 1) = \binom{N_0}{1}(m+1);
$$

which is the binomial coefficients in (6.32) for $k = m+1$ and $j = m$, with an extra multiplier $m + 1$ as well.

For $j = 1, \cdots, m - 1$, coefficients are the summation of those in (6.34) and (6.35):

$$
\begin{aligned}
&\binom{N_0}{m-j}\binom{m-1}{j}(N_0 - m + j) + \binom{N_0}{m-j+1}\binom{m-1}{j-1}(2m - j + 1) \\
=\ & \frac{N_0!(N_0 - m + j)}{(m-j)!(N_0 - m + j)!}\frac{(m-1)!}{j!(m-1-j)!} \\
&+ \frac{N_0!(2m + 1 - j)}{(m+1-j)!(N_0 - m - 1 + j)!}\frac{(m-1)!}{(j-1)!(m-j)!} \\
=\ & \frac{N_0!(m-1)!\left[(m+1-j)(m-j) + j(2m+1-j)\right]}{(m-j)!(N_0 - m + j - 1)!j!(m+1-j)!} \\
=\ & \frac{N_0!(m-1)!m(m+1)}{(m-j)!(N_0 - m + j - 1)!j!(m+1-j)!} \\
=\ & \frac{N_0!}{(N_0 - (m+1) + j)!(m+1-j)!}\frac{m!}{(m-j)!j!}(m+1) \\
=\ & \binom{N_0}{m+1-j}\binom{m}{j}(m+1).
\end{aligned}
$$

which is identical to the binomial coefficients in (6.32) times $m + 1$ when $k = m + 1$.

Therefore, we proved (6.32) holds for any $k \ge 1$ by induction. $\qquad \square$

Theorem 6.3.4. *The distribution of the normal tissue numbers can be calculated by the following*

$$P_k(t) = \left(\frac{a}{c}\right)^{N_0-k} \left(\frac{d}{c}\right)^k \sum_{j=0}^{k-1} \binom{N_0}{k-j} \binom{k-1}{j} \left(\frac{ad-bc}{dc}\right)^{k-j} \left(\frac{a}{c}\right)^j, \qquad (6.36)$$

for $k \geq 1$ and $P_0(t) = \left(\frac{a}{c}\right)^{N_0}$. where a, b, c, d are all function of t which are defined as (6.28-6.31).

Proof. Recall that $r = \frac{b}{d}$ and $\delta = \frac{ad-bc}{d}$, therefore by (6.32)

$$
\begin{aligned}
P_k(t) &= \frac{1}{k!} \frac{\partial^k A(s,t)}{\partial s^k}\bigg|_{s=0} \\
&= \left[r+\frac{\delta}{c}\right]^{N_0-k} \left(\frac{d}{c}\right)^k \sum_{j=0}^{k-1} \binom{N_0}{k-j} \binom{k-1}{j} \left(\frac{\delta}{c}\right)^{k-j} \left[r+\frac{\delta}{c}\right]^j \\
&= \left(\frac{a}{c}\right)^{N_0-k} \left(\frac{d}{c}\right)^k \sum_{j=0}^{k-1} \binom{N_0}{k-j} \binom{k-1}{j} \left(\frac{\delta}{c}\right)^{k-j} \left(\frac{a}{c}\right)^j.
\end{aligned}
$$

replacing δ by $\frac{ad-bc}{d}$, we obtain (6.36). $\qquad\square$

In [35], L. Hanin derived a formula for $P_k(t), k \geq 1$ for the distribution of tumor cell numbers from the k-th derivative of a rational function $\left[\frac{a-bs}{c-ds}\right]^{N_0}$, where his formula is

$$P_k(t) = \left(\frac{a}{c}\right)^{N_0} \left(\frac{b}{a}\right)^k \sum_{j=1}^{k} \binom{N_0+j-1}{j} \binom{k-1}{k-j} \left(\frac{ad-bc}{bc}\right)^j. \qquad (6.37)$$

The two formulas (6.36) and (6.37) look quite different from each other. But we could prove that the two formulas are equivalent to each other by the following Lemma.

Lemma 6.3.5. *Formula (6.36) and (6.37) are equivalent to each other.*

Proof. (6.36) could be written as

$$P_k(t) = \left(\frac{a}{c}\right)^{N_0} \left(\frac{d}{a}\right)^k \sum_{j=0}^{k-1} \binom{N_0}{k-j} \binom{k-1}{j} \left(\frac{ad-bc}{dc}\right)^{k-j} \left(\frac{a}{c}\right)^j$$

Times $\left(\frac{b}{d}\right)^k$ to $\left(\frac{d}{a}\right)^k$, $\left(\frac{d}{b}\right)^{k-j}$ to $\left(\frac{ad-bc}{dc}\right)^{k-j}$ and $\left(\frac{d}{b}\right)^j$ to $\left(\frac{a}{c}\right)^j$, we have,

$$
\begin{aligned}
P_k(t) &= \left(\frac{a}{c}\right)^{N_0}\left(\frac{b}{a}\right)^k \sum_{j=0}^{k-1}\binom{N_0}{k-j}\binom{k-1}{j}\left(\frac{ad-bc}{bc}\right)^{k-j}\left(\frac{ad}{bc}\right)^j \\
&= \left(\frac{a}{c}\right)^{N_0}\left(\frac{b}{a}\right)^k \sum_{l=k}^{1}\binom{N_0}{l}\binom{k-1}{k-l}\left(\frac{ad-bc}{bc}\right)^l\left(\frac{ad}{bc}\right)^{k-l}. \quad (6.38)
\end{aligned}
$$

Equation (6.38) has the same multipliers as (6.37) prior to the summation notation. We are going to only calculate the summation terms of (6.38). Denote $\Delta = \frac{ad-bc}{bc}$, $\frac{ad}{dc} = \Delta + 1$, the summation in (6.38) changes into

$$
\begin{aligned}
&\sum_{l=1}^{k}\binom{N_0}{l}\binom{k-1}{k-l}\Delta^l(\Delta+1)^{k-l} \\
&= \sum_{l=1}^{k}\binom{N_0}{l}\binom{k-1}{k-l}\Delta^l\sum_{i=0}^{k-l}\binom{k-l}{i}\Delta^i \\
&= \sum_{l=1}^{k}\binom{N_0}{l}\binom{k-1}{k-l}\sum_{i=0}^{k-l}\binom{k-l}{i}\Delta^{i+l}
\end{aligned}
$$

In order to compare (6.38) and (6.37), we need to check the coefficients of the term of $\Delta^{i+l} = \Delta^j$. The coefficient Δ^j of in the above equation is

$$
\begin{aligned}
&\sum_{l=1,i=j-l}^{j}\binom{N_0}{l}\binom{k-1}{k-l}\binom{k-l}{i} \\
&= \sum_{l=1}^{j}\binom{N_0}{l}\binom{k-1}{k-l}\binom{k-l}{j-l} \\
&= \sum_{l=1}^{j}\binom{N_0}{l}\frac{(k-1)!}{(k-l)!(l-1)!}\frac{(k-l)!}{(j-l)!(k-j)!} \\
&= \sum_{l=1}^{j}\binom{N_0}{l}\frac{(k-1)!}{(j-1)!(k-j)!}\frac{(j-1)!}{(j-l)!(l-1)!} \\
&= \binom{k-1}{k-j}\sum_{l=1}^{j}\binom{N_0}{l}\binom{j-1}{j-l} \quad\quad (6.39)
\end{aligned}
$$

while in (6.37), the coefficient of Δ^j is

$$
\binom{N_0+j-1}{j}\binom{k-1}{k-j} \quad\quad (6.40)
$$

By Chu-Vandermonde's identity [6], we have

$$\sum_{l=1}^{j} \binom{N_0}{l} \binom{j-1}{j-l} = \binom{N_0+j-1}{j} \tag{6.41}$$

because when $l = 0$, $\binom{j-1}{j-l} = 0$. This complete the proof that the two formulas are equivalent. $\qquad\square$

Simulations in Figure 6.5 also show that we have the same probability distribution as what Hanin obtained by using the parameter values listed in [35]. However, our formula take less time for the computation.
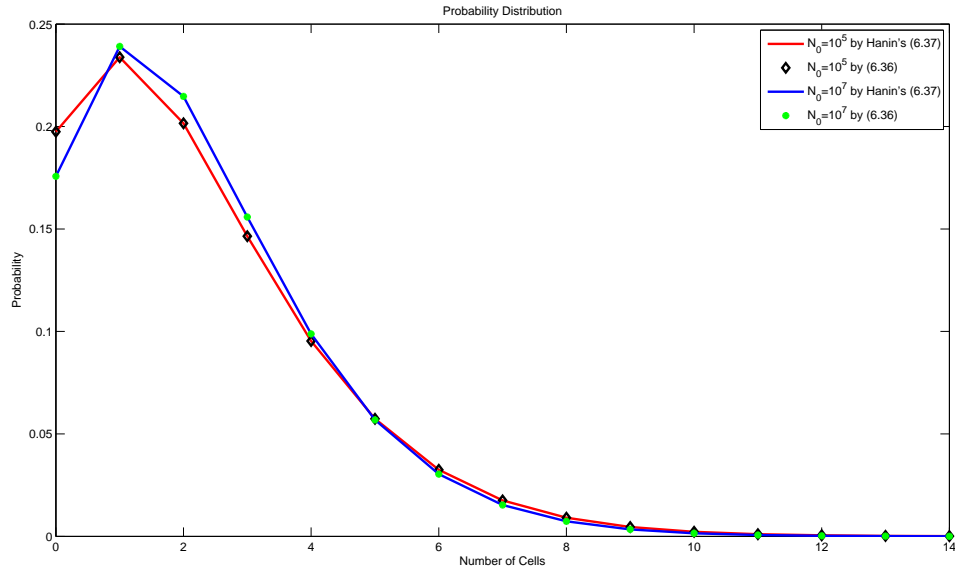
Figure 6.5: **Comparison of simulation by formula (6.37) and (6.36).** a, b, c, d are chosen the same as in Hanin [35] rather than calculated by (6.28-6.31).

It is obvious that we have formula for NTCP based on (6.26) and (6.36).

Theorem 6.3.6. *The Normal Tissue Complication Probability is*

$$NTCP = \sum_{k=0}^{L} P_k(t). \tag{6.42}$$

where $P_k(t)$ is in the form of (6.36).

111

6.4 Numerical Simulation

In this section, we are going to give some examples to calculate NTCP. We use formula (6.36) here. When the number of initial cells are large, the multiplications in formula (6.36) are huge. To reduce the number of multiplications, we rewrite it for the sake of efficient computation:

$$P_k(t) = \left(\frac{a}{c}\right)^{N_0} \left(\frac{ad - bc}{ac}\right)^k \sum_{j=0}^{k-1} \binom{N_0}{k-j} \binom{k-1}{j} \left(\frac{ad}{ad - bc}\right)^j \qquad (6.43)$$

Another challenge of the calculation by computer is that when N_0 is large, the binomial coefficient $\binom{N_0}{k-j}$ is out of the range that our computer can store, and the N_0 power of a smaller number $\frac{a}{c}$ will be close to 0. We are grateful for the advice from Professor L. G. Hanin at Idaho State University, and store the number and power separately. For example, $f = \binom{1000}{3} = 166167000$, we store this number by $f_1 = 0.166167$ with power $f_2 = 9$, then instead of f, we use $f_1 10^{f_2}$.

We calculate the NTCP for the standard treatment of $d = 2$ Gy with $N_0 = 10^5$ in Figure 6.6. The parameters we used are birth rate $\mu = 0.0655$ Day^{-1}, radiosensitive parameters $\alpha = 0.145$ Gy^{-1}, $\beta = 0.0353$ Gy^{-2}.
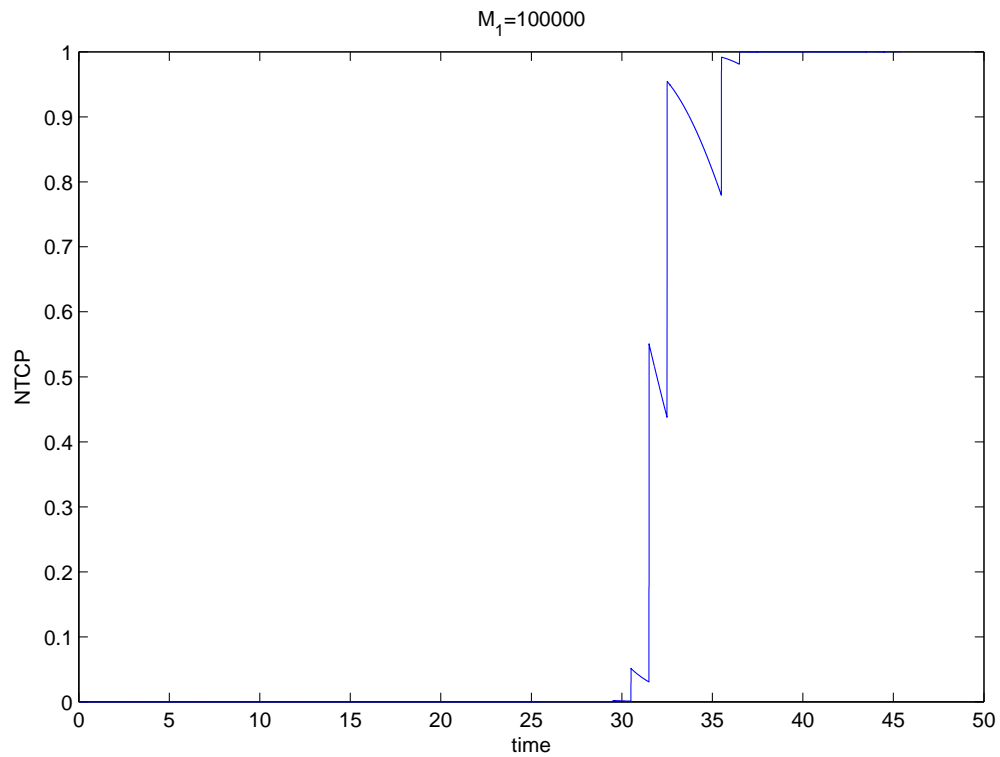
Figure 6.6: **NTCP calculation for initial normal cells** $N_0 = 10^5$. The treatment is standard treatment with dose $d = 2$ Gy, we calculate only until day around 45 days.

Chapter 7

TCP Based on the First Passage Time Problem

I modeled a stochastic process as a birth-death process to derive a TCP model in Chapter 5. In this Chapter, I study a stochastic process by its advection-diffusion equations: *the backward Kolmogorov equation* and *the first passage time problem*. I got inspired by the Ecology where this method was used to estimate the time taken for an animal to reach a specified site for the first time by McKenzie *et al* [60].

The first passage time problem is used to study the probability and the time that a random variable X arrives at a preset target for the first time. Applying this idea to tumor radiation treatment, I want to study the time needed for the numbers of tumor cells X to arrive at the target $X = 0$ and the probability that the number of tumor cells reduces to 0, which is the tumor control probability (TCP).

The Kolmogorov equation is a partial differential equation (PDE) of advection-diffusion type which describes the time evolution of the probability density function (p.d.f) of the position of the random variable. It is used as forward or backward Kolmogorov equation, where *forward* means future in time evolution, it is used to find a future time p.d.f, given the current position and *backward* refers to an earlier time, it is used to find a p.d.f at a previous time if current position is known. I will review the classical theory of both

Kolmogorov equations in Section 7.1.

Moreover, I will review the survival probability and mean first passage time problem related to the backward Kolmogorov equation in Section 7.2. In Section 7.3, I will extend the survival probability and the mean first passage time problem to tumor radiation treatment. Here I study two special cases where in both cases the tumor size X is in a finite domain $[0, M_0]$. The first case assumes that tumor can exit this domain either by treatment success at $x = 0$ or at $x = M_0$. This case results in a homogeneous boundary parabolic equation which can be solved using *splitting probability* which is the probability of exiting one boundary before hitting the other boundary. The other case supposes the tumor size at $x = M_0$ is uncontrollable: once the tumor reaches size $x = M_0$, it will persist until the patient dies, we call this *no hope boundary*. This case leads to an interesting and new boundary condition for the mean exit time equation. We will study this new problem in detail and we will show that the eigenfunction expansion of the tumor persistent probability results in the unbounded mean exit time. We finally give a conclusion in Section 7.4 for this method.

7.1 Backward and Forward Kolmogorov Equation

Suppose $X(t)$ is the random variable of positions (also called states) of the particle we are interested in. The allowable set of states of the random variable is the whole real line and the initial state is $X(t_0) = x_0$. For simplicity, we denote $p(x, t)$ as the probability density function ($p.d.f$) of the random variable $X(t)$: we define it as the conditional probability of a particle to stay at x at time t if a given initial state is $X(t_0) = x_0$, that is,

$$p(x, t) = p(x, t; x_0, t_0) = Prob\{X(t) = x | X(t_0) = x_0\}, t > t_0.$$

More generally, we can define the transition probability density function ($p.d.f$) of X as the probability of a particle to stay at y at time s if it is at x at an

earlier time t:

$$p(y, s; x, t) = Prob\{X(s) = y | X(t) = x\}, s > t$$

The $p.d.f$ is a special case of the transition $p.d.f$.

Besides the property of Markov chain (1.7) and Chapman-Kolmogorov equation

$$p(y, s; x, t) = \int_z p(y, s; z, \tau) p(z, \tau; x, t) dz, \quad s > \tau > t. \tag{7.1}$$

we further assume that the transition probability density function satisfies the following properties:

(1). The transition p.d.f $p(y, s; x, t)$ is continuously differentiable with respect to both space x, y and time t, s.

(2). Particles will always go somewhere. Therefore the transition p.d.f satisfies the following normalization equation,

$$\int_y p(y, s; x, t) dy = 1, \ s > t. \tag{7.2}$$

(3). For physical reason, $p(y, s; x, t)$ and all of its derivatives need to vanish at infinity [43].

It is sufficient to assume that $p(y, s; x, t) \geq 0$, $p \in C^1$ and $\int_x p(y, s; x, t) < \infty$, Then $\lim_{x \to \infty} p(y, s; x, t) dx = 0$. The same arguments hold for the other three variables.

Let us start with the *backward Kolmogorov equation*. Suppose Δt is a small time interval,

$$
\begin{aligned}
&p(y, s; x, t) - p(y, s; x, t - \Delta t) \\
=\ &p(y, s; x, t) - \int_z p(y, s; z, t) p(z, t; x, t - \Delta t) dz \\
=\ &p(y, s; x, t) \int_z p(z, t; x, t - \Delta t) dz - \int_z p(z, t; x, t - \Delta t) p(y, s; z, t) dz \\
=\ &\int_z p(z, t; x, t - \Delta t) \left[p(y, s; x, t) - p(y, s; z, t) \right] dz \\
=\ &-\int_z p(z, t; x, t - \Delta t) \left[\frac{\partial p(y, s; x, t)}{\partial x} (z - x) + \frac{\partial^2 p(y, s; x, t)}{\partial x^2} \frac{(z - x)^2}{2} \right] dz \\
&+ \int_z p(z, t; x, t - \Delta t) o\left((z - x)^3 \right) dz.
\end{aligned}
$$

Here we use Chapman-Kolmogorov equation (7.1) in the first equality and property (2) in the second equality. Divide Δt on both sides and take the limit of Δt approaching 0, we have

$$\frac{\partial p(y, s; x, t)}{\partial t} = -a(x, t)\frac{\partial p(y, s; x, t)}{\partial x} - \frac{b(x, t)}{2}\frac{\partial^2 p(y, s; x, t)}{\partial x^2}. \qquad (7.3)$$

where the drift coefficient is given by

$$a(x, t) = \lim_{\Delta t \to 0} \frac{1}{\Delta t} \int_z (z - x)p(z, t; x, t - \Delta t)dz, \qquad (7.4)$$

and the diffusion coefficient given by

$$\frac{b(x, t)}{2} = \lim_{\Delta t \to 0} \frac{1}{2\Delta t} \int_z (z - x)^2 p(z, t; x, t - \Delta t)dz. \qquad (7.5)$$

Note:

- Equation (7.3) is called *backward Kolmogorov equation*, which is normally used to solve the following problem: If we know that the position of the particle is at y at time s, what is the probability that it begins from x at a former time moment t. The initial condition of (7.3) is normally chosen as

$$p(y, s; x, s) = \delta(y - x). \qquad (7.6)$$

where $\delta(x)$ is the Dirac delta distribution, which is defined by its action on continuous function as,

$$\int_{\mathbb{R}} \delta(x)f(x)dx = f(0), \quad \forall f \in C^0(\mathbb{R}). \qquad (7.7)$$

Based on this definition, it is easy to see the following properties:

$$\int_{-\infty}^{\infty} \delta(x)dx = 1 \qquad (7.8)$$

$$\int_y f(y)\delta(y - x)dy = f(x) \qquad (7.9)$$

$$f(t)\delta(t - a) = f(a)\delta(t - a). \qquad (7.10)$$

For other properties of the Dirac δ−function, please see Evans [26].

- In the definition of $a(x,t)$ and $b(x,t)$, they both include the first order time step Δt, $a(x,t)$ includes the first order spatial moment, while $b(x,t)$ includes the second order spatial moment. Therefore $a(x,t)$ can be explained as the expected value of displacement of a particle in one step jump, $b(x,t)$ is the second moment of displacement of the particle in one step jump, characterizing the variance of each jump.

- The definition of $a(x,t)$ and $b(x,t)$, together with the following assumption,

$$0 = \lim_{\Delta t \to 0} \frac{1}{\Delta t} \int_z (z-x)^\delta p(z,t;x,t-\Delta t)dz, \delta > 2.$$

  make this Markov Process a diffusion process (see the books of L. Allen [2] and C. Gardiner [30]).

- **Time Homogeneous Case:** We say the transition p.d.f $p(y,s;x,t)$ is time homogeneous, if it only depends on the time interval and independent of the beginning and ending time moments, i.e.,

$$p(y,s;x,t) = p(y,0;x,t-s) = p(y,s-t;x,0), \qquad (7.11)$$

  The semigroup property (7.11) allows us to write a backward Kolmogorov equation (7.3) in a different way. We introduce $\tau := s - t \geq 0$ and write $p(y,s;x,t) = p(y,0;x,t-s) = p(y,s-t;x,0) = p(y,\tau;x,0)$, then $\frac{\partial}{\partial \tau} = -\frac{\partial}{\partial t}$ and the backward Kolmogorov equation (7.3) becomes

$$\frac{\partial p(y,\tau;x,0)}{\partial \tau} = a(x)\frac{\partial p(y,\tau;x,0)}{\partial x} + \frac{b(x)}{2}\frac{\partial^2 p(y,\tau;x,0)}{\partial x^2}. \qquad (7.12)$$

  Note: This equation looks like forward in time as $\tau > 0$, but the space derivative is with respect to the position x of the earlier time.

A closely related equation is the *forward Kolmogorov equation*. It is used to solve the following problem: given the state of the particles at a earlier time t, what is the probability distribution at a later time moment s. Therefore we need to find the transition p.d.f to solve it. The *forward Kolmogorov equation* can also be derived from the Chapman-Kolmogorov equation by using equation

(7.3).

$$
\begin{aligned}
&p(y, s + \Delta s; x, t) - p(y, s; x, t) \\
&= \int_z p(y, s + \Delta s; z, s)p(z, s; x, t)dz - p(y, s; x, t) \\
&= \int_z \left[p(y, s + \Delta s; z, s) - \delta(y - z) \right] p(z, s; x, t)dz \\
&= \int_z \left[p(y, s + \Delta s; z, s) - p(y, s + \Delta s; z, s + \Delta s) \right] p(z, s; x, t)dz \\
&= -\int_z \left[\left. \frac{\partial p(y, s + \Delta s; z, t)}{\partial t} \right|_{t=s} \Delta s + o(\Delta s)^2 \right] p(z, s; x, t)dz \quad (7.13)
\end{aligned}
$$

Using equation (7.3) for $\left. \frac{\partial p(y, s + \Delta s; z, t)}{\partial t} \right|_{t=s}$ and integrating by parts

$$
\begin{aligned}
&p(y, s + \Delta s; x, t) - p(y, s; x, t) \\
&= \Delta s \int_z \left[a(z, s)\frac{\partial p(y, s + \Delta s; z, s)}{\partial z} + \frac{b(z, s)}{2}\frac{\partial^2 p(y, s + \Delta s; z, s)}{\partial z^2} \right] p(z, s; x, t)dz \\
&\quad + \Delta s \int_z o(\Delta s)p(z, s; x, t)dz \\
&= \Delta s \int_z \left[-\frac{\partial\left(a(z, s)p(z, s; x, t)\right)}{\partial z} + \frac{\partial^2\left(\frac{b(z,s)}{2}p(z, s; x, t)\right)}{\partial z^2} \right] p(y, s + \Delta s; z, s)dz \\
&\quad + \left[a(z, s)p(z, s; x, t)p(y, s + \Delta s; z, s) + \frac{b(z, s)}{2}p(z, s; x, t)p(y, s + \Delta s; z, s) \right. \\
&\quad \left. \left. -\frac{\partial\left(\frac{b(z,s)}{2}p(z, s; x, t)\right)}{\partial z}p(y, s + \Delta s; z, s) \right] \right|_{z=\pm\infty} + o(\Delta s)^2 \quad (7.14)
\end{aligned}
$$

the non-integral terms will disappear in the last equation because of the property (3) that the transition *p.d.f* $p(z, s; x, t)$ and its derivative vanish at infinity. By dividing Δs on both sides and taking the limit of $\Delta s \to 0$, we have $\lim_{\Delta s \to 0} p(y, s + \Delta s; z, s) = \delta(y - z)$ and

$$
\frac{\partial p(y, s; x, t)}{\partial s} = -\frac{\partial\left(a(y, s)p(y, s; x, t)\right)}{\partial y} + \frac{1}{2}\frac{\partial^2\left(b(y, s)p(y, s; x, t)\right)}{\partial y^2}. \quad (7.15)
$$

where $a(y, s), b(y, s)$ are the same as in definition (7.4) and (7.5). Equation (7.15) is known as Fokker-Planck Equation, or forward Kolmogorov equation.

7.1.1 The Drift and Diffusion Coefficients Derived from a Discrete Random Walk

This derivation is given in A. Okubo and S. A. Levin in Chapter 5 [5].

In the following we will derive $a(x,t)$ and $b(x,t)$ from a discrete random walk. A random walk is a discrete space Markovian chain, i.e. $X(t)$ can only stay on the lattice $\cdots, x - \Delta x, x, x + \Delta x, \cdots$. Suppose the transition probability is defined as follows,

$$
\begin{aligned}
p(x + \Delta x, t + \Delta t; x, t) &= x\mu(t)\Delta t, & (7.16) \\
p(x - \Delta x, t + \Delta t; x, t) &= xh(t)\Delta t, & (7.17) \\
p(x, t + \Delta t; x, t) &= 1 - (h(t) + \mu(t)) x\Delta t, & (7.18) \\
p(x + k\Delta x, t + \Delta t; x, t) &= o(\Delta t)^2, \quad |k| \geq 2. & (7.19)
\end{aligned}
$$

where $\mu(t), h(t)$ represent the birth rate and death rate per capita, respectively, and x is denotes a population size. Define

$$
\begin{aligned}
R(x,t) &:= p(x + \Delta x, t + \Delta t; x, t) = \mu(t)x, & (7.20) \\
L(x,t) &:= p(x - \Delta x, t + \Delta t; x, t) = h(t)x. & (7.21)
\end{aligned}
$$

Therefore, $R(x,t), L(x,t)$ are the birth rate and death rate of the whole population, respectively. We have, by the discrete Chapman-Kolmogorov equation

$$
\begin{aligned}
p(x, t + \Delta t; y, \tau) &= R(x - \Delta x, t)\Delta t p(x - \Delta x, t; y, \tau) + o(\Delta t) \\
&\quad + L(x + \Delta x, t)\Delta t p(x + \Delta x, t; y, \tau) \\
&\quad + (1 - (L(x,t) + R(x,t))\Delta t) p(x, t; y, \tau). \quad (7.22)
\end{aligned}
$$

Expanding the both sides at $p(x, t; y, \tau)$ by Taylor series and taking $\Delta t \to 0$, we have

$$
\begin{aligned}
\frac{\partial p(x, t; y, \tau)}{\partial t} &= -\frac{\partial \left(\Delta x \left(R(x) - L(x)\right) p(x, t; y, \tau)\right)}{\partial x} \\
&\quad + \frac{1}{2}\frac{\partial^2 \left((\Delta x)^2 \left(R(x) + L(x)\right) p(x, t; y, \tau)\right)}{\partial x^2} \quad (7.23)
\end{aligned}
$$

If $a(x,t)$ and $b(x,t)$ are

$$
a(x,t) = \Delta x(R(x) - L(x)) = (\mu(t) - h(t))x\Delta x. \quad (7.24)
$$

and

$$b(x,t) = (\Delta x)^2(R(x) + L(x)) = (\mu(t) + h(t))x(\Delta x)^2. \qquad (7.25)$$

then (7.23) is the Fokker-Planck Equation (7.15).

The above advection-diffusion equation has been used in Ecology for the modeling of distribution of the species [88]. Recently, the mean first passage time problem has been used to study the movement of red fox by McKenzie *et al* [60].

7.2 Survival Probability and the Mean First Passage Time Problem

The material in this part is mainly from the book written by Gardiner [30].

The *First Passage Time Problem* is also called the first exit time, or persistent time problem, it is the time needed for a random variable to arrive at a certain predefined end position from its initial position [73]. Suppose the state of a stochastic process $X(t)$ is restricted in some bounded domain $(x_l, x_r) \subset \mathbb{R}$ and $X(0) = x, \quad x_l < x < x_r$. Let $T_{x_l x_r}(x)$ be the time moment that a particle starting at x exits the domain for the first time, that is the predefined ending points are $\{x_l, x_r\}$. Mathematically it is defined as

$$T_{x_l x_r}(x) = sup\{t | x_l < X(\tau) < x_r, 0 \le \tau < t, X(0) = x \in (x_l, x_r)\}. \qquad (7.26)$$

If x_l, x_r are fixed, we write $T(x)$ for short. If we assume that once a particle arrives at the boundary, it stays at the boundary or exits the system, then the boundary is called absorbing. $T(x_l) = 0$ or $T(x_r) = 0$ means the left or right boundary is an absorbing boundary. If both boundaries are absorbing, then $T(x_l) = T(x_r) = 0$.

Normally, $T(x)$ is not easy to find, but the probability density function of $T(x)$ is easy to find, denoted as $g(x,t)$. When the both boundaries are absorbing, $\forall x \in (x_l, x_r)$, we consider the probability of mean exit time $T(x)$ is greater than t, i.e. at time t, the particle is still within the domain (x_l, x_r):

$$P(T(x) > t) = \int_{x_l}^{x_r} p(y, t; x, 0) dy := G(x, t). \qquad (7.27)$$

$G(x,t)$ is called survival probability (see [73]), it has the following properties:

- $G(x,0) = 1, \ x_l < x < x_r,$

- $G(x,\infty) = 0, x_l < x < x_r$ because of the property (3) of $p(y, s; x, t)$,

- $G(x,t) = P(T(x) > t) = \int_t^\infty -G_t(x, s)ds$. Therefore, $g(x,t) = -G_t(x,t)$ is the probability density function of $T(x)$.

The boundary condition of $G(x,t)$ depends on the physical properties of the boundaries. For absorbing boundaries,

$$G(x_l, t) = 0, G(x_r, t) = 0, \quad \forall t \geq 0.$$

Integrating the backward Kolmogorov equation (7.3) by y from x_l to x_r, we obtain an equation for the survival probability $G(x,t)$

$$\begin{aligned}
\frac{\partial G(x,t)}{\partial t} &= -a(x,t)\frac{\partial G(x,t)}{\partial x} - \frac{b(x,t)}{2}\frac{\partial^2 G(x,t)}{\partial x^2}, \quad \forall x \in (x_l, x_r) \\
G(x,0) &= 1, \quad x \in (x_l, x_r), \\
G(x_l, t) &= 0, \quad G(x_r, t) = 0, \forall t > 0.
\end{aligned} \quad (7.28)$$

The mean first exit time, denoted as $\tilde{T}(x)$, could be derived from the survival probability,

$$\tilde{T}(x) = E(T(x)) = \int_0^\infty tg(x,t)dt = \int_0^\infty G(x,t)dt. \quad (7.29)$$

Here we use the integration by parts with assumption $lim_{t\to\infty}tG(x,t) = 0$. We can solve for $G(x,t)$ first and then integrate with respect to t to receive $\tilde{T}(x)$. Normally, it is not easy to find an explicit formula for $G(x,t)$, not to mention for $\tilde{T}(x)$. However, for some special cases, we could simplify the equation for $\tilde{T}$ into a second order ODE and find an explicit solution.

Time-homogeneous Case: For the time homogeneous case, $a(x,t) = a(x)$, $b(x,t) = b(x)$, the equation for the survival probability $G(x,t)$ in (7.28) can be written as

$$\frac{\partial G(x,t)}{\partial t} = a(x)\frac{\partial G(x,t)}{\partial x} + \frac{b(x)}{2}\frac{\partial^2 G(x,t)}{\partial x^2}, \quad \forall x \in (x_l, x_r) \quad (7.30)$$

with the boundary and initial conditions given in (7.28).

Then we can integrate (7.30) by time t to receive an ordinary differential equation for $\tilde{T}(x)$.

$$-1 = a(x)\tilde{T}'(x) + \frac{b(x)}{2}\tilde{T}''(x). \tag{7.31}$$

with absorbing boundary condition $\tilde{T}(x_l) = \tilde{T}(x_r) = 0$. Here the $'$ is the derivative with respect to x. This ordinary equation can be solved explicitly by integrating twice with respect to x [30],

$$
\begin{aligned}
\tilde{T}(x) &= \frac{\int_{x_l}^{x_r} \frac{dz}{A(z)} \int_{x_l}^{z} \frac{2A(y)}{b(y)} dy}{\int_{x_l}^{x_r} \frac{dy}{A(y)}} \int_{x_l}^{x} \frac{dy'}{A(y')} - \int_{x_l}^{x} \frac{dz}{A(z)} \int_{x_l}^{z} \frac{2A(y)}{b(y)} dy \\
&= 2\frac{\int_{x_l}^{x_r} \frac{dz}{A(z)} \int_{x_l}^{z} \frac{A(y)}{b(y)} dy \int_{x_l}^{x} \frac{dy'}{A(y')} - \int_{x_l}^{x_r} \frac{dy}{A(y)} \int_{x_l}^{x} \frac{dz}{A(z)} \int_{x_l}^{z} \frac{A(y)}{b(y)} dy}{\int_{x_l}^{x_r} \frac{dy}{A(y)}}.
\end{aligned} \tag{7.32}
$$

where $A(y) = exp\{\int_{x_l}^{x_r} \frac{2a(s)}{b(s)} ds\}$.

First passage time analysis has a long history in physics and chemistry [82] [73] [92] [30], and it has been recently been introduced into Ecology, to study the animal movement and the impact of environment on the animal movement distribution. For example, McKenzie *et al* [60] used it to study red fox arriving a certain position (static prey) for the first time.

In the following, I will use this idea to study the tumor control probability (TCP), given the predefined target of no tumor, we ask what is the probability of an initial tumor to arrive at this target after treatment.

7.3 Tumor Control Probability

When it comes to radiation treatment of tumor, we let $X(t)$ denote the number of tumor cells at time t. The tumor control probability could be solved from the survival probability $G(x, t)$ (of tumor). To avoid the confusion of the survival probability of patients, we will call $G(x, t)$ as *tumor persistent probability* in the following sections.

Now, let us assume that the number of tumor cells is in the interval of $[0, M_0]$ (M_0 could be chosen, for example, the uncontrolled tumor size). The transition p.d.f $p(y, s; x, t)$ is the probability to have y tumor cells at time s, given x tumor

cells at time t; $\tilde{T}(x) = \tilde{T}_{0,M_0}(x)$ is the mean time to first exit the tumor size domain $[0, M_0]$.

We are going to study the parabolic equation in (7.28), the required Mathematical background regarding to parabolic problem is reviewed in Appendix A, all the results are from Evans [26]. Parabolic equation in (7.28) with both absorbing boundary condition has been studied in Redner [73]. To distinguish the probability of the particle to exit on the left or right boundary, respectively, Redner studied the splitting probability which is defined on exit from one boundary before hitting the other. In Section 7.3.1, we will study the treatment success probability that tumor exit $x = 0$ before hitting $x = M_0$ and the mean time needed for treatment success. We use the method of eigenfunction expansion to solve the corresponding boundary problem. The related Mathematical results are listed in Appendix B, which are from Walter [93] and Duffy [21].

Besides, we study the parabolic equation in (7.28) with *no hope boundary* condition at $x = M_0$, we call it *treatment failure problem* in Section 7.3.2. In this problem, we let $x = M_0$ be the uncontrollable tumor size: once the tumor arrive this size, it will persist until the patient dies. This treatment failure problem results in an interesting boundary problem for the mean treatment success time. Eigenfunction expansion of the treatment failure problem shows that the mean treatment success time will be unbounded. We will study this problem in detail in Section 7.3.2 and Section 7.3.3.

7.3.1 Two-side Absorbing Boundary Problem

In the following, we study the time-homogeneous case (7.30). This corresponds to the case of constant treatment, where the birth rate and death rate per capita are independent of time and $a(x,t) = a(x), b(x,t) = b(x)$. Including the boundary and initial condition, we have

$$\begin{cases} \frac{\partial G(x,t)}{\partial t} = a(x)\frac{\partial G(x,t)}{\partial x} + \frac{b(x)}{2}\frac{\partial^2 G(x,t)}{\partial x^2}, & \forall x \in (0, M_0) \times (0, T]. \\ G(0,t) = 0, G(M_0, t) = 0, \forall t \in [0, T]. \\ G(x, 0) = 1, \forall x \in (0, M_0). \end{cases} \quad (7.33)$$

Based on the Theorems in Appendix A, our problem (7.33) has $U = (0, M_0) \subset \mathbb{R}$, and differential operator $\mathcal{L}G = -\frac{b(x)}{2}\frac{\partial^2 G}{\partial x^2} - a(x)\frac{\partial G}{\partial x}$. From (7.25), we know that the coefficient of the second derivative $c(x, t) = b(x, t) > 0$, which means that our problem (7.33) is parabolic. Because the coefficients $a(x), b(x) \in L^\infty(U_T)$, the known functions $f = 0 \in C^\infty(U_T), g = 1 \in C^\infty(U)$, based on the note after Theorem A.2, we have the tumor persistent probability $G(x, t)$ in the constant treatment is $C^\infty(U_T)$.

Theorem 7.3.1. *There is a unique solution for the tumor persistent probability $G(x, t) \in C^\infty(U_T)$ to solve the time homogeneous problem (7.33).*
Because the boundary condition is 0 and initial condition is 1, by the Maximum Principle Theorem, $G(x, t)$ has values between 0 and 1, $\forall (x, t) \in U_T$.

We simulate the tumor persistent probability $G(x, t)$ and draw the contour lines for $G(x, t)$ in Figure 7.1 (left), the x-axis is the initial number of tumor cells and the y-axis is the time. The right graph plots $G(x, t)$ as a function of t for three chosen initial tumor cells $x = M_0/4, \ M_0/2, \frac{3}{4}M_0$. We can see from Figure 7.1 (right) that $G(x, t)$ stays in the interval of $[0, 1]$.

We could continue to compute the mean first exit time $\tilde{T}(x)$, which is not a useful quality for our problem, since it describes the mean time that tumor 'exits' the domain $[x_l, x_r] = [0, M_0]$ either by treatment success from '0' or from 'M_0'. We are more interested in the probability of treatment success, so we look at the probability of exit from $x = 0$ before hitting $x = M_0$.

Probability of Treatment Success

We study this problem based on the personal communication with Professor Mark Lewis at the Center for Mathematical Biology, at the University of Alberta. Related background can be found in the book of Redner [73], where instead of *splitting probability*, we give it a name of *probability of treatment success* here.

Denoted $\mathcal{E}_-(x)$ as the probability of exit from $x = 0$ before hitting $x = M_0$ with x the initial tumor cell numbers. Denote

$PT_-(x) := \{\text{all paths that a particle goes from } x \text{ to } 0 \text{ before hitting } M_0\}.$
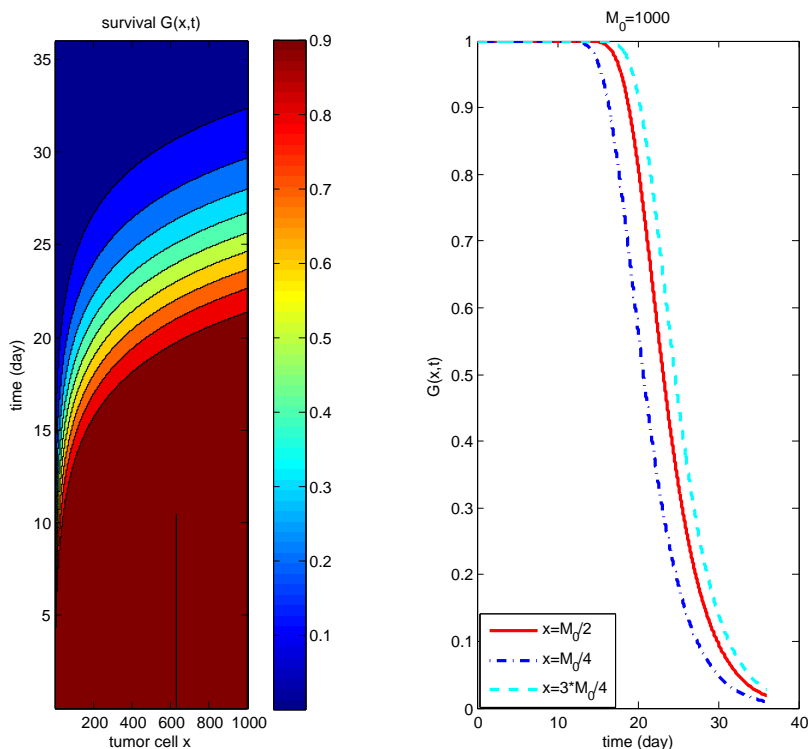
Figure 7.1: **Tumor persistent probability with two absorbing boundary conditions.** The left graph is the contour of $G(x,t)$ as a function of number of tumor cells x and time t, the right graph plot $G(x,t)$ as a function of time t when the initial number of tumor cells x is fixed to $x = M_0/2, M_0/4, \frac{3}{4}M_0$.

Note that the set of possible paths might be uncountable. If this is the case, more formal probability arguments need to be used (see Dynkin's formula [67]). Here we only present the formal derivation where we implicitly assume that PT_- is countable.

$P_{p_-}(x)$ the probability of a path $p_- \in PT_-(x)$. Therefore,

$$\mathcal{E}_-(x) = \sum_{p_-} P_{p_-}(x). \tag{7.34}$$

We assume the time step Δt is small enough such that, if the initial number of tumor cells is x, after one time step Δt, it will be either $x+1$ or $x-1$ or x

with probability of $R(x), L(x)$ and $1 - (R(x) + L(x))$, respectively. We derive a recursive relation for $\mathcal{E}_-(x)$:

$$
\begin{aligned}
\mathcal{E}_-(x) &= \sum_{p_- \in PT_-(x+1)} R(x) \Delta t P_{p_-}(x+1) + \sum_{p_- \in PT_-(x-1)} L(x) \Delta t P_{p_-}(x-1) \\
&\quad + \sum_{p_- \in PT_-(x)} (1 - R(x)\Delta t - L(x)\Delta t) P_{p_-}(x) \\
&= R(x) \Delta t \mathcal{E}_-(x+1) + L(x) \Delta t \mathcal{E}_-(x-1) + (1 - R(x)\Delta t - L(x)\Delta t)\mathcal{E}_-(x) \\
&= \mathcal{E}_-(x) + a(x) \Delta t \mathcal{E}'_- + \tfrac{b(x)}{2} \Delta t \mathcal{E}''_- + h.o.t.
\end{aligned}
$$

(7.35)

where we use Taylor expansion theorem in the last equation and $a(x), b(x)$ are defined by (7.24, 7.25). So for the leading order we have boundary problem for $\mathcal{E}_-$ as following

$$
\begin{cases}
\dfrac{b(x)}{2}\mathcal{E}''_-(x) + a(x)\mathcal{E}'_- = 0, \\
\mathcal{E}_-(0) = 1, \\
\mathcal{E}_-(M_0) = 0.
\end{cases}
$$

(7.36)

Example. For constant treatment, $a(x) = (\mu - h)x$ and $b(x) = (\mu + h)x$, define $\alpha = 2(\mu - h)/(\mu + h)$, the first equation of problem (7.36) is $\mathcal{E}''_- + \alpha \mathcal{E}'_- = 0$. Denote $p(x) = e^{\alpha x}$, problem (7.36) changes into

$$
\begin{cases}
\left(p(x)\mathcal{E}'_-(x) \right)' = 0, \\
\mathcal{E}_-(0) = 1, \\
\mathcal{E}_-(M_0) = 0.
\end{cases}
$$

(7.37)

It can be solved by integrating twice:

$$
\mathcal{E}_-(x) = \frac{e^{-\alpha M_0} - e^{-\alpha x}}{e^{-\alpha M_0} - 1}.
$$

(7.38)

$\mathcal{E}_-$ is a decreasing function of x, that means, the larger the initial tumor, the harder it is to kill the tumor. We plot the probability of treatment success $\mathcal{E}_-$ as a function of α in Figure 7.2. We find that when $\alpha = \frac{2(\mu - h)}{h + \mu} < 0$, $\mathcal{E}_-$ is a concave down function and when $\alpha > 0$, $\mathcal{E}_-$ is concave up. That is to say, when the birth rate μ is bigger than the death rate h induced by radiation ($\alpha > 0$), then the probability of treatment success is small for larger initial tumor size; however, when the birth rate μ is smaller than the death rate h, the tumor is easier to treat, so for most of initial tumor cells, $\mathcal{E}_-$ remains at a number close to 1.
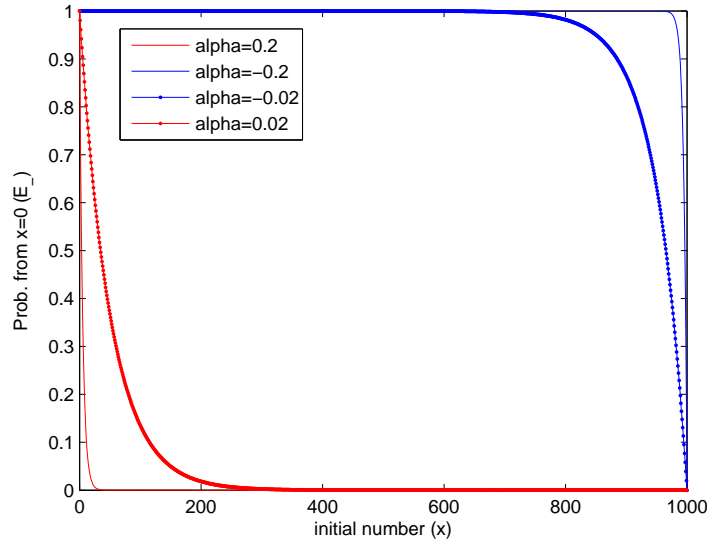
Figure 7.2: **The left exit probability before hitting the right boundary for four choices of α value.** When $\alpha > 0$, the probability of treatment success is quite small, while $\alpha < 0$ brings the probability of treatment success to a high level near 1.

Mean Time of Treatment Success

Next we compute the time needed to exit the left boundary before hitting the right boundary.

Assume we initially have x tumor cells, denote $t_{p_-}(x)$ as the time for each path in $PT_-(x)$ to exit from the left boundary $x = 0$ before touching the right boundary $x = M_0$. Define the mean exit time from the left boundary as

$$t_-(x) = \frac{\sum_{p_-} t_{p_-}(x) P_{p_-}(x)}{\sum_{p_-} P_{p_-}(x)} = \frac{\sum_{p_-} t_{p_-}(x) P_{p_-}(x)}{\mathcal{E}_-(x)}. \tag{7.39}$$

Similarly as the the derivation of $\mathcal{E}_-$, we have

$$
\begin{aligned}
t_-(x)\mathcal{E}_-(x) &= \sum_{p_-\in PT_-(x)} t_{p_-}(x)P_{p_-}(x) \\
&= \sum_{p_-\in PT_-(x+1)} R(x)\Delta t P_{p_-}(x+1)\left[t_{p_-}(x+1)+\Delta t\right] \\
&\quad + \sum_{p_-\in PT_-(x-1)} L(x)\Delta t P_{p_-}(x-\Delta x)\left[t_{p_-}(x-1)+\Delta t\right] \\
&\quad + \sum_{p_-\in PT_-(x)} \left(1-(R(x)+L(x))\,\Delta t\right) P_{p_-}(x)\left[t_{p_-}(x)+\Delta t\right] \\
&= R(x)\Delta t\left[t_-(x+1)\mathcal{E}_-(x+1)\right]+(\Delta t)^2 R(x)\mathcal{E}_-(x+1) \\
&\quad + L(x)\Delta t\left[t_-(x-1)\mathcal{E}_-(x-1)\right]+(\Delta t)^2 L(x)\mathcal{E}_-(x-1) \\
&\quad + \left(1-(R(x)+L(x))\,\Delta t\right)\left[t_-(x)\mathcal{E}_-(x)\right]+\left(1-(L(x)+R(x))\,\Delta t\right)\Delta t\mathcal{E}_-(x) \\
&= t_-(x)\mathcal{E}_-(x)+(R(x)-L(x))\Delta t\left(t_-(x)\mathcal{E}_-(x)\right)' \\
&\quad + \frac{(R(x)+L(x))\Delta t}{2}\left(t_-(x)\mathcal{E}_-(x)\right)''+\Delta t\mathcal{E}_-(x)+h.o.t.
\end{aligned}
$$

where we use Taylor expansion and (7.36) in the last equation. We can further simplify it as follows,

$$
\begin{cases}
\frac{(R(x)+L(x))}{2}(t_-(x)\mathcal{E}_-)''(x)+(R(x)-L(x))(t_-(x)\mathcal{E}_-)'=-\mathcal{E}_-(x), & \text{in } J=(0,M_0) \\
t_-(0)\mathcal{E}_-(0)=0 \\
t_-(M_0)\mathcal{E}_-(M_0)=0.
\end{cases}
\tag{7.40}
$$

Note, the first boundary condition follows because $t_-(0)=0$ and the second comes from $\mathcal{E}_-(M_0)=0$. The treatment success probability $\mathcal{E}_-(x)$ is known from (7.38). We know that $R(x)-L(x)=a(x)=(\mu-h)x$, $\frac{R(x)+L(x)}{2}=\frac{b(x)}{2}=\frac{h+\mu}{2}x$. Let $\alpha=a(x)/b(x)$, we can obtain an equation for $w(x):=t_-(x)\mathcal{E}_-(x)$ as follows

$$
\begin{cases}
w''(x)+\alpha w'(x)=-\frac{\mathcal{E}_-(x)}{b(x)}=-\frac{e^{-\alpha x}-e^{-\alpha M_0}}{(1-e^{-\alpha M_0})b(x)}=\theta\frac{e^{-\alpha M_0}-e^{-\alpha x}}{x}:=g(x), \\
w(0)=0, \\
w(M_0)=0.
\end{cases}
\tag{7.41}
$$

where $\theta=-\frac{2}{(1-e^{-\alpha M_0})(h+\mu)}$.

Let us study the eigenvalue problem corresponding to (7.41),

$$
\tilde{w}''+\alpha\tilde{w}'=-\lambda\tilde{w}, \quad \text{in } J=(0,M_0), \quad \tilde{w}(0)=\tilde{w}(M_0)=0.
$$

Lemma 7.3.2. *When $\Delta = \alpha^2 - 4\lambda \geq 0$, the above problem only has the trivial solution. When $\Delta = \alpha^2 - 4\lambda < 0$, the above problem has nontrivial solutions at some particular values of λ, denoted as λ_k and called eigenvalues, their corresponding eigenfunction w_k as follows,*

$$\lambda_k = \frac{(k\pi/M_0)^2 + \alpha^2}{4}, \quad w_k(x) = e^{-\frac{\alpha}{2}x} sin(\frac{k\pi}{M_0}x), \quad k = 1, 2, \cdots. \quad (7.42)$$

and w_k, $k \geq 1$ are orthogonal to each other by a weighted inner product in L^2, i.e.,

$$< w_k, w_m >_\rho = \int_0^{M_0} e^{\alpha x} w_k(x) w_m(x) = \begin{cases} 0, & k \neq m \\ \frac{M_0}{2}, & k = m. \end{cases} \quad (7.43)$$

By the superposition principle, $\tilde{w}(x) = \sum_{k=1}^{n} c_k w_k$ is also a solution of the above problem, where c_k are any constants. We use the method of eigenfunction expansion to solve (7.41).

Theorem 7.3.3. *The solution of semihomogeneous problem (7.41) is*

$$w(x) = -\sum_{k=1}^{\infty} \frac{g_k}{\lambda_k} w_k(x). \quad (7.44)$$

where w_k, λ_k are defined as (7.42) and g_k are the coefficients of Fourier expansion of $g(x)$ corresponding to w_k, i.e.,

$$\begin{aligned} g_k(x) &= \frac{< g, w_k >_\rho}{< w_k, w_k >_\rho} = \frac{\int_0^{M_0} e^{\alpha x} g_1(x) w_k(x) dx}{\int_0^{M_0} e^{\alpha x} w_k(x) w_k(x) dx} \\ &= \frac{2\theta}{M_0} \left[e^{-\alpha M_0} \int_0^{M_0} \frac{e^{\frac{\alpha}{2}x}}{x} sin\left(\frac{k\pi}{M_0}x\right) dx \right. \\ &\quad \left. - \int_0^{M_0} \frac{e^{-\frac{\alpha}{2}x}}{x} sin\left(\frac{k\pi}{M_0}x\right) dx \right], \quad (7.45) \end{aligned}$$

where $\theta = -\frac{2}{(1-e^{-\alpha M_0})(\mu+h)}$.

Notice that $\frac{sin(x)}{x}$ is continuous and integrable at $x = 0$, hence there is no singularity in the integral of (7.45).

In the left of Figure 7.3 and 7.4, we plot the Fourier series (7.44) up to $K_{max} = 700$ for $\alpha = 0.02$ and $\alpha = -0.02$, respectively. We find in Figure 7.3 that w has
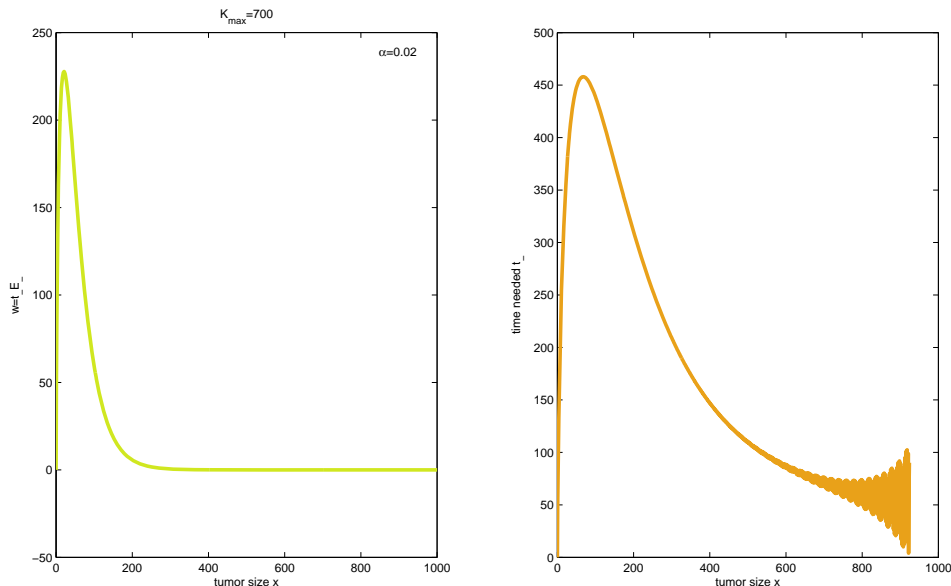
Figure 7.3: **The computation of w (left) and time t_- for $\alpha = 0.02$.** Calculation is up to $K_{max} = 700$.

values of near zero for $x \geq 300$, since $\mathcal{E}_-$ is close to zero in that region. The oscillation of $w(x)$ in Figure 7.4 comes from the $sin\left(\frac{k\pi}{M_0}x\right)$ in the eigenfunction w_k and our truncation of calculation to $K_{max} = 700$. When we increase this K_{max} into a higher number, the amplitude of oscillation will decrease and eventually disappear.

Once $w(x)$ is found, we could solve the mean time to kill the tumor as

$$t_-(x) = \frac{w(x)}{\mathcal{E}_-} = \frac{w(x)}{\frac{e^{-\alpha M_0} - e^{-\alpha x}}{e^{-\alpha M_0} - 1}}. \tag{7.46}$$

We show $t_-(x)$ in the right panel of Figure 7.3 and Figure 7.4. Because of the oscillations of the w below zero at the right boundary, we only calculate the corresponding $t_-(x)$ for $w > 0$. The time $t_-(x)$ shows a hump: it increases for a small initial tumor sizes and then decreases for larger initial tumor size. This happens because $t_-(x)$ is the expected time for tumor cells to die before treatment failure over all the paths that tumor cells die out. When the tumor cell numbers become large enough, the number of paths that reach zero before hitting $x = M_0$ decrease quickly such that the mean time for tumor to die, over all successful treatment paths, decreases.

131
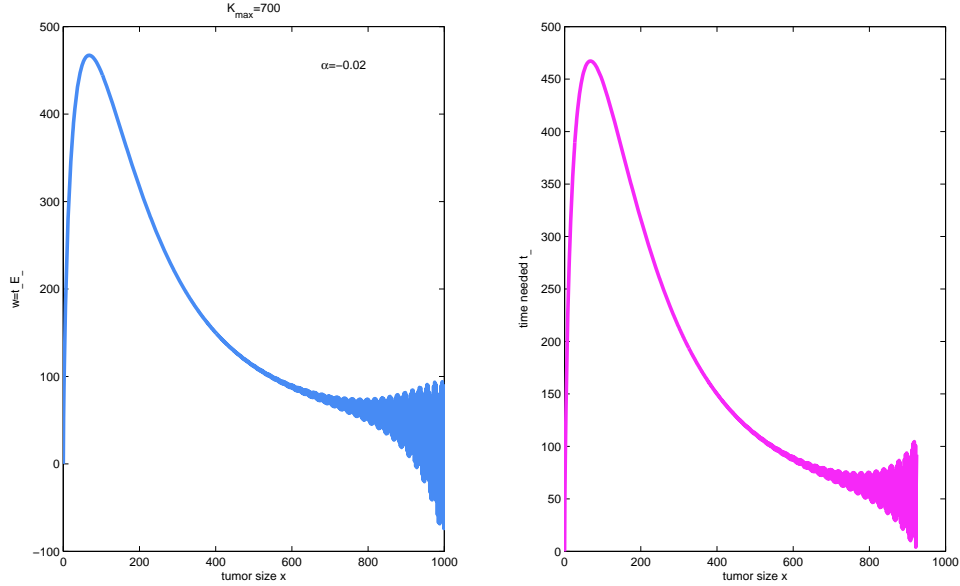
Figure 7.4: **The computation of** w **(left) and time** t_- **for** $\alpha = -0.02$. Calculation is up to $K_{max} = 700$.

7.3.2 Treatment Failure Problem

Here we still consider the domain as $[x_l, x_r] = [0, M_0]$, but we assume that tumor can only exit the domain from $x_l = 0$, which means successful treatment. This problem is not derived from the definition of tumor persistent probability; instead we study this problem for the sake of mathematical curiosity, because it leads to an interesting mathematical problem. Now we have the survival probability satisfies:

$$
\begin{cases}
\frac{\partial G(x,t)}{\partial t} &=& a(x)\frac{\partial G(x,t)}{\partial x} + \frac{b(x)}{2}\frac{\partial^2 G(x,t)}{\partial x^2}. & (x,t) \in (0, M_0) \times (0, \infty) \\
G(x,0) &=& 1, \forall x \in [0, M_0] \\
G(0,t) &=& 0, \forall t \in [0, \infty). \\
G(M_0, t) &=& 1, \forall t \in [0, \infty).
\end{cases}
\tag{7.47}
$$

We choose the right hand side boundary condition as $G(M_0, t) = 1$, because we consider the situation that once the number of tumor cells arrive the size M_0, the tumor is out of control, and tumor will persist until the patient dies; we also name this boundary as *no hope boundary condition*.

132

Compared to the parabolic problem (A.1), problem (7.47) has an inhomogeneous boundary condition. We could easily find a C^∞ function $\phi(x,t)$ such that $\phi(0,t) = 0, \phi(M_0,t) = 1$, for example $\phi(x,t) = \frac{x}{M_0}$. Define $u(x,t) = G(x,t) - \phi(x,t)$, then

$$u_t = G_t, \quad \frac{\partial u}{\partial x} = \frac{\partial G}{\partial x} - \frac{1}{M_0}, \quad \frac{\partial^2 u}{\partial x^2} = \frac{\partial^2 G}{\partial x^2}.$$

and $u(x,t)$ satisfies

$$
\begin{cases}
\frac{\partial u(x,t)}{\partial t} = a(x)\frac{\partial u(x,t)}{\partial x} + \frac{b(x)}{2}\frac{\partial^2 u(x,t)}{\partial x^2} + \frac{a(x)}{M_0}. & (x,t) \in (0, M_0) \times (0,\infty) \\
u(x,0) = 1 - \frac{x}{M_0}, & \forall x \in [0, M_0] \\
u(0,t) = 0, & \forall t \in [0,\infty). \\
u(M_0,t) = 0, & \forall t \in [0,\infty).
\end{cases}
$$

(7.48)

Using theorems as in Appendix A, we can prove the existence of solutions in $U_T = [0, M_0] \times [0,T]$ and the solution is in $C^\infty(U_T)$ provided $a(x), b(x) \in C^\infty$. Also, by the Maximum Principle, $G(x,t)$ has values between 0 and 1. Then we can extend the problem to $[0, M_0] \times [nT, (n+1)T], n \geq 1$ and use the same theorems to prove the existence of the solution for $G(x,t)$ in $(0, M_0) \times (0,\infty)$. The *tumor control probability* can be defined as $TCP(x,t) = 1 - G(x,t)$. We can solve for the $G(x,t)$ function to receive TCP and integrate by t to receive mean exit time $\tilde{T}(x)$.

Example. We choose the birth rate μ as a constant. In Dawson *et al* [20], they choose birth rate for active and quiescent cells as $\mu_a = 0.0655$ day $^{-1}$ and $\mu_q = 0.0476$ day $^{-1}$ respectively. Here we just have one compartment, we choose $\mu = \frac{\mu_q}{\mu_a + \mu_q}\mu_a$, and for death rate, $h(t)$ only comes from the radiation treatment as we assume the natural death is negligible. We take the effective hazard function with finite window (see [20]), i.e.

$$h(t) = (\alpha + 2\beta\,(D(t) - D(t - \omega))\,\dot{D}(t).$$

where $\dot{D}(t)$ is the dose rate, ω is the interaction window that two DSB can interact with each other, and α, β are radiosensitivity parameters. We choose $\alpha = 0.26\ Gy^{-1}$ and $\beta = 0.031\ Gy^{-2}$ the same as Nahum *et al* [62]. These choice of parameters makes $a(x)$ in (7.24) < 0 and $b(x)$ in (7.25) > 0, equation (7.47) is a advection-diffusion problem, and values of $a(x), b(x)$ allow

us to solve the problem by a *forward-center scheme*. We calculate the problem (7.47) in the domain $[0, M_0]$, and draw $TCP(x,t) = 1 - G(x,t)$ values for initial tumor cell numbers $x = M_0/2$ as a function of time t on the left of Figure 7.5. We also compute the mean time for treatment success $\tilde{T}(x)$ from its definition (7.29). Instead of the integral, we sum up all the discrete values of $G(x,t)$ up to our simulation time T and plot $\tilde{T}(x)$ as a function of initial tumor cell numbers x on the right of Figure 7.5.
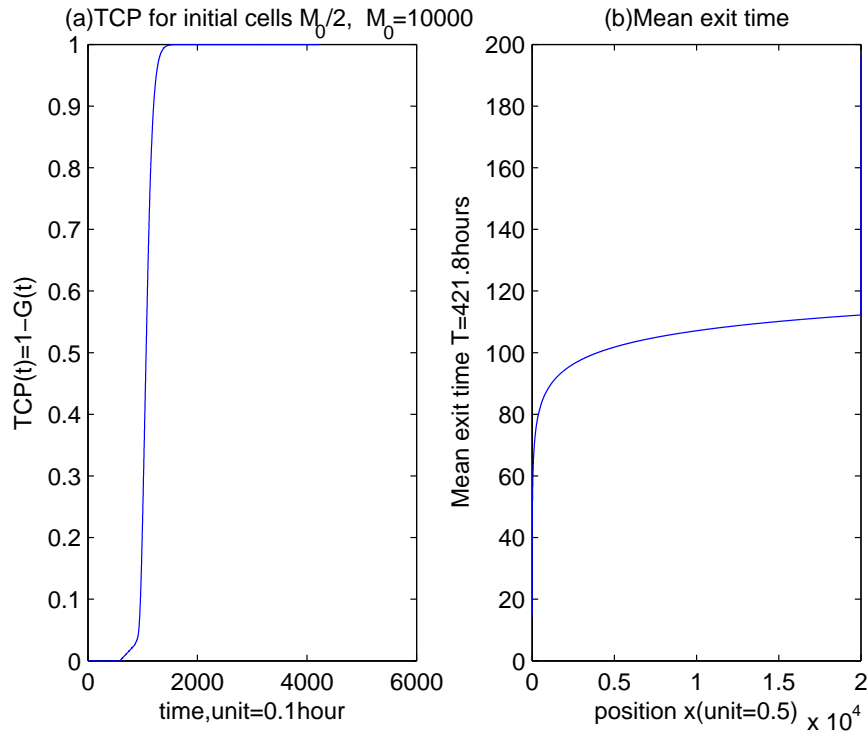
Figure 7.5: **TCP for treatment failure problem.** On the left, we compute the TCP as a function of time with initial tumor cell numbers of $x = M_0/2$; on the right, we calculate the mean treatment success time $\tilde{T}(x)$ as a function of initial tumor cell numbers up to our simulation time $T = 421.8$ hours.

Note we can also derive the ODE for mean exit time $\tilde{T}(x)$ with interesting boundary conditions. The right hand side boundary has changed into $\tilde{T}(M_0) =$

∞. i.e.

$$
\begin{cases}
a(x)\frac{d\tilde{T}(x)}{dx} + \frac{b(x)}{2}\frac{d^2\tilde{T}(x)}{dx^2} &= -1, \quad x \in (0, M_0) \\
\tilde{T}(0) &= 0 \\
\tilde{T}(M_0) &= \infty.
\end{cases}
\tag{7.49}
$$

Mathematically this is a very interesting boundary value problem. To see whether a solution to this problem exists, we go back to study the problem (7.48). This problem could have a Fourier series solution. To make things easier, we first look at the constant coefficients a, b, then the time-homogeneous coefficients $a(x), b(x)$.

7.3.3 Green Function For Parabolic Equation (7.48)

To solve equation (7.48), we use the method of eigenfunction expansion. We first look at the corresponding homogeneous equation and look for a non-trivial solution in a form of $u(x, t) = V(x)T(t)$, which gives

$$
VT' = aV'T + \frac{b}{2}V''T,
$$

by dividing $V(x)T(t)$ on both sides, we have

$$
\frac{T'}{T} = \frac{aV' + \frac{b}{2}V''}{V}
$$

The first term of the above equation is a function of time t and the second term is a function of x, the only situation which make them equal is when they are constants, denoted as $-\lambda$. We end up with a problem of $V(x)$ as

$$
\begin{cases}
aV' + \frac{b}{2}V'' &= -\lambda V \quad (x, t) \in (0, M_0) \\
V(0) &= 0 \\
V(M_0) &= 0.
\end{cases}
\tag{7.50}
$$

This problem has a non-trivial solution when $\frac{a^2}{b^2} < \frac{2\lambda}{b}$, there are infinitely many such λ and corresponding $V(x)$, we denote each one with a subscript n as

$$
\lambda_n = \frac{\mu_n^2 b^2 + a^2}{2b}, \quad n = 1, 2, \cdots
\tag{7.51}
$$

$$
V_n(x) = e^{-\frac{a}{b}x}sin(\mu_n x), \quad n = 1, 2, \cdots
\tag{7.52}
$$

where $\mu_n = \sqrt{\frac{2b\lambda_n - a^2}{b^2}} = \frac{n\pi}{M_0}$. Note $V_n(x)$ are orthogonal to each other with a weight

$$\rho(x) = e^{\frac{2a}{b}x}$$

i.e.,

$$\int_0^{M_0} \rho(x)V_n(x)V_m(x)dx = \int_0^{M_0} sin(\mu_n x)sin(\mu_m x)dx = \begin{cases} 0, & m \neq n \\ \frac{M_0}{2}, & m = n. \end{cases} \tag{7.53}$$

We denote the ρ-weighted inner product in $L^2_\rho([0, M_0])$ as

$$< f, g >_\rho = \int_0^{M_0} \rho(x)f(x)g(x)dx \tag{7.54}$$

and the corresponding norm as

$$\| f \|^2_\rho = < f, f >_\rho .$$

Theorem 7.3.4. *Let $a(x) = a, b(x) = b$ be constants, given eigenvalue and eigenfunction pair $(\lambda_n, V_n(x))$ as defined in (7.51, 7.52), denote*

$$g(x) := 1 - \frac{x}{M_0} = \sum_{n=1}^{\infty} g_n V_n(x), \tag{7.55}$$

$$h(x) := \frac{a}{M_0} = \sum_{n=1}^{\infty} h_n V_n(x). \tag{7.56}$$

where $g_n = \dfrac{< g(x), V_n(x) >_\rho}{\| V_n \|^2_\rho}$ and $h_n = \dfrac{< h(x), V_n(x) >_\rho}{\| V_n \|^2_\rho}$. We have the following results,

(1) $\bar{u}(x,t) = \sum_{n=1}^{\infty} g_n e^{-\lambda_n t} V_n(x)$ is the solution of the homogeneous BVP corresponding to (7.48), i.e.

$$\begin{cases} \frac{\partial \bar{u}(x,t)}{\partial t} & = a\frac{\partial \bar{u}(x,t)}{\partial x} + \frac{b}{2}\frac{\partial^2 \bar{u}(x,t)}{\partial x^2}, & (x,t) \in (0, M_0) \\ \bar{u}(x,0) & = g(x), \ \forall x \in [0, M_0] \\ \bar{u}(0,t) & = \bar{u}(M_0, t) = 0, \ \forall t \in [0, \infty) \end{cases} \tag{7.57}$$

(2) We can write down the Green function for the linear operator $\mathcal{L} = \frac{\partial}{\partial t} - a\frac{\partial}{\partial x} - \frac{b}{2}\frac{\partial^2}{\partial x^2}$ as

$$\Phi(x, t; \xi, s) = \sum_{n=1}^{\infty} \frac{e^{-\lambda_n(t-s)}}{\| V_n \|_\rho^2} V_n(x) V_n(\xi) H(t - s), \quad t, s > 0; x, \xi \in [0, M_0].$$
(7.58)

where $H(t - s)$ is the Heaviside step function. $H(t)$ is defined as

$$H(t) = \begin{cases} 1, & t \geq 0 \\ 0, & t < 0 \end{cases}$$
(7.59)

and its derivative is a δ-distribution, i.e., $H_t(t) = \delta(t)$. In this case, $\bar{u}(x, t)$ in item (1) can be written as

$$
\begin{aligned}
\bar{u}(x, t) &= \sum_{n=1}^{\infty} g_n e^{-\lambda_n t} V_n(x) = \sum_{n=1}^{\infty} \frac{< g(x), V_n(x) >_\rho}{\| V_n \|_\rho^2} e^{-\lambda_n t} V_n(x) \\
&= \sum_{n=1}^{\infty} \frac{1}{\| V_n \|_\rho^2} e^{-\lambda_n t} V_n(x) \int_0^{M_0} \rho(\xi) g(\xi) V_n(\xi) d\xi \\
&= < \Phi(x, t; \xi, 0), g(\xi) >_\rho
\end{aligned}
$$
(7.60)

(3) The solution of the inhomogeneous problem (7.48) is

$$u(x, t) = < \Phi(x, t; \xi, 0), g(\xi) >_\rho + \int_0^t < \Phi(x, t; \xi, s), h(\xi) >_\rho ds. \quad (7.61)$$

When the coefficients $a(x), b(x)$ are not constant, the eigenvalue problem is

$$\begin{cases} a(x)V' + \frac{b(x)}{2}V'' &= -\lambda V \quad (x, t) \in (0, M_0) \\ V(0) &= 0 = V(M_0). \end{cases}$$
(7.62)

This divergent form can be written as the self-adjoint form as

$$\hat{\mathcal{L}} = \left(p(x)V(x)' \right)' = -\lambda \frac{2}{b(x)} p(x)V,$$
(7.63)

where $p(x) = e^{\int_0^x \frac{2a(s)}{b(s)} ds}$. By Sturm-Liouville Theorem B.7, we know there exist real value eigenvalue $\tilde{\lambda}_n$ and their corresponding eigenfunctions $\tilde{V}_n(x)$. Replacing $\lambda_n, V_n(x)$ by $\tilde{\lambda}_n$ and $\tilde{V}_n(x)$, we have a similar result.

Now let us go back to the inhomogeneous problem (7.47). Notice

$$\frac{x}{M_0} = 1 - g(x,t) = \frac{M_0}{a}h(x,t) - g(x,t) = \sum_n \left(\frac{M_0}{a}h_n - g_n\right)V_n(x)$$

Therefore, the solution of (7.47) is

$$
\begin{aligned}
G(x,t) &= u(x,t) + \frac{x}{M_0} = \sum_{n=1}^{\infty} u_n(t)V_n(x) + \sum_{n=1}^{\infty} \left(\frac{M_0}{a}h_n - g_n\right)V_n(x) \\
&= \sum_{n=1}^{\infty} \left[g_n e^{-\lambda_n t} + \frac{h_n}{\lambda_n}(1 - e^{-\lambda_n t}) + \frac{M_0}{a}h_n - g_n\right]V_n(x) \qquad (7.64)
\end{aligned}
$$

Integrating of the above $G(x,t)$ with respect to time t from 0 to ∞ will result in the mean first exit time $\tilde{T}(x)$ to be unbounded.

Corollary 7.3.5. *The solution $\tilde{T}(x)$ of (7.49) satisfies*

$$\tilde{T}(x) = \begin{cases} 0, & \text{for } x = 0, \\ \infty, & \text{for } x \neq 0. \end{cases} \qquad (7.65)$$

Proof. Assume $\tilde{T}(x) < \infty$ for $0 < x < \infty$. Then $\tilde{T}(x) = \int_0^{\infty} G(x,t)dt < \infty$. Since the solution $G(x,t)$ exists, its integral needs to coincide with $\tilde{T}(x)$. Now we consider $G(x,t) = u(x,t) + \frac{x}{M_0}$ with $u(x,t) \geq 0$ and study

$$\int_0^R G(x,t)dt = \int_0^R u(x,t)dt + \int_0^R \frac{x}{M_0}dt \geq \frac{xR}{M_0} \xrightarrow{R \to \infty} \infty \text{ for } x \neq 0$$

which contradicts the assumption of $\tilde{T}(x) < \infty$.

$\square$

Therefore, we restrict to our treatment period to the interval $[0, T]$. The mean first exit time $\tilde{T}(x) = \int_0^T G(x,t)dt$ can be solved explicitly

$$\begin{cases} a(x)\frac{d\tilde{T}(x)}{dx} + \frac{b(x)}{2}\frac{d^2\tilde{T}(x)}{dx^2} &= -1, \quad x \in (0, M_0) \\ \tilde{T}(0) &= 0 \\ \tilde{T}(M_0) &= T. \end{cases} \qquad (7.66)$$

which has the solution

$$\tilde{T}(x) = \frac{T + \int_0^{M_0} \frac{dz}{A(z)}\int_0^z \frac{2A(y)}{b(y)}dy}{\int_0^{M_0} \frac{dy}{A(y)}}\int_0^x \frac{dy'}{A(y')} - \int_0^x \frac{dz}{A(z)}\int_0^z \frac{2A(y)}{b(y)}dy \qquad (7.67)$$

where $A(y) = exp\{\int_0^y \frac{2a(s)}{b(s)}ds\}$.

138

7.4 Conclusion

In this chapter, we use two methods to study the tumor control probability. These two methods cannot be compared. The method in Section 7.3.1 studies the probability of tumor treatment success, under the assumption that treatment will eventually succeed. Therefore, this treatment success $\mathcal{E}_-(x)$ is just a function of initial tumor size rather than time. In contrast, the method in Section 7.3.2 is a function of both time and initial tumor size.

This chapter is full of mathematical results. To make it more clear, in this section, we are going to clarify the process how to use the above models to calculate the TCP for a given treatment.

We first need the information for the initial tumor size x_0, and determine the fatal tumor size M_0 such that $x_0 \in [0, M_0]$ for a treatable tumor.

Then we need to know the birth rate μ per capita, α, β values in the Linear Quadratic (LQ) model and the treatment schedule, such that we could calculate $R(x), L(x)$ as a random walk and therefore the advection-coefficient $a(x)$ and the diffusion coefficient $\frac{b(x)}{2}$ in equation (7.47).

After all the information has been given, we could solve the parabolic problem (7.47) to calculate the tumor persistent probability $G(x, t)$, then we could find the tumor control probability $TCP(x_0, t) = 1 - G(x_0, t)$, and we could compute the average time all the tumor cells are killed $\tilde{T}(x_0) = \int_0^T G(x_0, t) dt$.

Chapter 8

Conclusion

Radiotherapy has become an effective method to treat cancer. In this thesis, I mainly studied mathematical models to quantify radiation treatment schedules, for both cancer cell-killing and normal tissue complication. These models are extensions of classic cell survival models and are based upon ordinary differential equations (ODEs) and birth-death processes. I first reviewed classical cell survival models and generalized the hazard functions to include various formulations into one general framework. The hazard function describes the death rate caused by radiation and can be used within population models to describe radiation-induced cell death.

The tumor control probability (TCP) is a mathematical model to quantify the probability of tumor eradication. I began my analysis with the simple Poisson TCP where I included regrowth for realistic treatment schedules. I argued that the Gompertzian model is not useful for the study of tumor extinction since it overestimates the growth rate for small tumor size. Hence, I focused my optimization studies on exponential and logistic regrowth. I optimized the TCP under the constraint of limited cumulative radiation effect (CRE) onto normal tissue. My results support the usage of hyperfractionated treatments to reduce damage to healthy tissue. The Poisson model for the TCP and the CRE model are relatively simple models. They do not include many effects; for example, stochastic effects, which might be important for small tumor sizes. Motivated by extinction studies from Ecology, I considered models for

TCP and Normal tissue complication probability (NTCP) which are based on stochastic processes.

The first non-Poisson TCP I studied was the TCP from a birth-death process. First, I reviewed the models of Zaider-Minerbo [101] and Dawson-Hillen [20]. The Zaider-Minerbo model is the first TCP model that allows for arbitrary treatment schedules and it had a huge impact in this field. The Dawson-Hillen model is an extension to include cell-cycle dynamics. I generalized these two models into one framework and proposed a general algorithm to derive a TCP model from birth-death processes. Simulations of this generalized TCP model show that the Zaider-Minerbo model makes the same predictions as the more complicated Dawson-Hillen model and my general model for low dose rate, whereas the predictions differ for higher dose per fraction. Compared to the Zaider-Minerbo model, a large quiescent compartment requires more treatment dose or treatment time to cure the tumor. This result is confirmed by another project in which I was involved, but it is not included in this thesis. In that project with two other students, M. dos Santos and C. Finlay, and with Prof. T. Hillen, we compared six TCP models: Poisson TCP, birth-death TCP, and Monte-Carlo TCP with one and two compartments. We confirmed that the more complicated models indeed make the same predictions as the simplest Poisson TCP for a slow-growing tumor. When tumor cells have a shorter doubling time, however, the difference between non-Poisson TCP and Poisson TCP will increase. We presented these results in a paper appearing in *Mathematical Medicine Biology, a journal of the IMA* [31].

Furthermore, I was able to use the general algorithm from above to derive a TCP model for a tumor with tumor stem cells. This is, to my knowledge, the first time that tumor stem cells were included in a TCP model. I found that the proportion of the stem cells in a tumor cluster will affect the treatment: the less stem cells in the cluster, the easier the tumor is treated. In Hillen *et al* [38], the stem cell model has been used to explain the *tumor growth paradox*. It says that a partially treated tumor might grow bigger than it was before the treatment. Using my stem-cell TCP, I did not observe this paradox, since I am looking at the tumor eradication and not relapse.

Besides the TCP models mentioned above for tumor cells, I also derived a model for normal tissue complication probability (NTCP) from a birth-death process. The existent NTCP models do not consider the growth of the normal tissue. The new NTCP model, which I derived, includes growth and its mean field equation is characterized by logistic growth. Incidently, the calculation of the NTCP also provided an alternative proof to the formula proposed by Hanin [36] to compute the probability distribution $P_i(t)$ of tumor cells from the generating function $A(s,t)$. The formula provided here is faster in simulations. Finally, I studied a TCP model based on the *backward Kolmogorov equation* and *the first passage time problem*. The first passage time problem is used to study the probability that a stochastic process X arrives at a preset target for the first time. Applying this idea to the tumor radiation treatment, I studied the time needed for the numbers of tumor cells X to arrive at the target $X = 0$, i.e., the probability that the tumor cell amount reduces to 0. For this model, I studied two special cases where, in both cases, the tumor size X is in a finite domain $[0, M_0]$. The first case assumes that the tumor can exit this domain either by treatment success at $x = 0$ or patient death at $x = M_0$. This case results in an estimation of treatment success as a function of the initial number of tumor cells. We solve it by the method of eigenfunction expansion. The other case has a *no hope boundary* at $x = M_0$: once the tumor reaches size $x = M_0$, it will persist until the patient dies. This case leads to an interesting and new boundary condition for the mean exit time equation. I studied this new problem by Green's function method and I showed that the eigenfunction expansion of the tumor persistent probability results in an unbounded mean exit time.

The use of the CRE model has been discouraged by Fowler in 1989, and since then it has not been used extensively. I found that Fowler's criticism with the CRE might be related to the weak fitting of the corresponding exponents. Yet I think that there is still merit in the CRE model, if it assumes a general power-law relation between treatment dose, numbers of treatment, and intertreatment time with the damage on healthy tissue. I suggest that clinical data should be collected and fitted to the general power law CRE model

(4.3). It might be a good model for daily treatment planning because of its simplicity.

In my studies, I found that the Poisson TCP does a remarkably good job in estimating the TCP. This can potentially be seen in the wider context of cancer growth and treatment. Cancer growth is a very complex phenomenon, which includes various cell types, such as stem cells, transient cells, quiescent cells, invading cells, metastasis, and other genetic variants All of these cells interact with each other and with the healthy surrounding tissue in a complicated fashion (competition for nutrients, competition for space, interaction with the immune system, etc.). In addition, each tumor is different. A liver tumor of one patient might be quite different from a liver tumor of another patient. Hence it cannot be expected that a one-for-all treatment from the shelf would do an equally good job on all patients. More and more effort is focused on the design of individual treatment schedules, and I hope that my thesis can contribute to the individual treatment design. Mathematical Models, as discussed here, typically depend on a number of parameters, for example the α and β sensitivities. These could be measured individually. Hence, individual treatment can be designed.

A fully accurate model for cancer growth would need to include all the effects which are mentioned above. But this is not possible and also not quite useful. A good mathematical model should focus on the relevant issues and ignore the irrelevant issues. In the context of optimal radiation treatment, we showed that the Poisson model covers most of the complexity that is relevant in every day radiation treatment planning. It seems that inclusion of further complexities in these models is only warranted if absolutely necessary. Hence we might decide that the Poisson TCP is good enough and focus our efforts on other complexities, such as cell-immune interactions, volume constraints, cell-cell competitions and genetic instabilities.

Future research could study the optimization of treatment based on the Poisson TCP and NTCP from the birth-death process. All the models in this thesis only consider the change of the numbers of tumor cells. It would be interesting to study the spatial heterogeneous effects and the effect of the treatment on

these models.

References

[1] Cancer research UK. http://www.cancerhelp.org.uk/help/default.asp?page=52.

[2] L. Allen. *An Introduction to Stochastic Processes with Biology Applications.* Prentice Hall (first Edition), 2003.

[3] P. D. Allison. *Survival analysis using SAS: a practice guide.* SAS Institute, 2010.

[4] E. L. Alpen. *Radiation Biophysics.* Prentice Hall, 1990.

[5] A.Okubo and S. A. Levin. *Diffusion and Ecological Problems: Modern Perspectives (second Edition).* Springer, 2001.

[6] R. Askey. *Orthogonal polynomials and special functions.*, volume 21. 1975.

[7] National Cancer Institute at the National Institutes of Health. http://www.cancer.gov/cancertopics/factsheet/sites-types/metastatic.

[8] K. B. Athreya. *Measure theory and probability theory.* Springer, 2006.

[9] D. Bonnet and J. E. Dick. Human acute myeloid leukemia is organized as a hierarchy that originates from a primitive hematopoietic cell. *Nat. Med.*, 3:730–737, 1997.

[10] C. Burman, G. J. Kutcher, B. Emami, and M. Goitein. Fitting of normal tissue tolerence data to an analytic function. *Int. J. Radiat. Oncol. Biol. Phys.*, 47:295–312, 1991.

[11] D. A. Casciato. *Manual of Clinical Oncology.* Little, Brown and Company, 1988 (2nd edition).

[12] K. H. Chadwick and H. P. Leenhouts. *The Molecular Theory of Radiation Biology.* Springer-Verlag, Berlin, 1981.

[13] M. L. Citron, D. A. Berry, C. Cirrincione, C. Hudis, E. P. Winer, W. J. Gradishar, N. E. Davidson, S. Martino, R. Livingston, J. N. Ingle, E. A. Perez, J. Carpenter, D. Hurd, J. F. Holland, B. L. Smith, C.I. Sartor, E. H. Leung, J. Abrams, R. L. Schilsky, H. B. Muss, and L. Norton. Randomized trial of dose-dense versus conventionally scheduled and sequential versus concurrent combination chemotherapy as postoperative adjuvant treatment of node-positive primary breast cancer: first report of intergroup trial c9741/cancer and leukemia group b trial 9741. *J. Clin Oncol.*, 21(8):1431–1439, 2003.

[14] M. J. Clark, J. E. Dick, P. B. Dirks, C. J. Eaves, C. H. M. Jamieson, D. L. Jones, J. Visvader, I. L. Weissman, and G. M. Wahl. Cancer stem cells- perspectives on current status and future directions: Aacr workshop on cancer stem cells. *Cancer Research*, 66:9339, 2006.

[15] A. T. Collins. Prospective identification of tumorigenic prostate cancer stem cells. *Cancer Research.*, 46:191–224, 2005.

[16] S. B. Curtis. Lethal and potentially lethal lesions induced by radiation - a unified repair model. *Radiation Res.*, 106:252–271, 1986.

[17] M. E. Daly, G. Luxton, C. H. Choi, I. C. Gibbs, S. D. Chang, J. R. Adler, and S. G. Soltys. Normal tissue complication probability estimation by the lyman-kutcher-burman method does not accurately predict spinal cord tolerance to stereotactic radiosurgery. *Int. J. Radiation Oncology Biol. Phys*, doi:10.1016/j.ijrobp.2011.03.004:1–8, 2011.

[18] A. Dasu. Is the α/β value for prostate tumors low enough to be safely used in clinical trials? *Clinical Oncology*, 19:289–301, 2007.

[19] A. Dawson. An active-quiescent model for the radiation treatment of cancer and analysis of prostate cancer data, 2006. University of Alberta.

[20] A. Dawson and T. Hillen. Derivation of the tumour control prabability (TCP) from a cell cycle model. *Comput. and Math. Meth. in Medicine*, 7:121–142, 2006.

[21] D. G. Duffy. *Green′ Functions with Application.* Chapman and Hall/CRC, 2001.

[22] R. E. Pollock (eds). *UICC International Union Against Cancer: Manual of Clinical Oncology (7th Edition).* Wiley-liss, 1999.

[23] M. M. Elkind and G. F. Whitmore. *The Radiobiology of Cultured Mammalian Cells (Chapter 2).* Gordon and Breach Science Publishers, 1967.

[24] B. Emami, J. Lyman, A. Brown, L. Coia, M. Goitein, J. E. Munzenrider, B. Shank, L.J. Solin, and M. Wesson. Tolerance of normal tissue to therapeutic irradiation. *Int J Radiat Oncol Biol Phys*, 21:109–122, 1991.

[25] H. Enderling, A. R. A. Anderson, M. A. J. Chaplain, A. Beheshti, L. Hlatky, and P. Hahnfeldt. Paradoxical dependencies of tumor dormancy and progression on basic cell kinetics. *Cancer Research*, 69:8814–8821, 2009.

[26] L. C. Evans. *Partial Differential Equations.* Amer Math. Society, 1998.

[27] S. B. Field. The Ellis formulae for x-rays and fast neutrons. *Brit. J. Radiol.*, 45:315–316, 1972.

[28] J. F. Fowler. The linear-quadratic formula and progress in fractionated radiotherapy. *British Journal of Radiology*, 62(740):679–694, 1989.

[29] R. Ganguly and I. K. Puri. Mathematical model for the cancer stem cell hypothesis. *Cell Prolif.*, 39, 2006.

[30] C. W. Gardiner. *Handbook of Stochastic Methods for physics, chemistry and the natural sciences.* Springer, 1983.

[31] J. Gong, M. M. dos Santos, C. Finlay, and T. Hillen. Are more complicated tumor control probability models better? *Mathematical and Medicine Biology: A Journal of The IMA (accepted)*, 2011.

[32] D. T. Goodhead. An assessment of the role microdosimetry in radiobiology. *Radiation Res.*, 91, 1982.

[33] T. Guo, L. Kang, and Y. Li. A new algorithm for solving function optimization problem with inequality constraint. *Wuhan University Journal of Natural Science*, 4(4):409–419, 1999.

[34] E. J. Hall. *Radiobiology for the Radiobiologist (Fourth Edition) (Chapter 3)*. J. B. Lippincott Company, 1994.

[35] L. G. Hanin. Iterated birth and death process as a model of radiation cell survival. *Mathematical biosciences*, 169(1):89–107, 2001.

[36] L. G. Hanin. A stochastic model of tumor response to fractionated radiation: limit theorems and rate of convergence. *Math Biosci*, 91(1):1–17, 2004.

[37] T. Hillen, G. de Vries, J. Gong, and C. Finlay. From cell population models to tumour control probability: Including cell cycle effects. *Acta Oncologica*, 49:1315–1323, 2010.

[38] T. Hillen, H. Enderling, and P. Hahnfeldt. A mathematical model of the tumor growth paradox within the cancer stem cell hypothesis, 2011. In Preparation.

[39] T. Hillen and J. Lowengrub. Feedback control in a stem cell model can cause an allee effect, 2011. In Preparation.

[40] A. Jackson, G. J. Kutcher, and E. D. Yorke. Probability of radiation-induced complications for normal tissues with parallel architecture subject to non-uniform irradiation. *Medical Physics*, 20(3), 1993.

[41] J. H. A. M. Kaanders, L. A. M. Pop, H. A. M. Marres, I. Bruaset, F. J. A. van den Hoogen, M. A. W. Merkx, and A. J. van der Kogel.

Arcon: experience in 215 patients with advanced head-and-neck cancer. *Int. J. Radiat. Oncol. Biol. Phys.*, 52:769–778, 2002.

[42] P. Kallman, A. Agren, and A. Brahme. Tumor and normal tissue responses to fractionated non-uniform dose delivery. *Int. J. Radiat. Biol.*, 62(2), 1992.

[43] J. P. Keener and J. Sneyd. *Mathematical Physiology I: Cellular Physiology.* Springer, 2nd edition, 2008.

[44] A. M. Kellerer and H.H. Rossi. The theory of dual radiation action. *Curr. Top. Radiation Res. Q.*, 8:85–158, 1972.

[45] J. Kirk, W. Gray, and R. Watson. Cumulative radiation effect, part 1: Fractionated treatment regimes. *Clinical Radiol.*, 22:145–155, 1971.

[46] B. Koontz, S. Zhou, E. Evans, Z. Vujaskovic, R. Jazczack, T. Wong, M. Anscher, and L. Marks. Estimation of the α/β ratio for lung injury based on direct measurements of radiotherapy (RT)-induced reduction in regional perfusion in human patients. *Int. J. Rad. Oncol. Biol. Phys.*, 63(Supplement 1):S457, 2005.

[47] G. J. Kutcher and C. Burman. Calculation of complication probability factors for non-uniform normal tissue irradiation: The effective volume method. *Int. J. Rad. Oncol. Biol. Phys.*, 16, 1989.

[48] D. E. Lea. *Actions of Radiation on Living Cells.* Cambridge University Press, New York, 2nd edition, 1955.

[49] J. T. Leith, G. Padfield, L. E. Faulkner, P. Quinn, and S. Michelson. Effects of feeder cells on the x-ray sensitivity of human colon cancer cellsr. *Radiotherapy and Oncology*, 21:53–59, 1991.

[50] Y. Liao, M. Joiner, Y. Huang, and Jay Burmeister. Hypofractionation: What does it mean for prostate cancer treatment? *Brit. J. Radiol.*, 76:260–268, 2010.

[51] W. Lo, C.-S. Chou, K. K. Gokoffski, F. Y.-M. Wan, A. D. Lander, A. L. Calof, and Q. Nie. Feedback regulation in multistage cell lineages. *Math. Biosci. Eng.*, 6:doi:10.3934/mbe.2009.6.59, 2009.

[52] G. Luxton, P. J. Keall, and C. R. Kin. A new formula for normal tissue complication probability (NTCP) as a function of equivalent uniform dose (EUD). *Phys. Med. Biol*, 53:23–36, 2008.

[53] J. T. Lyman. Complication probability as assessed from dose-volume histograms. *Radiation Research*, 104:S13–S19, 1985.

[54] S. Ma, K.-W.W. Chan, L. Hu, T.K. Lee, J.Y. Wo, I.O. Ng, B.-J.J. Zheng, and X.-Y.Y. Guan. Identification and characterization of tumorigenic liver cancer stem/progenitor cells. *Gastroenterology.*, 132(7):2542–56, 2007.

[55] F. Macdonald and C.H. J. Ford. *The Molecular Biology of Cancer*. BIOS scientific Publishers Limited, Oxford., 1977.

[56] B. Maciejewski, H. R. Withers, J. M. G. Taylor, and A. Hliniak. Dose fractionation and regeneration in radiotherapy for cancer of the oral cavity and oropharynx - tumor dose-response and repopulation. *Int. J. Radiat. Oncol. Biol. Phys.*, 16(3):7831–843, 1989.

[57] K. Mah, J. van Dyk, and P. Y. Poon. Acute radiation induced pulmonary damage: A clinical study on the response to fractionated radiation therapy. *Int. J. Radiat. Oncol. Biol. Phys.*, 13:179–188, 1987.

[58] A. Marciniak-Czochra, T. Stiehl, A. D. Ho, W. Jger, and W. Wagner. Modeling of asymmetric cell division in hematopoietic stem cellsregulation of self-renewal is essential for efficient repopulation. *Stem cells and development*, 18(3):377–386, 2009.

[59] A. McAneney and S.F.C. O'Rourke. Inverstigation of various growth mechanisms of solid tumor growth within the linear-quadratic model for radiotherapy. *Phys. Med. Biol*, 52:1039–1054, 2006.

[60] H. W. McKenzie, M. A. Lewis, and E. H. Merrill. First passage time analysis of animal movement and insights into the functional response. *Bull. Math. Biol*, 71:107–129, 2009.

[61] K. Miettinen, P. Neittanmaki, M. M. Makela, and J. Periaux. *Evolutionary algorithm in engineering and computer science.* John Wiley and Sons Ltd, Baffins Lane, Chichester, England, 1999.

[62] A. E. Nahum, B. Movsas, E. M. Horwitz, C. C. Stobbe, and J. D. Chapman. Incorporating clinical mesaurement of hypoxia into tumor local control modeling of prostate cander: Implications for the α/β ratio. *Int J. Radiat. Oncol. Biol Phys.*, 57, 2003.

[63] C. Nieder, A. L. Grosu, N. Andratschke, and M. Molls. Proposal of human spinal cord reirradiation dose based on a collection of data from 40 patients. *Int. J. Rad. Oncol. Biol. Phys.*, 61:851–855, 2005.

[64] A. Niemierko. Reporting and analyzing dose distributions: A concept of equivalent uniform dose. *Med. Phys.*, 24(1), 1997.

[65] A. Niemierko and M. Goitein. Modeling of normal tissue response to radiation: the critical volume model. *Int. J. Rad. Onc. Biol. Phys.*, 25(1), 1993.

[66] L. Norton and R. Simon. The norton-simon hypothesis revisited. *Can. Treat. Res.*, 70:163–169, 1986.

[67] B. Oksendal. *Stochastic Differential Equation (Fourth Edition).* Springer, 1995.

[68] World Health Organization. Global health observatory data repository 2008.

[69] S. T. Peeters, J. V. Lebesque, W. D. Heemsbergen, W. L. van Putten, A. Slot, M. F. Dielwart, and P. C. Koper. Localized volume effects for late rectal and anal toxicity after radiotherapy for prostate cancer. *Int. J. Rad. Oncol. Biol. Phys.*, 64(5):1151–1161, 2006.

[70] N. U. Prabhu. *Stochastic processes: basic theory and its applications.* World Scientific, 2007.

[71] D. M. Prescott and A. S. Flexer. *Cancer: The Misguided Cell.* Sinauer Assoc. Inc., Massachusetts, 1982.

[72] T. T. Puck and P. I. Marcus. A rapid method for viable cell titration and clone production with Hela cells in tissue culture: The use of X-irradiated cells to supply conditioning factors. *Proc. Natl. Acad. Sci. U. S.*, 41:432–437, 1955.

[73] S. Redner. *A Guide to First-Passage Process.* Cambridge University Press, 2001.

[74] A. M. Reuther, T. R. Willoughby, and P. A. Kupelian. Toxicity after hypofractionated external beam radiotherapy (70 gy at 2.5 gy per fraction) versus standard fractionation radiotherapy (78 gy at 2.0 gy per fraction) for localized prostate cancer. *Int. J. Rad. Onc. Biol. Phys.*, 54(Suppl.1):187–188, 2002.

[75] R. K. Sachs, L. R. Hlatky, and P. Hahnfeld. Simple ODE models of tumor growth and anti-angiogenic or radiation treatment. *Mathematical and computer modelling*, 33:1297–1305, 2001.

[76] T. E. Schulteiss, C. G. Orton, and R. A. Peck. Models in radiotherapy, volume effects. *Med. Phys.*, 10:410–415, 1983.

[77] V. A. Semenenko and X. A. Li. Lyman-Kutcher-Burman NTCP model parameters for radiation pneumonitis and xerostomia based on combined analysis of published clinical data. *Phys. Med. Biol.*, 53(3):737, 2008.

[78] S. K. Singh, C. Hawkins, I. D. Clarke, J. A. Squire, J. Bayani, R. M. Henkelman T. Hide, M. D. Cusimano, and P. B. Dirks. Identification of human brain tumour initiating cells. *Nature*, 432:396–401, 2004.

[79] P. Stavrev, N. Stavevra, A. Niemerko, and M. Gotein. Generalization of a model of tissue response to radiation based on the idea of functional subunits and binomial statistics. *Phys. Med. Biol.*, 46:1501–1518, 2001.

[80] F. A. Stewart, Y. Oussoren, and H. Bartelink. The influence of cisplatin on the response of mouse kidneys to multifraction irradiation. *Radiotherapy and Oncology*, 15(1):93–102, 1989.

[81] G. W. Swanson and T. L. Vincent. Optimal control analysis in the chemotherapy of igg multiple myeloma. *Bull. Math. Biol.*, 39:317–337, 1977.

[82] E. Teramoto and N. Shigesada. Stochastic theory of chemical kinetic. *J. Phys. Soc. of Japan*, 29(2):273–283, 1970.

[83] H. D. Thames, S. M. Bentzen, I. Turesson, M. Overgaard, and W. Vandenbogaert. Time-dose factors in radiotherapy - a review of the human data. *Radiotherapy and Oncology*, 19(3):219–235, 1990.

[84] H. R. Thieme. *Mathematics in Population Biology.* Princeton University Press, 2003.

[85] C. A. Tobias, E. A. Blakeley, F. Q. H. Ngo, and T. C. H Yang. The repair-misrepair model of cell survival. In R.E. Meyn and H.R. Withers, editors, *Radiation Biology and Cancer Research*, pages 195–230. Raven Press, New York, 1980.

[86] E. L. Travis and S . L. Tucker. Isoeffect models and fractionated radiation-therapy. *International Journal of Radiation Oncology Biology Physics*, 13(2):283–287, 1987.

[87] H. C. Tuckwell and F. Y. M. Wan. First-passage time of markov process to moving barriers. *Journal of Applied Probability*, 21(4):695–709, 1984.

[88] P. Turchin. *Quantitative Analysis of Movement: measuring and modeling population redistribution in plants and animals.* Sinauer Associates Inc., 1998.

[89] J. R. Usher. Mathematical derivation of optimal uniform treatment schedules for the fractionated irradiation of human tumors. *Math. Biosci.*, 49:157–184, 1980.

[90] R. Valdagni, C. Italia, P. Montanaro, A. Lanceni, P. Lattuada, T. Magnani, C. Fiorino, and A. Nahum. Is the alphabeta ratio of prostate cancer really low? a prospective, non-randomized trial comparing standard and hyperfractionated conformal radiation therapy. *Radiotherapy and Oncology*, 75(1):74–82, 2005.

[91] R. Villadsen, A. J. Fridriksdottir, L. Ronnov-Jessen, T. Gudjonsson, F. Rank, M. A. LaBarge, M. J. Bissell, and O. W. Petersen. Evidence for a stem cell hierarchy in the adult human breast. *J. Cell Biology*, 177, 2007.

[92] M. O. Vlad and V. T. Popa. A first passage time problem for physico-chemical systems with age structure. *Physica A: Statistical Theoretical Physics*, 142:579–600, 1987.

[93] W. Walter. *Ordinary Differential Equation.* Springer-Verlag, 1988.

[94] T. E. Wheldon. *Mathematical models in cancer research.* Taylor and Francis, 1988.

[95] T. E. Wheldon and A. E. Amin. The linear quadratic model. *British Journal of Radiology*, 61(728):700–702, 1988.

[96] T. E. Wheldon and J. Kirk. Mathematical derivation of optimal treatment schedules for the radiotherapy of human tumors, franctioned irradiation of exponentially growing tumor. *Brit. J. Radiol.*, 49:441–449, 1976.

[97] T. E. Wheldon, J. Kirk, and J. S. Orr. Optimal radiotherapy of tumour cells following exponential-quadratic survival curves and exponential repopulation kinetics. *Brit. J. Radiol.*, 50:681–682, 1977.

[98] H. R. Withers, J. M. G. Taylor, and B. Maciejewski. The hazard of accelerated tumor clonogen repopulation during radiotherapy. *Acta Oncologica*, 27(2):131–146, 1988.

[99] R. J. Yaes. Linear-quadratic model isoeffect relations for proliferating tumor-cells for treatment with multiple fractions per day. *International Journal of Radiation Oncology Biology Physics*, 17(4):901–905, 1989.

[100] O. Yurtseven. Effects of the cell cycle on the tumor control probability (TCP) in radiation treatment and comparison of treatment protocols. M.Sc. Thesis, University of Alberta, 2006.

[101] M. Zaider and G.N. Minerbo. Tumour control probability: a formulation applicable to any temporal protocol of dose delivery. *Phys. Med. Biol*, 45:279–293, 2000.

Appendix A
Results for Parabolic Equations

Evans [26] proved, in his book, the unique existence of the weak solution for an initial-boundary-value (IBV) parabolic problem defined as (A.1-A.3) on a domain $U_T = U \times (0, T]$, where U is an open, bounded subset of $\mathbb{R}^n$ and $T > 0$ is some fixed time. The IVB problem is read as

$$
\begin{cases}
\frac{\partial u(x,t)}{\partial t} + \mathcal{L}u &=& f & in\ U_T \\
u &=& 0 & on\ \partial U \times [0, T] \\
u &=& g & on\ U \times \{t = 0\}
\end{cases}
\tag{A.1}
$$

here $f : U_T \to \mathbb{R}$ and $g : U \to \mathbb{R}$ are given, and $u : \bar{U}_T \to \mathbb{R}$ is unknown. The operator $\mathcal{L}$ denotes a second-order partial differential operator in the divergence form

$$
\mathcal{L}u = -\sum_{i,j=1}^{n} (c^{i,j}(x,t)u_{x_i})_{x_j} + \sum_{i=1}^{n} d^i(x,t)u_{x_i} + e(x,t)u
\tag{A.2}
$$

Definition A.1. *Assume $\mathcal{L}$ is given by (A.2). We say the differential operator $\frac{\partial}{\partial t} + \mathcal{L}$ is (uniformly) parabolic, if there exists a constant $\theta > 0$ such that*

$$
\sum_{i,j=1}^{n} c^{i,j}(x,t)\xi_i\xi_j \geq \theta|\xi|^2, \quad \forall (x,t) \in U_t, and\ \xi \in \mathbb{R}^n.
\tag{A.3}
$$

We also say the differential operator $\mathcal{L}$ is (uniformly) elliptic.

Theorem A.2. *(See Evans [26]) When $c^{i,j}(x,t), d^i(x,t), e(x,t) \in L^\infty(U_T), i, j = 1, \cdots, n,\ f \in L^2(U_T), g \in L^2(U)$ and $c^{i,j} = c^{j,i}, i, j = 1, \cdots, n$, considering*

$$
[\mathbf{u}(t)](x) := u(x,t), \quad and \quad [\mathbf{f}(t)](x) := f(t,x),\ x \in U, 0 \leq t \leq T,
$$

then there is an unique function $\mathbf{u} \in L^2(0, T; H_0^1(U))$ *with* $\mathbf{u}' \in L^2(0, T; H^{-1}(U))$ *which is a weak solution of (A.1) satisfying*

$$< \mathbf{u}', v > + B[\mathbf{u}, v; t] \ = \ (\mathbf{f}, v), \forall v \in H_0^1(U) \ and \ a.e. \ 0 \le t \le T \ \ (A.4)$$

$$u(0) \ = \ g. \quad\quad\quad\quad\quad\quad\quad\quad\quad\quad (A.5)$$

where $<,>$ *is the pairing of* $H^{-1}(U)$ *and* $H_0^1(U)$ *and* $B[\mathbf{u}, v; t]$ *is a bilinear operator defined as*

$$B[\mathbf{u}, v; t] := \int_U \sum_{i,j=1}^n c^{i,j}(\cdot, t) u_{x_i} v_{x_j} + \sum_{i=1}^n d^i(\cdot, t) u_{x_i} v + e(\cdot, t) uv dx, \quad\quad (A.6)$$

$\forall \mathbf{u}, v \in H_0^1(U)$ *and a.e.* $0 \le t \le T.$ $(\mathbf{f}, v)$ *denotes the inner product in* $L^2(U)$,

$$(\mathbf{f}, v) = \int_U f(\cdot, t) v dx, \ \ \forall v \in H_0^1(U) \ and \ a.e. \ 0 \le t \le T.$$

Note: The proof of this theorem uses the method of Galerkin approximations in Sobolev spaces. Furthermore, when the regularities of f, g increase, the regularity of u will also increase correspondingly. Especially, when $c^{i,j}(x, t), d^i(x, t), e(x, t) \in L^\infty(U_T), i, j = 1, \cdots, n$, if $g \in C^\infty(\bar{U}), f \in C^\infty(\bar{U}_T)$ and compatibility conditions

$$g_0 := g \in H_0^2(U), g_m := \frac{d^{m-1}}{dt^{m-1}} f(0) - \mathcal{L} g_{m-1} \in H_0^2(U), \quad m = 0, 1, 2, \cdots$$

hold, then the solution for (A.1) is infinitely times differentiable, i.e. $u \in C^\infty(U_T)$. I will refer to Chapter 7 of Evans's book [26] for details.

Theorem A.3. *(Maximum Principle, see Evans [26]) Assume* $u \in C_1^2(U_T) \cap C(\bar{U}_T)$ *and* $e(x, t) \equiv 0$ *in* $\mathcal{L}$, *denote* $\Gamma_T = \bar{U}_T - U_T$, *then*

$$If \ u_t + \mathcal{L}u \le 0 \ in \ U_T, \quad then \quad \max_{\bar{U}_T} u = \max_{\Gamma_T} u,$$

$$If \ u_t + \mathcal{L}u \ge 0 \ in \ U_T, \quad then \quad \min_{\bar{U}_T} u = \min_{\Gamma_T} u.$$

There is also Maximum Principle for $e(x, t) > 0$ in Evans [26], but we only need the case of $e \equiv 0$.

Appendix B
Boundary Value Problem of
Sturm-Liouville Type

The result of this subsection comes from the book of Walter [93] in Chapter 27 and this method is also called *Sturm-Liouville method.* Here we mainly list the results for a Sturm-Liouville form operator $\hat{\mathcal{L}}$

$$\hat{\mathcal{L}}v(x) = \Big(p(x)v'(x)\Big)' + q(x)v, \ \forall x \in J = (0, M_0) \tag{B.1}$$

with two boundary operators

$$\mathcal{R}_1 v(x) \ := \ \alpha_1 v(0) + \alpha_2 p(0)v'(0), \tag{B.2}$$

$$\mathcal{R}_2 v(x) \ := \ \beta_1 v(M_0) + \beta_2 p(M_0)v'(M_0). \tag{B.3}$$

and assumption

$$p(x) \in C^1(J), q(x), g(x) \in C^0(J) \text{ are real functions,}$$

$$p(x) > 0 \text{ in } J, \ \alpha_1^2 + \alpha_2^2 > 0, \ \beta_1^2 + \beta_2^2 > 0. \tag{B.4}$$

Note: A more general form of $\hat{\mathcal{L}}$ is written as $\tilde{\mathcal{L}}u = c(x)u'' + d(x)u' + e(x)$, this two forms are equivalent under the condition of (B.4) and $c(x) \neq 0$.
If $p(x) \in C^1(J)$, $\big(p(x)u'(x)\big)' + q(x)u = p(x)u''(x) + p'(x)u'(x) + q(x)u$ is in the form of $\tilde{\mathcal{L}}u$; on the other hand, when $c(x) \neq 0$, dividing $c(x)$ on both sides of equation $\tilde{\mathcal{L}}u = f$, then multiplying the integrating factor $p(x) = \exp\{\int_0^x \frac{d(s)}{c(s)}ds\} > 0$, we obtain a Sturm-Liouville operator $\hat{\mathcal{L}}$.

The following theorems tell us whether the inhomogeneous boundary value problem (BVP)

$$\hat{\mathcal{L}}u = g(x) \text{ in } J, \quad \mathcal{R}_1 u = \eta_1, \mathcal{R}_2 u = \eta_2. \tag{B.5}$$

has unique solution or not, depends on the solution of the homogeneous BVP

$$\hat{\mathcal{L}}u = 0 \text{ in } J, \quad \mathcal{R}_1 u = 0, \mathcal{R}_2 u = 0. \tag{B.6}$$

Theorem B.4. *The inhomogeneous BVP (B.5) has unique solution , if and only if, the homogeneous BVP (B.6) has only zero solution $u \equiv 0$. The latter is true, if and only if, the Wronskian of the boundary operator of u_1, u_2 satisfies*

$$\begin{vmatrix} \mathcal{R}_1 u_1 & \mathcal{R}_1 u_2 \\ \mathcal{R}_2 u_1 & \mathcal{R}_2 u_2 \end{vmatrix} \neq 0 \tag{B.7}$$

where $u_1(x), u_2(x)$ are fundamental system of solution to the homogeneous differential equation $\hat{\mathcal{L}}u = 0$ and (B.7) is independent of the choices of u_1, u_2.

This theorem tells us, once the fundamental system of differential equation $\hat{\mathcal{L}}u = 0$ is known, we know whether the inhomogeneous BVP (B.5) exists an unique solution or not; Moreover, we could use this fundamental system to construct the solution for (B.5). Now we assume homogeneous BVP (B.6) has only trivial solution in the following.

Definition B.5. *(Green function) A continuous function $\Gamma(x, \xi)$ defined in a square of $x\xi$-plane $(Q = J \times J)$ is called a Green function of problem (B.6) [21], if*

(i) $\hat{\mathcal{L}}\Gamma(x, \xi) = \delta(x - \xi), \forall x, \xi \in J,$

(ii) $\forall$ *fixed* $\xi \in J_0 := (a, b), \mathcal{R}_1\Gamma(a, \xi) = \mathcal{R}_2\Gamma(b, \xi) = 0,$

(iii) Γ_x, Γ_{xx} *exist and are continuous in $Q_1 : a \leq \xi \leq x \leq b$ and $Q_2 : a \leq x \leq \xi \leq b,$*

(iv) *On the diagonal of Q $(x = \xi)$, $\Gamma_x(x+, x) - \Gamma_x(x-, x) = \frac{1}{p(x)}, \forall x \in J = (a, b).$*

Here $\Gamma_x(x+,x)$ and $\Gamma_x(x-,x)$ are the right sided derivative and left sided derivative of Γ with respect to x, respectively.

A Green function is very useful to solve a differential equation. The following theorem provides us a method to construct a Green function and to find the solution of an inhomogeneous equation.

Theorem B.6. *Suppose (B.4) and (B.7) hold.*

(i) *The Green function for the homogeneous BVP (B.6) uniquely exists. It is symmetric $(\Gamma(x,\xi) = \Gamma(\xi,x))$ and defined by*

$$\Gamma(x,\xi) = \frac{1}{c} \begin{cases} u_1(\xi)u_2(x), & 0 \le \xi \le x \le M_0 \\ u_1(x)u_2(\xi), & 0 \le x \le \xi \le M_0 \end{cases} \quad \text{(B.8)}$$

where $c = p(x)\left(u_1 u_2' - u_1' u_2\right) \ne 0$ is a constant, u_1, u_2 are a fundamental system of $\hat{\mathcal{L}} u_i = 0$ in J.

(ii). *The semihomogeneous BVP*

$$\hat{\mathcal{L}} v = g(x) \text{ in } J, \quad \mathcal{R}_1 v = 0, \mathcal{R}_2 v = 0. \quad \text{(B.9)}$$

has a unique solution given by

$$v(x) = \int_a^b \Gamma(x,\xi)g(\xi)d\xi. \quad \text{(B.10)}$$

where $\Gamma(x,\xi)$ is defined in (B.8).

(iii). *For the inhomogeneous BVP (B.5), we could easily find function $\psi \in C^2(J)$ such that $R_i \psi = \eta_i$, $i = 1, 2$. Define $v = u - \psi$, then v satisfying a semihomogenous BVP*

$$\hat{\mathcal{L}} v = \hat{\mathcal{L}} u - \hat{\mathcal{L}} \psi = g(x) - \hat{\mathcal{L}} \psi \text{ in } J, \quad \mathcal{R}_1 v = 0, \mathcal{R}_2 v = 0. \quad \text{(B.11)}$$

therefore by part (ii),

$$u(x) = v(x) + \psi(x) = \int_a^b \Gamma(x,\xi)\left(g(\xi) - \hat{\mathcal{L}}\psi(\xi)\right)d\xi + \psi(x). \quad \text{(B.12)}$$

The construction of a fundamental system u_1, u_2 of differential equation $\hat{\mathcal{L}}u = 0$ can be done as follows.

Notice $\mathcal{R}_1 = \alpha_1 u(0) + \alpha_2 p(0) u'(0)$, we know $(\alpha_1, \alpha_2) \neq 0$, or else $\alpha_1^2 + \alpha_2^2 = 0$. We could always find a pair of constants (c_1, c_2), such that

$$\alpha_1 c_1 + \alpha_2 c_2 = 0$$

u_1 could be received by solving

$$\hat{\mathcal{L}}u_1 = 0 \text{ in } J, \quad u_1(0) = c_1, \; p(0)u_1'(0) = c_2. \tag{B.13}$$

That is, u_1 satisfies the differential equation and the first boundary condition. Similarly, find (d_1, d_2) such that $\beta_1 c_1 + \beta_2 c_2 = 0$ and solve u_2 from

$$\hat{\mathcal{L}}u_2 = 0 \text{ in } J, \quad u_2(0) = d_1, \; p(0)u_2'(0) = d_2. \tag{B.14}$$

It could be proved that u_1, u_2 are linear independent, please see Walter [93]. Another way to construct the Green function is to solve the eigenvalue problem corresponding to (B.6). The following theorem states the existence of the eigenvalue and eigenfunction for the Sturm-Liouville eigenvalue problem

$$\hat{\mathcal{L}}u = -\lambda \rho(x) u \quad \text{it } J = (a, b), \quad \mathcal{R}_1 u = \mathcal{R}_2 u = 0 \tag{B.15}$$

where $\hat{\mathcal{L}}, \mathcal{R}_1$ and $\mathcal{R}_2$ defined as (B.1-B.3).

Theorem B.7. *(see Walter [93]) When $p(x) \in C^1(J), q(x), \rho(x) \in C^0(J), p(x) > 0, \rho(x) > 0$ in $J; \alpha_1^2 + \alpha_2^2 > 0, \beta_1^2 + \beta_2^2 > 0$, the eigenvalue problem (B.15) has infinitely many simple real eigenvalues*

$$\lambda_1 < \lambda_2 < \cdots, \; \lambda_n \to \infty, n \to \infty$$

and no other eigenvalues. The eigenfunction $u_n(x)$ corresponding to λ_n has exactly n zeros in the open interval $J^0 = (a, b)$ and orthogonal to each other in the sense of

$$\int_x \rho(x) u_n(x) u_m(x) dx = 0, \quad m \neq n. \tag{B.16}$$

Any function $f(x) \in C^2(J)$ that satisfies the homogeneous boundary conditions can be expanded in terms of the eigenfunctions in a series

$$f(x) = \sum_{n=1}^{\infty} c_n u_n(x).$$

where c_n, $n \geq 1$ are uniquely calculated from $c_n = \frac{\int_x \rho(x) u_n(x) f(x) dx}{\int_x \rho(x) u_n^2(x) dx}$.

For semihomogeneous problem (B.9), we expand both $u(x)$ and $g(x)$ in series in terms of $u_n(x)$, the coefficients of $u(x)$ can be uniquely determined from the coefficients of $g(x)$. Use the same trick in Theorem B.6 to reduce the inhomogeneous boundary conditions into homogeneous boundaries, we could solve the inhomogeneous problem (B.5).

The construction of the Green function from the eigenfunctions are easy to be extended into time evolution operator $\frac{\partial}{\partial t} + \mathcal{L}$ after Laplace transformation (see Duffy [21]).

Definition B.8. *(Green function for parabolic problem.) For any $x, \xi \in J$ and $t, \tau > 0$, a function $\Phi(x, t; \xi, \tau)$ is called a Green function of problem (A.1) on $U_T = (a, b) \times (0, T]$, if it is continuous on both space and time, and Φ satisfies the following conditions with regards to the equation and boundaries*

(i) $\frac{\partial \Phi}{\partial t} + \mathcal{L}_x \Phi(x, t; \xi, \tau) = \delta(x - \xi) \delta(t - \tau)$,

(ii) $\forall$ *fixed* $\xi \in J$ *and* $\tau > 0$, $\mathcal{R}_1 \Phi(a, t; \xi, \tau) = \mathcal{R}_2 \Phi(b, t; \xi, \tau) = 0$,

(iii) $\Phi(x, 0; \xi, \tau) = 0$.

Theorem B.9. *(see Duffy [21]) Assume a parabolic problem is defined as (A.1), $\Phi(x, t; \xi, \tau)$ is its Green function satisfying all conditions in Definition B.8. The solution of (A.1) $u(x, t)$ can be obtained by*

$$u(x, t) = \int_0^t \int_a^b f(\xi, \tau) \Phi(x, t; \xi, \tau) d\xi d\tau + \int_a^b g(\xi) \Phi(x, t; \xi, 0) d\xi. \quad \text{(B.17)}$$